Quantifying Streambank Erosion and Phosphorus Load for Watershed Assessment and Planning

Daniel E. Storm, Professor, Room 121 Ag Hall, Stillwater, OK 74078, 405-762-1510, dan.storm@okstate.edu, Oklahoma State University, Department of Biosystems and Agricultural Engineering.

Aaron Mittelstet, Assistant Professor, 245 L.W. Chase Hall, Lincoln, NE, (402) 472-5527, amittelstet2@unl.edu, University of Nebraska-Lincoln, Biological Systems Engineering Department.

Start Date: 3/1/2015

End Date: 2/29/2016

Congressional District: 3

Focus Category: AG, GEOMOR, HYDROL, M&P, MOD, NPP, NU, SED, SW, WQL

Descriptors: Nonpoint Source Pollution, Streambank Erosion, Sediments, Nutrients

Students:

Student Status	Number	Disciplines
Undergraduate	1	Biosystems Engineering
M.S.	0	
Ph.D.	2	Biosystems Engineering
Post Doc	0	
Total	3	

Principal Investigators:

Daniel E. Storm, Professor, Oklahoma State University
Aaron Mittelstet, Assistant Professor, University of Nebraska

Publications:

Mittelstet, Aaron Ray, 2015, Quantifying Phosphorus Loads and Streambank Erosion in the Ozark Highland Ecoregion Using the Swat Model, Ph.D. Dissertation, Biosystems and Agricultural Engineering Department, Oklahoma State University, Stillwater, Oklahoma, College, University, City, State, 170 p.

Mittelstet, A.R., D.E. Storm, G.A. Fox and P.M. Allen. Using SWAT to Predict Watershed-Scale Streambank Erosion on Composite Streambanks, Transactions of the ASABE, manuscript NRES-11666-2015 (review complete, revisions requested, revisions submitted)

TABLE OF CONTENTS

LIST OF TABLES

Table **Page**

LIST OF FIGURES

Figure **Page**

EXECUTIVE SUMMARY

Problem and Research Objectives

Streambanks can be a significant source of sediment and P to aquatic ecosystems. Although the streambank-erosion routine in the Soil and Water Assessment Tool (SWAT) has improved in recent years, the lack of site or watershed-specific streambank data increases the uncertainty in SWAT predictions. For the first part of the project, the objectives were: 1) improve and apply the current streambank-erosion routine in SWAT on composite streambanks and 2) compare SWAT-default channel parameters to field-measured values and assess their influence on erosion. The second part of the project addressed the lack of previous SWAT modeling efforts to account for the contribution of stream banks as a P source due to lack of field data and model limitations. This was hypothesized to cause under predicting total and particulate P during large storm events. Therefore, the final objective was to 3) model the streambank erosion and P for the Barren Fork Creek using a modified SWAT model.

Methodology

For the first part of the project, modifications were made to the current streambank-erosion routine in SWAT: 1) replaced the empirical applied-shear stress equation with a process-based equation, 2) replaced bankfull width and depth with top width and bank height, and 3) incorporated an area-adjustment factor to account for heterogeneous trapezoidal cross-sections. The updated streambank-erosion routine was tested on the gravel-dominated streambanks of the Barren Fork Creek in northeastern Oklahoma. The study used data from 28 cross-sectional surveys, including bank height and width, bank slope, bank-gravel d_{50} and bank composition. Gravel d_{50} and k_d-τ_c relationships were used to estimate the critical shear stress (τ) and the erodibility coefficient (k_d), respectively. For the second part of the project, measured streambank and channel parameters were incorporated into a flow-calibrated SWAT model and used to estimate streambank erosion and P for the Barren Fork Creek using the latest streambank-erosion routine and newly incorporated process-based applied shear stress equation.

Principal Findings and Significance

For the first part of the project, incorporating the process-based shear stress equation increased erosion by 85%, the area-adjustment factor increased erosion by 31% and the erosion decreased 30% when using top width and bank height. Incorporating the process-based applied shear stress equation, sinuosity, radius of curvature and measured bed slope improved the predicted vs observed Nash-Sutcliffe Efficiency and R^2 at the ten study sites from -0.33 to 0.02 and 0.49 to 0.65, respectively. Although the process-based applied shear stress equation was the most influential modification, incorporating the top width, bank height and area-adjustment factor more accurately represented the measured irregular cross-sections and improved the model predictions compared to observed data.

For the second part of the project, the predicted streambank erosion was 215,000 Mg/yr versus the measured 160,000 Mg/yr (34% relative error), which was considered excellent. Streambank erosion contributed 47% of the total P to the Barren Fork Creek and also improved P predictions compared to observed data, especially during the high flow events. Due to this influx of streambank P to the system and the current in-stream P routine's limitations, the in-stream P routine was modified by introducing a long-term storage coefficient, thus converting some of the particulate P to long-term storage. Of the total P entering the stream system, approximately 65% left via the watershed outlet and 35% was stored in the floodplain and stream system. This study not only provided local, state and federal agencies with accurate estimates of streambank erosion and P contributions for the Barren Fork Creek watershed, it demonstrated how watershed-scale model, such as SWAT, can be used to predict both upland and streambank P.

CHAPTER 1

USING SWAT TO PREDICT WATERSHED-SCALE STREAMBANK EROSION ON COMPOSITE STREAMBANKS

Abstract

Streambanks can be a significant source of sediment and P to aquatic ecosystems. Although the streambank-erosion routine in the Soil and Water Assessment Tool (SWAT) has improved in recent years, the lack of site or watershed-specific streambank data increases the uncertainty in SWAT predictions. There were two primary objectives of this research: (1) improve and apply the current streambank-erosion routine in SWAT on composite streambanks and (2) compare SWAT-default channel parameters to field-measured values and assess their influence on erosion. Three modifications were made to the current streambank-erosion routine: replaced the empirical applied-shear stress equation with a process-based equation, replaced bankfull width and depth with top width and bank height and incorporated an area-adjustment factor to account for heterogeneous trapezoidal cross-sections. The updated streambank-erosion routine was tested on the gravel-dominated streambanks of the Barren Fork Creek in northeastern Oklahoma. The study used data from 28 cross-sectional surveys, including bank height and width, bank slope, bank-gravel d_{50} and bank composition. Gravel d_{50} and k_d - τ_c relationships were used to estimate the critical shear stress (τ_c) and the erodibility coefficient (k_d), respectively. Incorporating the process-based shear stress equation increased erosion by 85%, the area-adjustment factor increased erosion by 31% and the erosion decreased 30% when using top width and bank height. Incorporating the process-based applied shear stress equation, sinuosity, radius of curvature and measured bed slope improved the predicted vs observed Nash-Sutcliffe Efficiency and R^2 at the ten study sites from -0.33 to 0.02 and 0.49 to 0.65, respectively. Although the process-based applied shear stress equation was the most influential modification, incorporating the top width, bank height and area-adjustment factor more accurately represented the measured irregular cross-sections and improved the model predictions compared to observed data.

Introduction

Sediment is a primary pollutant to surface waters and the fifth leading cause of water quality impairment in the US (USEPA, 2015a). Though erosion is a natural process, the rate of erosion has been accelerated due to anthropogenic activities, such as farming and urbanization. Although sediment loss from agricultural fields, deforestation, and construction sites is significant, in some watersheds streambank erosion can be the most significant contributor of sediment to rivers and streams (Simon and Darby, 1999; Simon et al., 2002; Wilson et al., 2008). Streambank erosion has been observed to increase 10 to 15 times with the advent of European settlement. Rates cited range from 37% to up to 92% (Walling et al., 1999; Simon, et al., 1996). Excess sediment in our streams and reservoirs affects water chemistry, water clarity, increases the cost of treating drinking

water, harms fish gills and eggs, reduces benthic macroinvertebrates densities and diversities and increases turbidity. Increased turbidity not only affects the water aesthetics, but reduces photosynthesis and organisms' visibility. Siltation alters flow in streams and decreases the storage area in our reservoirs, which in turn affects flooding, drinking water and recreation.

Although streambank erosion can contribute a significant quantity of sediment and phosphorus to stream systems (Miller et al., 2014; Kronvang et al., 2012), most watershed-scale models are limited in their ability to predict streambank erosion (Merritt et al., 2003). Two types of models are used to predict streambank erosion: empirical and process-based (Lai et al., 2012). Empirical models, those that predict erosion based on data alone, do a poor job of predicting erosion with changing boundary conditions (Narasimhan et al., 2015). Process-based models simulate the streambank erosion processes, i.e. subaerial processes, fluvial erosion and mass wasting. While process-based models, such as the Bank-Stability and Toe-Erosion Model (BSTEM) (USDA ARS, 2013; Daly et al., 2015a) and CONservation Channel Evolution and Pollutant Transport System (CONCEPTS) (USDA-ARS, 2000), estimate erosion on a single cross-section or reach (Staley et al., 2006), data requirements on a watershed scale are vast and often not practical for most projects. While HEC-RAS recently incorporated BSTEM into the watershed-scale model (Gibson, 2013), few projects have the resources to gather and incorporate the required data. In order to estimate streambank erosion for an entire watershed and require relatively simple inputs, the Soil and Water Assessment Tool (SWAT) model (Arnold et al., 1998) uses both process-based and empirical routines. This combination of processes allows SWAT to model the physical properties involved in streambank erosion, yet make it more practical to use for large watersheds.

Background

Streambank Erosion Routine and Parameter Estimation

The current streambank erosion routine from SWAT 2005 (Neitsch et al., 2011) only permits streambank erosion if there is sufficient transport capacity and after the deposited sediment from the previous time step is removed (Table 1.1). The routine uses the excess shear stress equation (Partheniades, 1965; Neitsch et al., 2011) to calculate the streambank erosion rate, ε (m s^{-1}), given as:

$$\varepsilon = k_d(\tau_e - \tau_c) \tag{1.1}$$

where k_d is the erodibility coefficient (cm^3 N-s^{-1}), τ_e is the effective shear stress (N m^{-2}), and τ_c is the soil's critical shear stress (N/m^2). The k_d and τ_c coefficients are functions of numerous soil properties. SWAT estimates the critical shear stress based on silt and clay content (Julian and Torres, 2006) using the following equation:

$$\tau_c = 0.1 + 0.1779(SC) + 0.0028(SC)^2 - 0.0000235(SC)^3 \tag{1.2}$$

where *SC* is the percent silt and clay content. SWAT predicts k_d using the relationship proposed by Hanson and Simon (2001) based on 83 *in situ* jet erosion tests:

$$k_d = 0.2 * \tau_c^{-0.5} \quad (1.3)$$

Effective shear stress is calculated using the following equations (Eaton and Miller, 2004):

$$\frac{\tau_e}{\gamma * d * s} = \frac{SF_{bank}}{100}\left(\frac{(W + P_{bed}) * \sin\theta}{4 * d}\right) \quad (1.4)$$

$$\log(SF_{bank}) = -1.40 * \log\left(\frac{P_{bed}}{P_{bank}} + 1.25\right) + 2.25 \quad (1.5)$$

where SF_{bank} is the proportion of shear force acting on the bank (N m^{-2}), γ is the specific weight of water (9800 N m^{-3}), d is the depth of water in the channel (m), W is the top width of the bank (m), P_{bed} is the wetted perimeter of the bed (m), P_{bank} is the wetted perimeter of the channel bank (m), θ is the angle of the channel bank from horizontal and s is the slope of the channel (m m^{-1}).

SWAT uses a digital elevation model (DEM) to estimate bed slope and drainage area, assumes the channel has a 2:1 side slope and uses regression equations to estimate bankfull height and width (Neitsch et al., 2011). Currently the same equations are applied worldwide to estimate bankfull width, *BW*, and bankfull height, *BH*, given as:

$$BW = 1.278 * A^{0.6004} \quad (1.6)$$

$$BD = 0.1291 * A^{0.4004} \quad (1.7)$$

where *BW* and *BD* are in meters, and *A* is the drainage area in km^2.

The current streambank-erosion routine has several limitations. Although streambanks on the outside of a meander experience more shear stress (Sin et al., 2012) and erosion (Purvis, 2015), the current routine does not account for the sinuosity of the stream system. The routine does a poor job of redefining channel dimensions after streambank erosion occurs. Therefore, most users assume a balance between erosion and deposition at a cross-section and thus channel dimensions remain constant. Unlike BSTEM and CONCEPTS, which can model multiple bank layers and simulate mass wasting, SWAT assumes a uniform bank and only considers fluvial erosion. Modeling only one layer can lead to large errors in erosion estimates if the critical shear stress and erodibility coefficients of a multilayer streambank are significantly different. Modeling on a large spatial scale leads to many assumptions and simplifications since data are not often available. Some assumptions include average shear stress on the bank, *BW* and *BD* correctly define channel dimensions and the channel is homogeneous and symmetrical.

Proposed Streambank Erosion Routine

Streambank erosion dependent on transport capacity and bed erosion can underestimate the erosion and does not represent the actual processes. A proposed routine (Narasimhan et al., 2015), currently being beta tested, also uses the excess shear

stress equation, but erodes the streambank independent of transport capacity and bed erosion (Table 1.1). The new routine increases the applied shear stress based on the radius of curvature and sinuosity of the reach. The maximum effective shear stress occurs on the outside of the meander and is affected by the degree of sinuosity. Sin et al. (2012) developed a dimensionless multiplication bend factor to adjust the effective shear stress on the meander, which was the ratio of the maximum shear stress experienced at the bends divided by the average channel shear. The dimensionless bend factor (K_b) is estimated using (Sin et al., 2012; Narasimhan et al., 2015):

$$K_b = 2.5\left(\frac{R_c}{W}\right)^{-0.32} \tag{1.8}$$

where R_c is the radius of curvature (m) and W is the top width (m). R_c is estimated using the empirical relationship based on several studies and has a wide range of applicability over widths ranging from 1.5 m (Friedkin, 1945) to 2,000 m (Fisk, 1947) given as (Williams, 1986):

$$R_c = 1.5 * W^{1.12} \tag{1.9}$$

The maximum effective shear stress on the outside of the meander, τ_e^*, is calculated using:

$$\tau_e^* = K_b * \tau_e \tag{1.10}$$

To calculate the total mass of sediment eroded from streambanks, the channel is divided into straight and meandering reaches. The length of the reach affected by meandering is calculated using the inverse of the sinuosity (ratio of channel length to the straight-line length). The effective shear stress of the reach affected by the sinuosity is then multiplied by K_b while the straight section is not. For the meandering section of a reach, erosion is only calculated from the critical bank while both banks erode for the straight section.

Objectives

The proposed routine has only been tested on cohesive soils in the Cedar Creek watershed in North-Central Texas with lateral bank erosion rates ranging from 0.025 to 0.37 m yr^{-1}. More testing is needed before the routine is incorporated into the official SWAT release and used by watershed modelers worldwide. Although the proposed routine addressed some of the current model limitations, several additional limitations and assumptions remain. Therefore, three modifications were made to the proposed routine and tested on the Barren Fork Creek watershed in northeastern Oklahoma. The Barren Fork Creek watershed has non-cohesive soils and lateral bank erosion rates ranging from 0.5 to 8.7 m yr^{-1} (Heeren et al., 2012; Midgley et al., 2012; Daly et al., 2015a). The Barren Fork Creek is representative of non-cohesive gravel-dominated channels and will add important information to the streambank erosion routine validation and assessment.

At a watershed-scale there is typically limited site specific streambank data, both spatially and temporally. While stream reaches range in length from a few hundred

meters to several kilometers, only one value for each parameter may be used to characterize the reach in SWAT. Gathering data for channel parameters by reach is a daunting task and for most projects is not feasible; therefore, the most critical parameters need to be identified to focus data collection efforts. Although there is considerable uncertainty in each of these parameters (Chaubey et al., 2005; Wechsler, 2007; Bieger et al., 2015), no study has compared field-measured to SWAT derived parameters and their influence on streambank erosion.

The objectives of this research were to (1) improve the current SWAT streambank erosion routine, (2) test the routine on the composite streambanks and (3) compare SWAT-default channel parameters to field-measured values and assess their influence on erosion. Results of this study will provide recommendations to watershed modelers and managers to focus data collection and parameter estimation efforts on the most critical streambank erosion parameters, thus providing more accurate model predictions.

Methods

Proposed SWAT Streambank Erosion Modifications

Three proposed modifications were made to the SWAT 2015 streambank-erosion routine beta version to address some of the model's current limitations. The first replaced the empirical applied shear stress equation with a process-based equation. The second replaced the bankfull width and depth with the top width and bank depth. Finally, the third added an area-adjustment factor to account for heterogeneous stream channels (Table 1.1).

To accurately predict streambank erosion, a good estimate of the applied shear stress is essential. Currently, SWAT uses an empirical equation derived from laboratory studies using symmetrical trapezoidal channels (Eaton and Miller, 2004). This can introduce error when used outside the conditions under which the equation was developed. The proposed replacement equation is process-based and used by CONCEPTS (USDA-ARS, 2000):

$$\tau = \gamma * R * S_f \tag{1.11}$$

where R is the hydraulic radius (m) and S_f is the friction slope (m m^{-1}). The friction slope is computed using the following equation:

$$S_f = \frac{n^2 * Q^2}{A^2 * R^{\frac{4}{3}}} \tag{1.12}$$

where Q is the average flow rate (m^3 s^{-1}), n is Manning's roughness coefficient and A is the cross-sectional area (m^2).

SWAT currently assumes a symmetric trapezoidal channel with dimensions derived from bankfull width and depth. There are two primary reasons to replace bankfull parameters with top width and bank height. First, identifying and measuring bankfull width

is subjective and thus carries considerable uncertainty (Johnson and Heil, 1996). Second, bankfull measurements are often less than top width and bank height measurements, thus resulting in inaccurate modeling of stream flow depth (Figure 1.1). In summary, replacing bankfull parameters with top width and bank height more accurately defines the stream system being modeled.

To accurately model streambank erosion, channel dimensions must mimic those of the studied stream system. Although the current SWAT model is constrained by its symmetrical trapezoidal channel dimensions, a simple area-adjustment factor to account for a heterogeneous channel cross-section is proposed (Figure 1.2). No natural channel is symmetrical with a flat and level streambed, and thus assuming a trapezoidal channel will result in errors predicting flow depth. The proposed equation is:

$$A_{adj} = a * A \tag{1.13}$$

where A_{adj} is the adjusted channel cross-sectional area (m^2), A is the irregular cross-sectional area (m^2), and a is a dimensionless adjustment factor less than or equal to 1.0. The variable a is calculated by dividing the irregular cross-sectional area by the trapezoidal area. The trapezoidal area is based on the SWAT input for top width, channel depth and side slope.

Study Site

The streambank erosion routine was tested on the Barren Fork Creek watershed, located in the Ozark Highland Ecoregion in northeast Oklahoma and northwest Arkansas. Recent research on the Barren Fork Creek, an Oklahoma designated Scenic River, has shown that streambank erosion is a significant P source (Miller et al., 2014). Miller et al. (2014) estimated that 36% of the streambanks in the Barren Fork Creek watershed were unstable and eroding. In another study by Heeren et al. (2012), lateral bank erosion on 23 reaches on the Barren Fork Creek and Spavinaw Creek, approximately 50 km north, averaged more than 7 m from 2003 to 2008, with one reach losing 55 m.

The watershed has a drainage area of 890 km^2 (Figure 1.3) and is composed of 55% forest, 30% pasture and 13% hay meadow (Storm and Mittelstet, 2015). The headwaters begin in Washington County, Arkansas, flow through Adair County, Oklahoma before discharging into the Illinois River in Cherokee County, Oklahoma just north of Ferry Tenkiller Lake. The streambanks consist of a fining upward sequence of basal gravels and overlying silts and clays derived from overbank deposition (Figure 1.4). Due to readily available information, the ten study sites from Miller et al. (2014) were used in this study (Figure 1.3). Available information for each site included pebble counts used to define the median particle size (d_{50}), bank height, and streambank total and water soluble soil P. Seven of the ten sites historically had riparian vegetation protection while three were unprotected. Since SWAT only models one streambank layer, the entire streambank was modeled as a gravel layer. Although fluvial erosion is the dominant streambank process in the watershed, ignoring mass wasting of the cohesive layer may lead to the under prediction of the streambank erosion, especially during those events where the top cohesive layer becomes saturated and unstable (Fox and Wilson, 2010).

Parameter Measurement

Parameter measurement was divided into two categories, data mining and field data collection. Data mining included existing online digital data and derivatives, such as bed slope, R_c and sinuosity. Field data included measured stream and streambank information, i.e. *BW, BD*, top width, bank height, side slope and τ_c.

Kocian (2012) found that aerial images and topographic maps were highly correlated with measured data. Therefore, bed slope for each study site reach was calculated using 1:24,000 USGS topography maps and National Aerial Imagery Program (NAIP) aerial images to estimate elevation change and stream length, respectively. Both sinuosity and R_c were calculated using NAIP images from 2003, 2008 and 2013 and averaging the calculated values. The R_c was calculated for each of the meandering reaches by visually overlaying and fitting a circle to each bend (Figure 1.5), and then comparing estimates obtained from Equation 1.9 using *BW* and top width.

A total of 28 stream cross-sections, starting from the Oklahoma/Arkansas state line to the confluence of Barren Fork Creek and the Illinois River (Figure 1.6; Appendix A) were surveyed using a laser level, measuring tape and survey rod; eight at cross-over points, nine at meanders and eleven at straight cross sections (Figures 1.6 and 1.7). Locations of cross-sections were based on available access points. Cross-over points were defined as the river reaches where the thalweg crossed from one side of the channel centerline to the other, straight reaches were defined as reaches with a sinuosity less than 1.1 (Dey, 2014) and meanders were the remaining reaches with a sinuosity greater than 1.1. Two of the straight reaches included surveys completed at the USGS gage stations near Eldon, Oklahoma (07197000) and Dutch Mills, Arkansas (07196900). At each of the 28 sites, the following data were collected: *BW*, *BD*, top width, bank height and side slope.

The measured irregular channel cross section for each of the straight and meandering reaches were compared to the trapezoidal cross section, which was calculated from the measured top width and side slope to obtain the *a*. FlowMaster V8 (Bentley, 2015) was used to estimate the water depth of the irregular cross-section versus the water depth using a trapezoidal cross-section with and without using *a*. Three representative cross-sections were chosen: meander, and heterogeneous and homogenous straight reaches. Flow depths were calculated assuming uniform flow and Manning's formula.

BW was identified by physical stream indicators, such as change in elevation, deposited sediment and vegetation (USGS, 2004). The bankfull area, calculated using the cross-sectional survey, was divided by *BW* to obtain the average *BD*. The measured bankfull parameters were compared to the values calculated by SWAT as well as two equations proposed by Bieger et al. (2015). The equations currently used by the SWAT model to estimate *BW* and *BD* were derived several years ago based on limited measured data. Bieger et al. (2015) compiled *BW* and *BD* data from 51 studies across the US, one equation for the entire US and eight regional equations based on physiographic divisions. The entire US equations for BW_{us} and BD_{us}, in m, are (Bieger et al., 2015):

$$BW_{US} = 2.70 * A^{0.352} \quad (1.14)$$

$$BD_{US} = 0.30 * A^{0.213} \quad (1.15)$$

Dutnell (2000) developed regional equations for the Internal Highland Region, which includes the Barren Fork Creek, for BW_{ihr} and BW_{ihr}, in m, given as:

$$BW_{ihr} = 23.23 * A^{0.121} \quad (1.16)$$

$$BD_{ihr} = 0.27 * A^{0.267} \quad (1.17)$$

Measured d_{50} coupled with an alternative τ_c equation were used to estimate τ_c for the streambank gravel layer using the following algorithm developed specifically for non-cohesive gravel particles (Millar, 2005):

$$\tau_c = 0.05 * \tan(\varphi) * \rho * g(SG-1)d_{50} * \sqrt{1 - \frac{\sin^2 * \theta}{\sin^2 * \phi}} \quad (1.18)$$

where ρ is the density of water (1000 kg m^{-3}), g is gravitational acceleration (9.81 m s^{-2}), SG is the specific gravity of the bank soil (assumed to be 2.65 for all soils), d_{50} is the mean particle diameter of the soil (m), φ is the angle of repose (degrees), and θ is the bank angle (assumed to be 25° for all streambank soils and 0° for all streambed sediments) (Daly et al., 2015a). Although Equation 1.3 was derived using cohesive soils, the equation was successfully used for gravel layers at similar sites by Daly et al. (2015a) and Midgley et al. (2012) and thus will be used in this study.

SWAT Model Setup

The landcover dataset, developed from 2010 and 2011 Landsat images, was used as well as the 10-m USGS DEM and SSURGO soil data. The watershed had minor point sources at Westville, Oklahoma and Lincoln, Arkansas, two USGS stream gages located near Eldon, Oklahoma and Dutch Mills, Arkansas, and three weather stations (Figure 1.8). Outlets were added to the model upstream and downstream of the ten study sites (Miller et al., 2014) to produce SWAT output files for each study reach to predict stream flow and streambank erosion. Management practices, litter application rates and Soil Test Phosphorus for each subbasin were obtained from Mittelstet (2015). The final SWAT model consisted of 73 subbasins, 2,991 HRUs and eight land covers. The primary land covers were forest (55%), pasture (30%) and hay meadow (13%).

Model Evaluation

Streamflow and Flow Depth

The SWAT model was calibrated to observed daily and monthly baseflow, peak flow and total flow at USGS gage stations 07197000 and 07196900. Since Oklahoma's Mesonet began in November 1994, streamflow was calibrated and validated from 2004 to 2013 and 1995 to 2003, respectively. The USGS Hydrograph Separation Program

(HYSEP) was used to estimate baseflow (Sloto and Crouse, 1996). Channel dimensions, obtained from the cross-sectional surveys at the two USGS gage stations, were used in the SWAT model along with an initial Manning's *n* of 0.025 (Daly et al., 2015a). Manning's *n*, the only value not measured, was manually adjusted to calibrate flow depth. The Coefficient of Determination (R^2) and Nash Sutcliff Efficiency (NSE) (Nash and Sutcliffe, 1970) were used to evaluate the model's performance (Moriasi et al., 2007).

Streambank Erosion

NAIP images from 2003 to 2013 were used to estimate the lateral streambank retreat (Figure 1.9) (Heeren et al., 2012; Miller et al., 2014). The NAIP images were used to estimate the eroded streambank widths and lengths, and to calculate the eroded surface area (*EA*). Streambank depth (D_{ts}), in m, was based on Miller et al. (2014) and the 28 surveys, which was used to calculate the total sediment loading (*TS*), in kg, from each reach using:

$$TS = EA * D_{ts} * \rho_b \tag{1.19}$$

where ρ_b is the soil bulk density (g cm^{-3}). A weighted ρ_b based on the bank composition (Miller et al., 2014) was used to estimate the average ρ_b for the bank.

Results and Discussion

Area Adjustment Factor Verification

Figure 1.10 illustrates differences in *a* and flow depth for three cross-sectional reaches: meander (a=0.72), heterogeneous straight reach (a=0.77) and homogenous straight reach (a=0.93). Due to land cover changes and deforestation, gravel has eroded from the upland areas throughout the Barren Fork Creek watershed. Much of this gravel has reached the Barren Fork Creek, resulting in changes in the channel dimensions and flow dynamics of the creek. The highly irregular cross-sections (Figure 1.10a,b) were more representative of the cross-sections on the Barren Fork Creek. The more irregular the measured channel cross section, the more important *a* becomes in accurately estimating the flow depth. For each cross-section, the flow depth was simulated more accurately when using a.

Flow and Flow Depth Calibration

Streamflow calibration predictions were 'very good' (Moriasi et al., 2007) with monthly R^2 and NSE for the calibration (2004 to 2013) and validation (1995 to 2003) periods ranging from 0.78 to 0.82. Based on the cross-sectional surveys, a trapezoidal channel with a top width of 136 m, D_{ts} of 4.97 m and side slopes of 1.35 m m^{-1} were used to calculate *A* at USGS gage station 07197000. This *A* was then compared and adjusted using *a* (Equation 1.13) until it matched the irregularly-shaped surveyed *A* (see Figure 1.2). An α of 0.66 was calculated, which signifies that water is not flowing in 34% of the trapezoidal *A* at a flow depth of 4.97 m. The procedure was repeated at the upstream USGS gage station 07196900 using an α of 0.95.

Flow-depth calibration at the two USGS gage stations yielded the same Manning's *n*, 0.05, which was applied to each reach in the watershed. The calibrated daily flow depth at gage station 07197000 had an R^2 of 0.64 and NSE of 0.56 (Figure 1.11), while the USGS gage station upstream near Dutch Mills, Arkansas had an R^2 and NSE of 0.49. The calibrated Manning's *n* of 0.05 was in the range for other gravel bed streams (Chow, 1959; USGS, 1989) based on the procedure developed by Cowan (1956).

SWAT Calculated Vs Measured Parameters

Data Mining Parameters

The estimated bed slope using topographic maps and NAIP aerial images were not normally distributed; therefore, a Mann-Whitney Rank Sum Test was used to compare bed slopes. At a 95% confidence level, the bed slope calculated using the topographic maps and NAIP aerial images was not significantly different than the bed slope estimated from the 10-m DEM (Figure 1.12). However, the DEM underestimated the bed slope near the watershed outlet and overestimated the bed slope in the head waters. Kocian (2012) also found low accuracy with the 10-m DEM in estimating bed slope compared to LIDAR and topographic maps. Based on these findings and those by Kocian (2012), the bed slope measurements derived from aerial images and topographic maps were utilized.

The sinuosity at the ten study sites ranged from 1.0 to 2.5 with an average of 1.3. Of the ten study sites, four were classified as straight reaches (less than 1.1), three sinuous (1.1-1.5) and three meandering (greater than 1.5) (Dey, 2014). Note that Equation 1.9 was valid for reaches with a sinuosity greater than 1.2 (Williams, 1986). The average radius of curvature for the four study reaches with a sinuosity greater than 1.2 was 151 m. Applying Equation 1.9, the average R_c of the four sites was 131 m and 216 m using *BW* and top width, respectfully (Figure 1.13). An analysis of covariance was conducted at a 95% confidence level to compare the measured R_c versus those derived from Equation 1.9 and the top width or *BW*. Neither the slope nor slope intercept were significantly different for either the top width or *BW*.

Field-measured Parameters

Field measurements at cross-over points and the corresponding drainage area were used to derive equations for *BW* and *BD* (Dutnell, 2000). The measured *BW* had an R^2 of 0.72 and was compared to the values derived from the three empirical equations using an analysis of covariance with a 95% confidence level (Figure 1.14). Neither the slope nor the slope intercept for the SWAT global regression (Equation 1.6) were significantly different with p-values of 0.23 and 0.07, respectively. For the proposed regional regression (Equation 1.17), the slope was significantly different, but the slope intercept was not with a p-value of 0.08. Both the slope and slope intercept were significantly different for the proposed US regression (Equation 1.15).

The measured *BD* versus *DA* had an R^2 of 0.66 and was also compared to the values derived from the three empirical equations using an analysis of covariance with a 95% confidence level (Figure 1.15). The slope was not significantly different for the SWAT global regression (Equation 1.6), yet the slope intercept was significantly different with p-values of 0.07 and 0.02, respectively. For the proposed regional and US regression (Equation 1.17 and 1.15), neither the slope nor the slope intercept were significantly different with p-values of 0.49 and 0.11 for the proposed regional regression and 0.19 and 0.72 for the US regression, respectively.

These results support the findings by Bieger et al. (2015) that concluded that the regional curves were more reliable than the US equations. The regional equations can be improved by incorporating additional sites, especially for the Internal Highlands (seven sites) and Laurentian Upland (six sites) (Bieger et al., 2015). With the large number of SWAT users outside the US, there is a need for counties outside the US to develop their own regional or watershed specific regression equations; however, in this study the global regression estimated the bankfull parameters adequately.

SWAT defined the gravel bank containing 65% gravel, 15% sand, 15% silt and 5% clay, which was similar to the ten study sites that measured 68% gravel, 15% sand, 10% silt and 7% clay. Based on the measured *SC* content of the banks (Julian and Torres, 2006), τ_c was 4.6 Pa and k_d was 0.093 $cm^3\ N^{-1}\ s^{-1}$ (Equations 1.2, 1.3). Using the measured d_{50} of the ten study sites (1.3 to 2.5 cm) and Equation 1.18, τ_c ranged from 3.5 Pa to 8.7 Pa with an average of 5.6 Pa. Both methods produced similar results for τ_c, 4.6 versus 5.6, which agrees with Daly et al. (2015b).

The field surveys measured stream channel side slope, top width and D_{ts}. Average measured side slopes for the straight reaches and meanders were 4.8:1 and 1.4:1, respectively (Figure 1.16). Based on an ANOVA with a Tukey's multiple comparison test at a 95% confidence level, the measured side slopes from straight and meandering reaches and SWAT default values were all significantly different. Top width measurements taken at straight reaches were used to characterize all the stream reaches (Figure 1.17). Measurements were attempted at cross-over and meandering reaches, but many of the cross sections had 25 to 100 m of thick vegetation preventing accurate measurements. Based on an analysis of covariance at a 95% confidence level, the measured *BW* and top width were not significantly different. However, both the slope and slope intercept were significantly different for the measured D_{ts} and *BD* (Figure 1.18).

Observed vs Simulated Streambank Erosion

SWAT-estimated parameters were replaced with parameter estimates based on measured data using a regression equation with watershed area as the independent variable or an average measured value. The following regression equations were derived using measured bed slope and top width:

$$BS = 4.3*10^{-9}*WA^2 - 6.7*10^{-6}*DA + 0.00369 \quad (1.20)$$

$$TW = 0.0787*DA + 35.384 \quad (1.21)$$

where *BS* is the bed slope in m m^{-1}, *TW* is the top width in m and *DA* is the watershed area in km^2. The sinuosity measured at each site using aerial photographs was used in the model. However, R_c could not be measured using aerial photographs for large reaches. Therefore, Equation 1.9 was used to estimate the R_c based on *DA*. It should be noted that the R_c measurements were taken from the aerial photographs were not significantly different at the 95% confidence level from the estimates using Equation 1.9. Since there was no longitudinal trend with *DA* along the length of the Barren Fork Creek, the average τ_c (5.6 Pa), k_d (0.085 cm^3 N^{-1} s^{-1}), side slope (3.1:1), D_{ts} (2.8 m) and *a* (0.78) were used for each reach in the model simulations.

The average observed streambank erosion (gravel and topsoil) from 2004 to 2013 at the ten sites was 2,830 Mg yr^{-1}, and ranged from 219 Mg yr^{-1} at site J to 10,300 Mg yr^{-1} at site F (Figure 1.19). Using the SWAT model with default parameters, the SWAT 2015 streambank erosion routine beta version was tested using two methods, the empirical and proposed applied shear stress equations. The average simulated streambank erosion using the empirical equation was 1,360 Mg yr^{-1} compared to 2,510 Mg yr^{-1} for the process-based equation (Figure 1.19). Both models under predicted the streambank erosion at sites F and E and over predicted the erosion at several other sites, such as D and J. Though the correlation with observed erosion was poor for both equations, the NSE was better for the proposed shear stress equation (Table 1.2).

Data Mining

Incorporating measured *BS* into the model resulted in an improvement in both the R^2 and NSE (Table 1.2). Much of this improvement was due to the incorporation of measured *BS* for sites E and F. Based on the SWAT default using DEM, the *BS* at sites E and F were 0.00095 and 0.00054, respectively. The measured values using the topographic maps and NAIP images were 0.0015 for both sites, which were slope increases of 58 and 180 percent. Incorporating the measured sinuosity and R_c further improved model predictions. Though the average erosion for the data mining scenario decreased overall by 4 to 5% using the two applied shear stress equations, the simulated erosion at the meandering reaches (sites E and F) increased as did the R^2 and NSE (Table 1.2). Based on these results, model simulations can be improved by incorporating measured *BS*, sinuosity and R_c, which can all be measured without field-collected data. The correlation between observed and measured streambank erosion for both the empirical and process-based model had an R^2 of 0.65, even though the average erosion was under predicted using the empirical equation.

Bankfull Parameters

Replacing SWAT default *BW* and *BD* with measured values resulted in an average streambank erosion reduction of 41% and 30% for the empirical and process-based equations, respectively. While the *BW* and *BD* from the proposed regional equation reduced the average erosion by only 4 to 10%, the quantity of erosion increased 46 to

126% when the bankfull parameters derived from the US equation were incorporated into the model (Table 1.3). Using an ANOVA and Tukey's comparison test at 95% confidence level, none of the simulation results using the proposed shear stress equation were significantly different, yet the simulation results using the empirical shear stress equation and the US regression equations was significantly different compared to the other simulation results using the empirical equations. This re-enforces the need for US SWAT applications to use the regional regression equation instead of the US regression equation.

Field Data

Incorporating measured τ_c into the model resulted in a 22 to 25% reduction in the predicted average erosion for the two applied shear stress equations. Increasing τ_c by just one Pa influenced the erosion significantly and corroborates the findings by Narasimhan et al. (2015) that streambank erosion is very sensitive to τ_c. This supports the need for further research evaluating τ_c and k_d using empirical equations and field-measured data. Although the τ_c using the silt and clay content was within the range of measured values in this study, Daly et al. (2015b) found out the Julian and Torres (2006) relationship predicted a smaller range of values over a large range of silt and clay content for cohesive soils.

Replacing the SWAT default side slope of 2:1 with the field-measured side slope of 3.1:1 increased erosion at each site by 34% and 80% for the empirical and applied shear stress equation, respectively (Table 1.3). Issues arise when adjusting side slope, but not the *W* and bank height. Modifying the side slope, but using the smaller bankfull width instead of the *W*, decreases the stream channel *A* and results in excessive shear stress applied to the banks. Replacing the default *BW* and *BH* with the measured *W* and bank height increased the stream channel *A* and reduced the erosion by approximately 30% for the two applied shear stress equations. Replacing all of the measured values, side slope, T*W* and D_{ts}, with the measured values only increased the erosion by 15% using the empirical equation and reduced the erosion by 2% using the process-based equation. Incorporating *a* resulted in an increase of 172% for the empirical equation and 28% for the process based equation. The sensitivity of the empirical applied shear stress equation to decreases in the *A* is a result of more shear stress applied to the streambank instead of the streambed (Equations 1.4 and 1.5). Although replacing the default values with field measurements did not improve model predictions in this study (Table 1.3), more confidence can be given to the model predictions. Further research is needed to determine if replacing the *BS*, sinuosity and R_c is sufficient or if cross-sectional surveys should be conducted.

Cover Factor

Seven of the ten study sites were protected with riparian vegetation while three sites (F, E, and A) were unprotected (Miller et al., 2014). The average observed erosion from 2003 to 2013 at the three unprotected sites was 6,160 Mg yr^{-1} compared to 1,450 Mg yr^{-1} for the protected sites. Although quantifying the impact of riparian vegetation on

streambank erosion is challenging on a watershed scale, vegetation can significantly impact the streambank erosion (Daly et al., 2015a; Harmel et al., 1999). While vegetation does not reduce the erodibility of the gravel layer, the stability of the cohesive top layer increases with root density. Micheli and Kirchner (2002) studied similar banks in California and found that the protected sedge banks only failed after the bank was significantly undercut. After the geotechnical streambank failure, the overbank soil remained partially attached providing temporary armoring against further erosion. The unprotected meadow banks failed more frequently and detached completely from the bank, thus preventing temporary armoring. Although the gravel layer is not affected by vegetation, the streambank erosion of the top cohesive soil layer is reduced. Therefore, due to the current limitations of the model, the τ_c was increased for the seven banks with riparian protection based on the following equation (Julian and Torres, 2006):

$$\tau_c^* = \tau_c * CH_{\text{cov}} \tag{1.22}$$

where τ_c^* is the effective critical shear stress (N m^{-2}) adjusted for vegetative cover and CH_{COV} is the multiplication factor called channel cover factor. Based on Narasimhan et al. (2015), we chose to use a CH_{COV} of two for forest. Therefore, the τ_c for the seven protected sites was increased from 5.6 to 11.2 N m^{-2} and the k_d was decreased to 0.06 cm^3 N^{-1} s^{-1} using Equation 1.3. Including the channel CH_{COV} improved the R^2 and overall model predictions (Figure 1.20). R^2 and NSE were 0.58 and 0.42 using the empirical equation and 0.66 and 0.52 using the process-based equation, respectfully. Both shear stress equations using the CH_{COV} adequately predicted streambank erosion except at reaches E and I. Reach E had an unusually large quantity; more than twice as much as the other two unprotected sites. Although reach I had good riparian protection in 2003 (Figure 1.21), it had 4,330 Mg yr^{-1} streambank erosion compared to a combined total of 5,800 Mg yr^{-1} for the remaining six protected sites. Results from these two reaches demonstrate that models cannot account for all processes occurring in the natural world.

Conclusions

The modified streambank-erosion routine for the SWAT model improved the predicted streambank erosion for composite streambanks. Although the process-based applied shear stress equation was the most influential modification, incorporating the top width, streambank depth and area-adjustment factor more accurately represented the measured irregular cross-sections and improved the model predictions compared to observed data. Since field-data collection is not feasible for every project, simulations were performed using literature and field-based data.

If collecting stream data to estimate channel parameters is not possible due to financial, geographic or time constraints, literature-based data can provide good streambank-erosion estimates. The current SWAT and proposed regional regression equations adequately estimated bankfull width and bankfull depth. The proposed US equation, on the other hand, produced poor results and therefore should not be used for the conditions studied. While Equation 1.9 provided an adequate estimate of the radius of curvature, the measured bed slope using aerial images and topography maps should

be used in place of the DEM-derived estimates. Incorporating the radius of curvature, sinuosity, bed slope and the global or regional bankfull parameters improved model predictions at the ten study sites. The R^2 increased from 0.01 to 0.65 and the NSE increased from -0.92 to 0.49.

Although results from this study demonstrated that using field-measured parameter estimates may not statistically improve model predictions for the conditions studied, other time periods or watersheds may be different. If limited field work can be conducted, multiple measurements of the critical shear stress (τ_c) are recommended. The τ_c was one of the most sensitive parameters and it can be incorporated into the model without affecting the cross-sectional area of the stream channel. If resources permit, complete cross-section surveys should be conducted throughout the stream system to quantify the top width, streambank depth, side slope and area-adjustment factor. Each of these parameters affects the cross-sectional area and should be replaced together. In general, the more watershed-specific measured data incorporated into the model, the more confident the user can be in the model predictions.

Further testing of the ability to predict τ_c using the silt and clay content is needed as well as exploring other τ_c and erodibility coefficient relationships. More research is also needed to quantify how root density from different types of riparian vegetation impact τ_c. Future research also needs to address the streambank-erosion routine limitations, specifically incorporating multiple-layer banks and the modification of channel dimensions throughout the simulation.

Table 1.1. Streambank erosion processes and equations for the current version (SWAT 2005), the 2015 beta version and the proposed modifications to the beta version.

Process	2005 SWAT	2015 Proposed Subroutine	2015 Proposed Subroutine Modifications
Streambank erosion	Excess shear stress equation; function of transport capacity	Excess shear stress equation	Excess shear stress equation
Applied shear stress equation	Equations 1.4, 1.5	Equations 1.4, 1.5	Equations 1.15, 1.16
Incorporates sinuosity	No	Yes	Yes
Bank dimensions	Bankfull width/depth	Bankfull width/depth	Top width/bank depth
Channel heterogeneity	No	No	Yes; area adjustment factor

Table 1.2. SWAT simulated streambank erosion using different methods to estimate streambank erosion parameters using both the empirical and proposed process-based equations for Barren Fork Creek. Empirical is the empirical applied shear stress equation currently used by the SWAT model. Process-Based is the proposed process-based applied shear stress equation. Methods include SWAT default parameters and replacing default parameters with several measured parameters: bed slope, literature based and bankfull width and depth. Literature based parameters include bed slope, sinuosity and radius of curvature. NS=Nash Sutcliff Efficiency.

Parameter	Applied Shear Stress Equation					
	Empirical			Process-Based		
	Erosion (Mg yr^{-1})	R^2	NSE	Erosion (Mg yr^{-1})	R^2	NSE
SWAT default	1,150	0.02	-0.33	2,510	0.01	-0.16
Bed slope	1,000	0.03	-0.20	2,230	0.57	0.38
Literature based	1,090	0.02	-0.12	2,410	0.65	0.49
Measured bankfull parameters	680	0.01	-0.55	1,750	0.05	-0.14
Regional bankfull regression	1,100	0.55	-0.35	2,260	0.01	-0.26
Proposed United States regression	2,600	0.65	-0.47	3,660	0.01	-0.92

Table 1.3. Influence field-measured parameters have on simulated streambank erosion using both the empirical and proposed process-based applied shear stress equations. Empirical is the empirical applied shear stress equation currently used by the SWAT model and Process-Based is the proposed process-based applied shear stress equation. Each method includes literature based parameters, which includes bed slope, sinuosity and radius of curvature. All measured data includes the following: critical shear stress, side slope, top width and bank height. A_{adj} = area adjustment factor.

Parameter	Applied Shear Stress Equation					
	Empirical			Process-Based		
	Erosion (Mg yr^{-1})	R^2	NSE	Erosion (Mg)	R^2	NSE
Literature based (baseline)	1,090	0.65	-0.12	2,410	0.65	0.49
Critical shear stress	850	0.27	-0.37	1,800	0.32	0.10
Side slope	1,960	0.38	0.16	3,240	0.35	0.31
Top width and bank height	720	0.30	-0.42	1,740	0.46	0.15
All measured data	1,250	0.28	-0.14	2,350	0.46	0.32
All measured data + A_{adj}	2,960	0.34	0.31	3,080	0.47	0.41

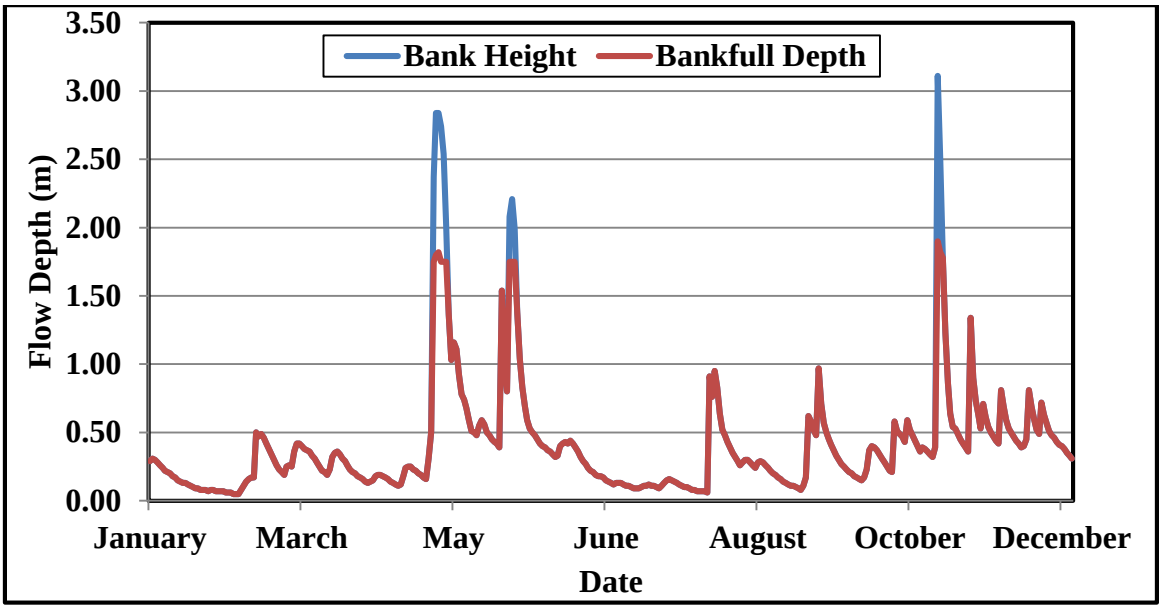

Figure 1.1. SWAT simulated flow depth when using bankfull depth or bank depth to define the channel cross section on the Barren Fork Creek for 2011.

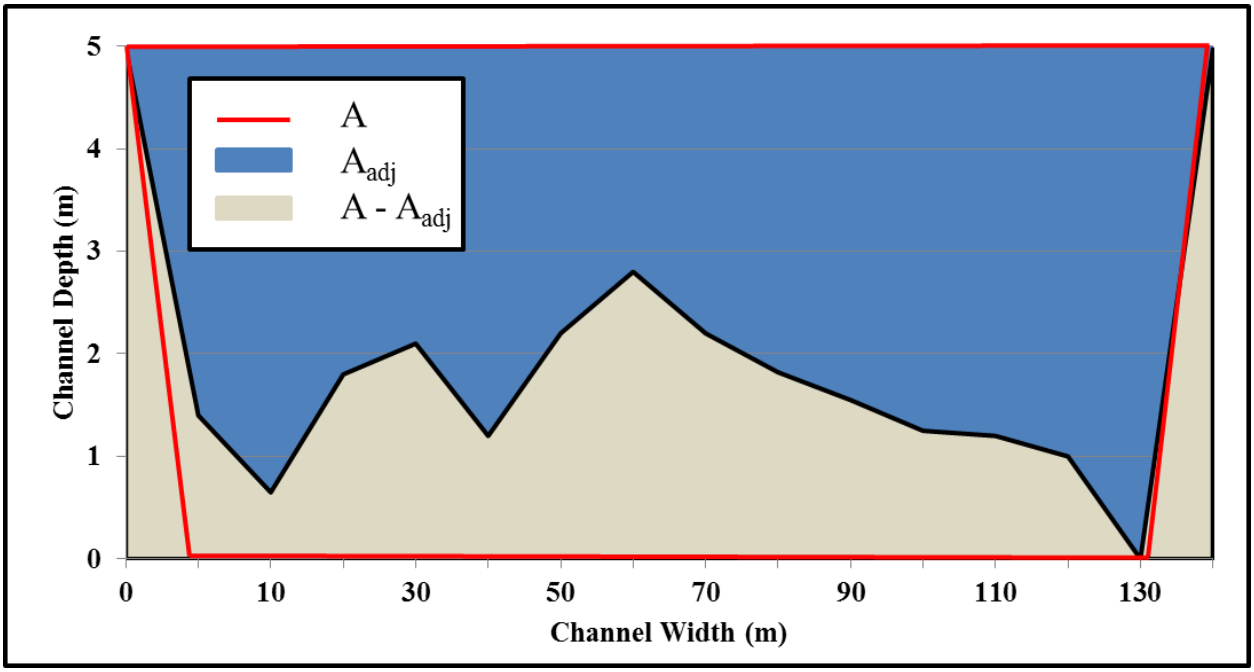

Figure 1.2. SWAT trapezoidal and measured stream cross sections at the United States Geological Survey gage station 07197000 used to adjust cross sectional area and calibrate flow depth. A_{adj} is the measured cross-sectional area of the natural channel, A is the cross-sectional area of an assumed trapezoidal channel, A-A_{adj} is the difference between the trapezoidal and measured cross sections.

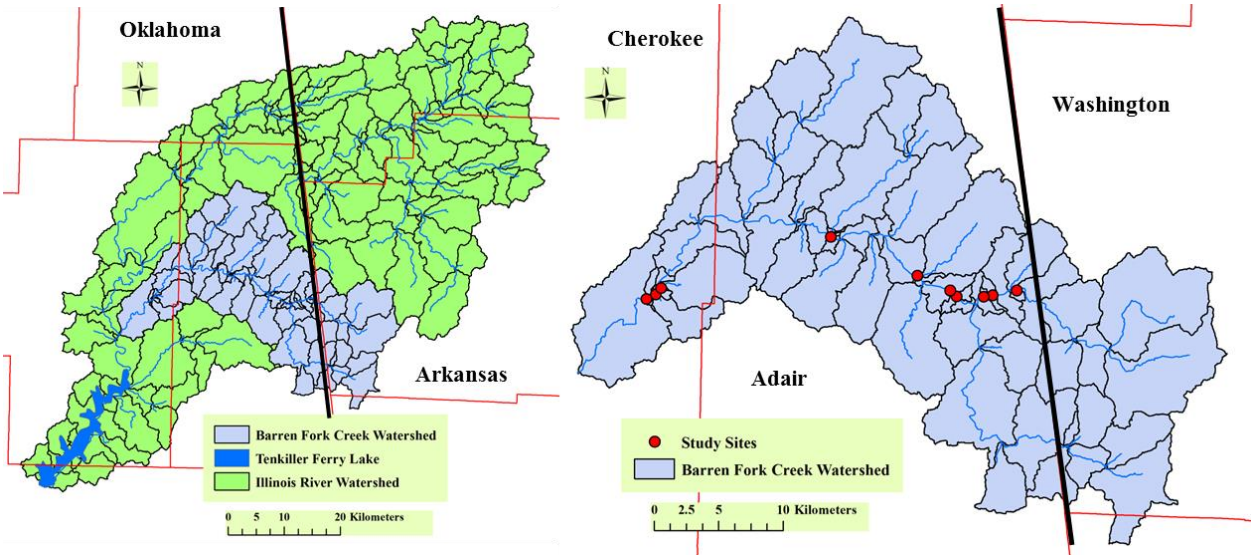

Figure 1.3. Illinois River and Barren Fork Creek watersheds in Oklahoma and Arkansas (left) and the Barren Fork Creek watershed showing ten study sites (right).

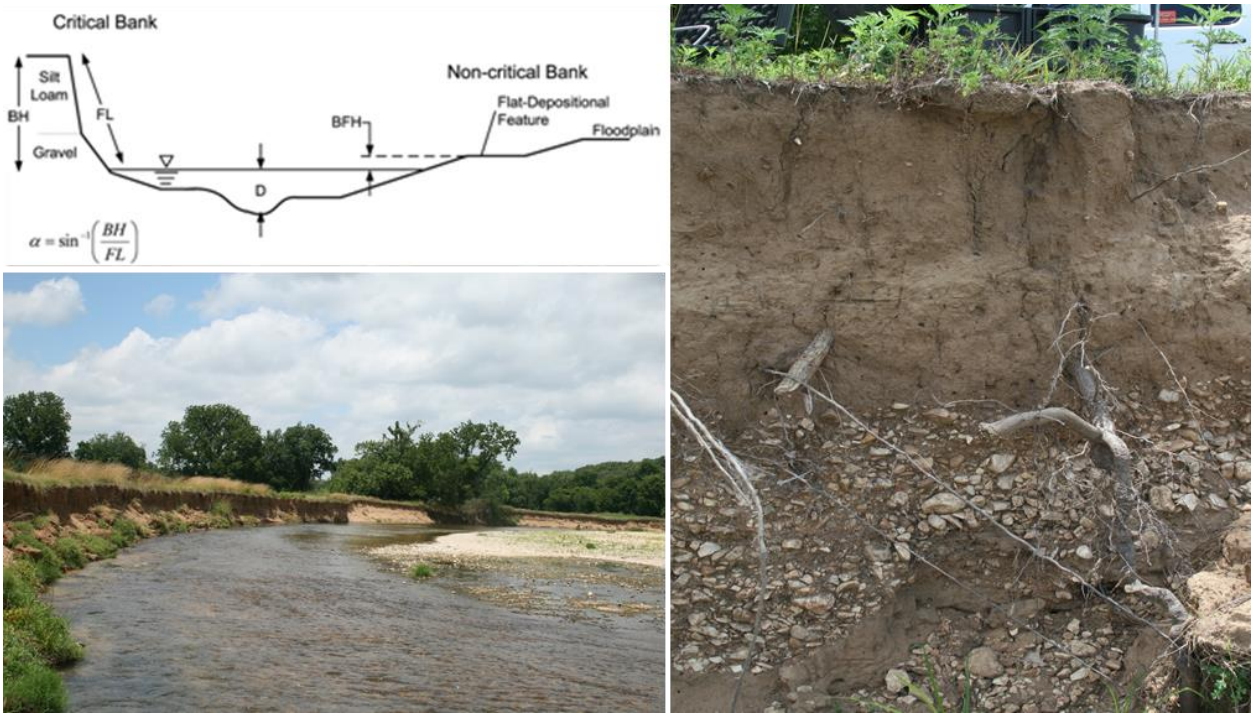

Figure 1.4. Typical stream channel profile in the Barren Fork Creek with one critical bank and one non-critical bank. Right image illustrates the underlying gravel layer and the silty loam topsoil for the critical bank (Heeren et al., 2012).

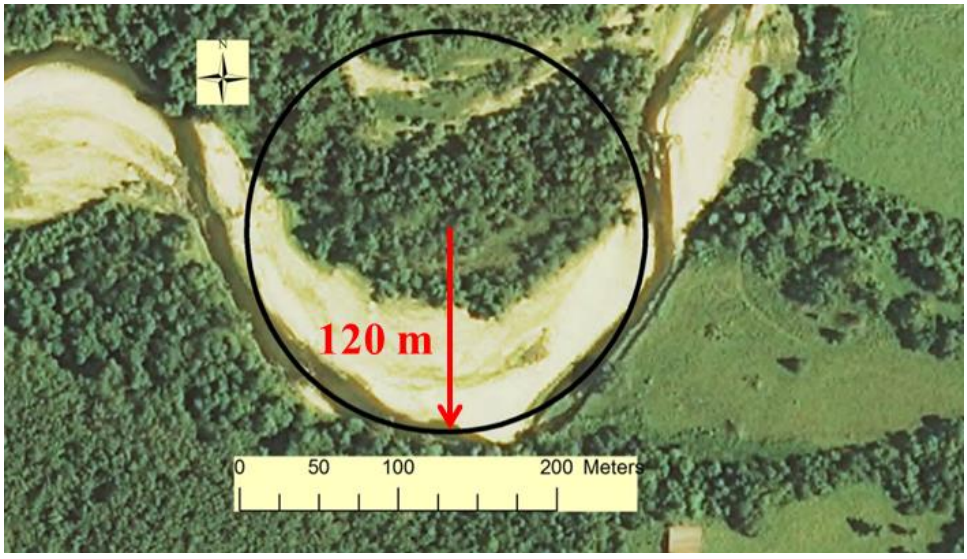

Figure 1.5. Radius of curvature estimate at site F on the Barren Fork Creek using a 2013 National Agriculture Imagery Program image.

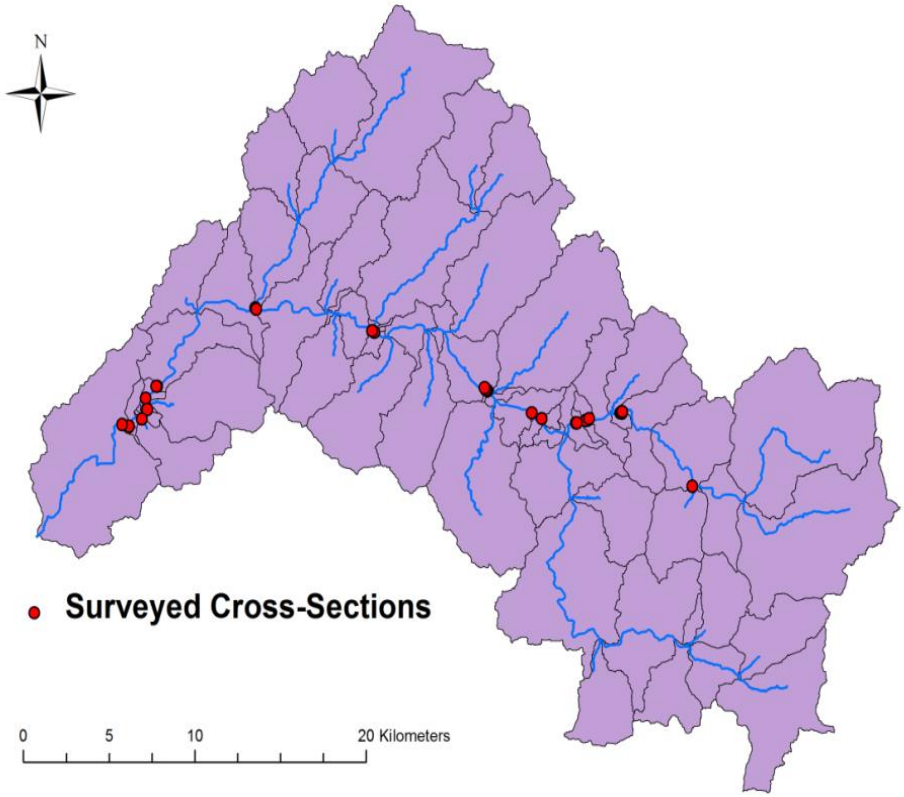

Figure 1.6. Location of 28 surveyed cross-sections surveyed on the Barren Fork Creek 2015.

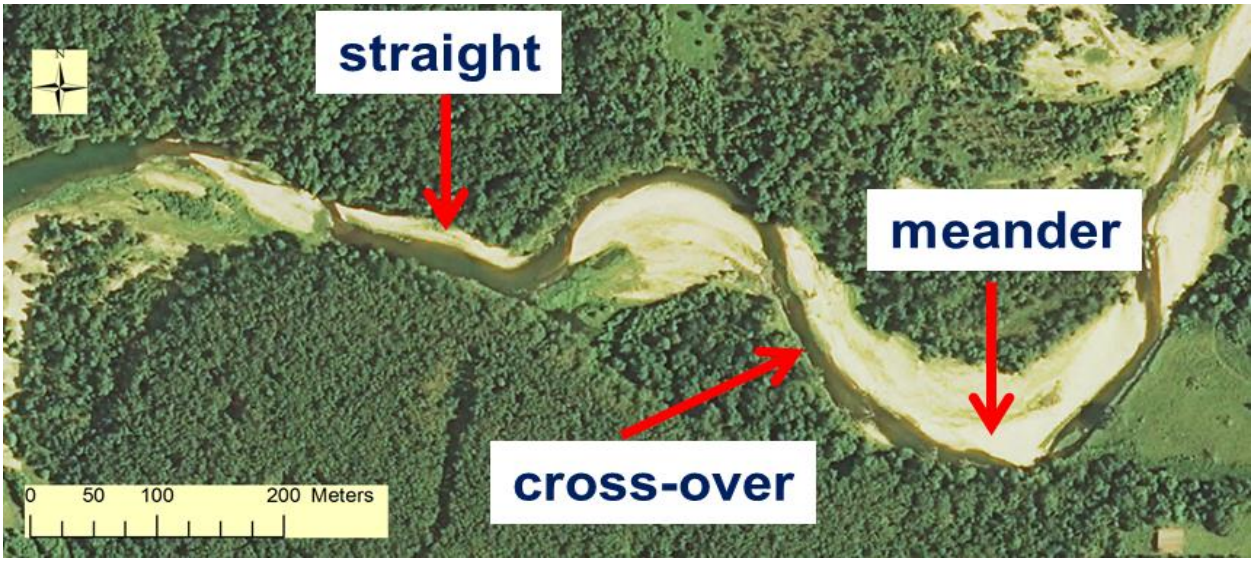

Figure 1.7. Examples of straight, meandering and cross-over stream reaches on a 2013 National Agriculture Imagery Program image.

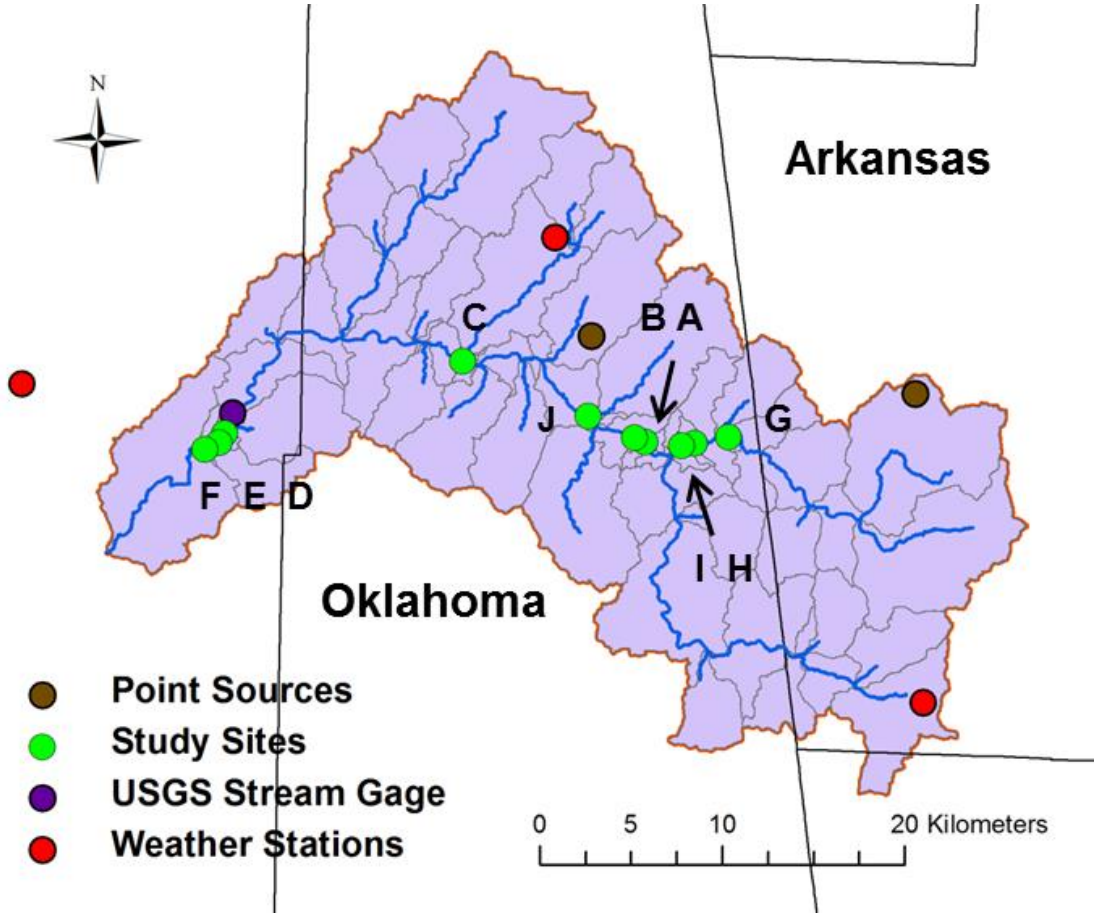

Figure 1.8. United States Geological Survey gage station, weather stations and stream reach study sites for the Barren Fork Creek watershed.

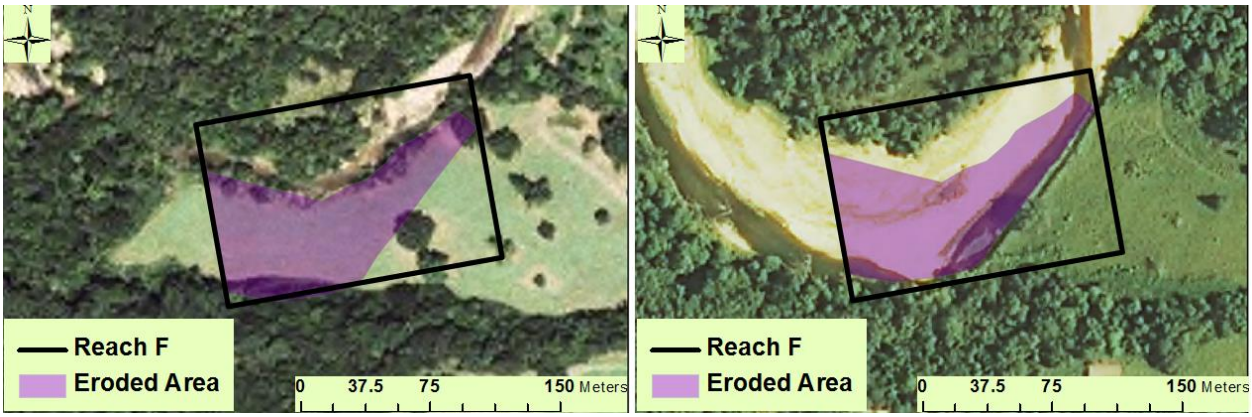

Figure 1.9. 2003 (left) and 2013 (right) National Agricultural Imagery Program aerial images with polygons illustrating the streambank retreat (purple) during the period for study Site F on the Barren Fork Creek.

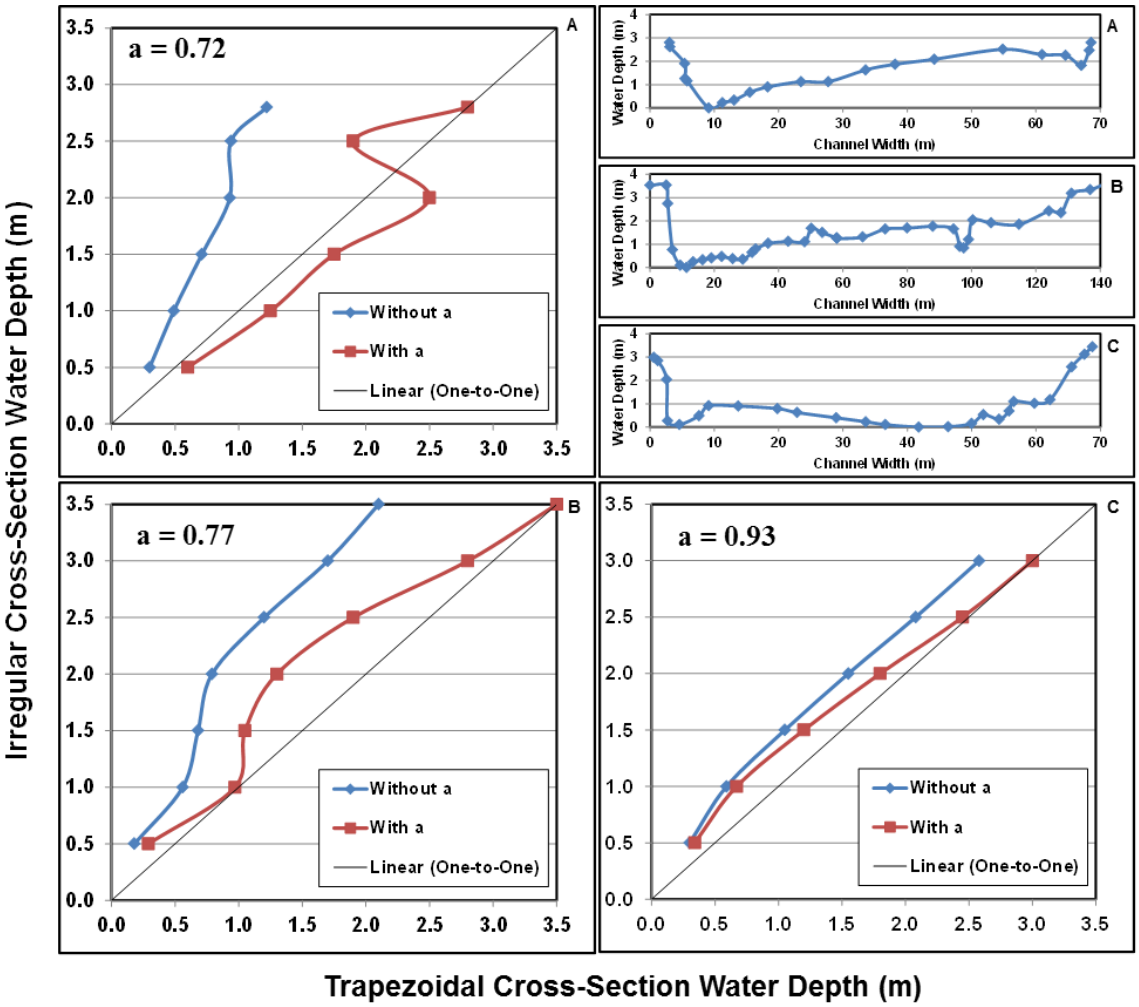

Figure 1.10. FlowMaster-calculated flow depth for the irregular cross-section compared to the trapezoidal cross-section with and without the area adjustment factor (a). Cross-section A is a meander, B is a heterogeneous straight reach and C is a homogenous straight reach.

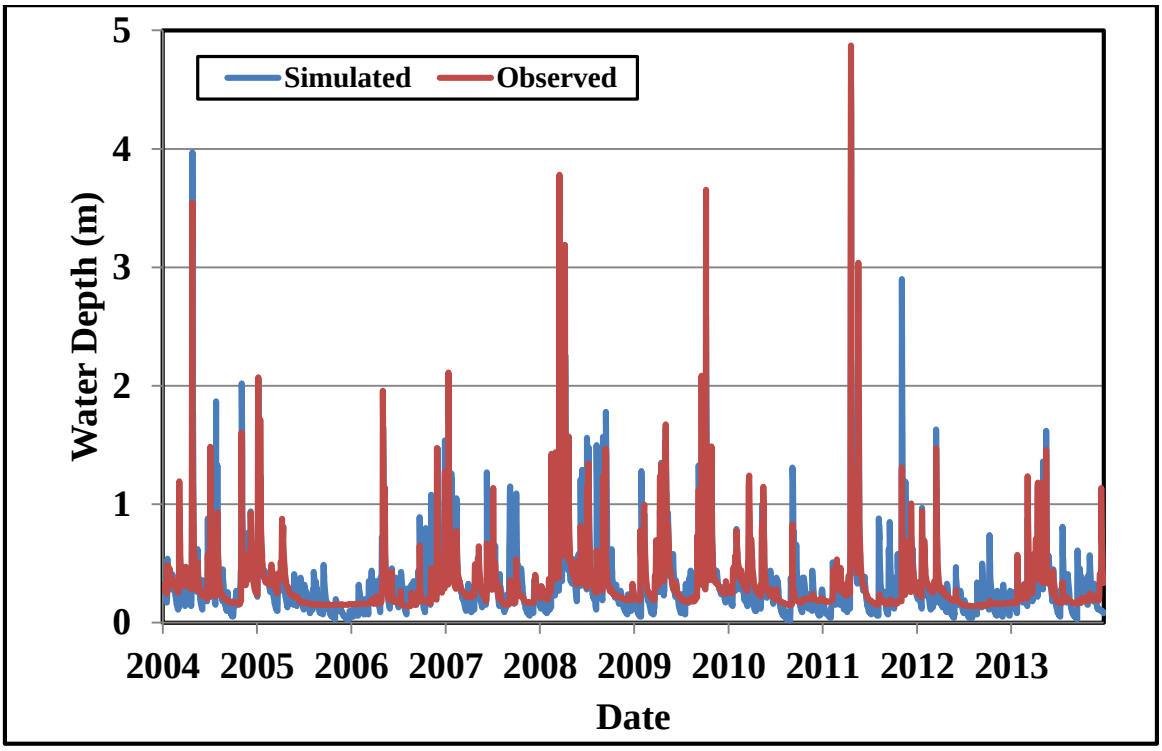

Figure 1.11. Observed and simulated water depth at the United States Geological Survey gage station 07197000 for the period 2004 to 2013.

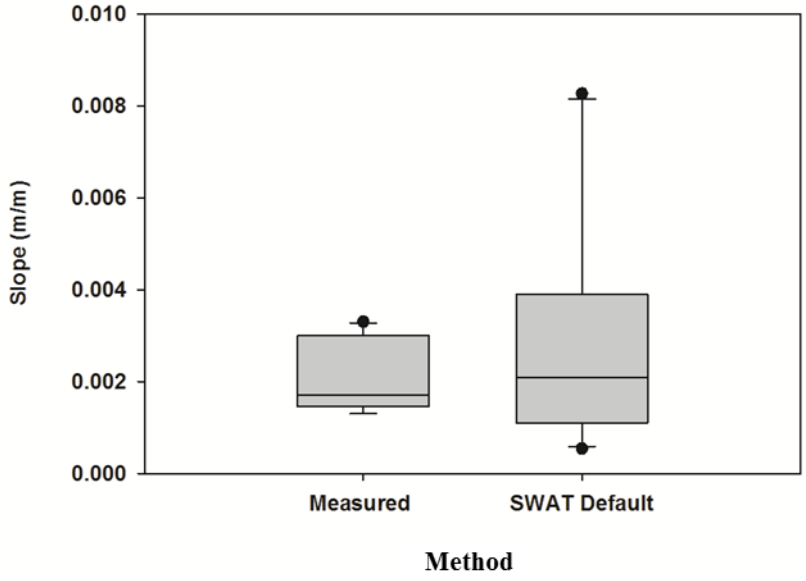

Figure 1.12. Channel bed slope calculated from the topographic map and aerial images (measured) and digital elevation model (SWAT default) for the Barren Fork Creek.

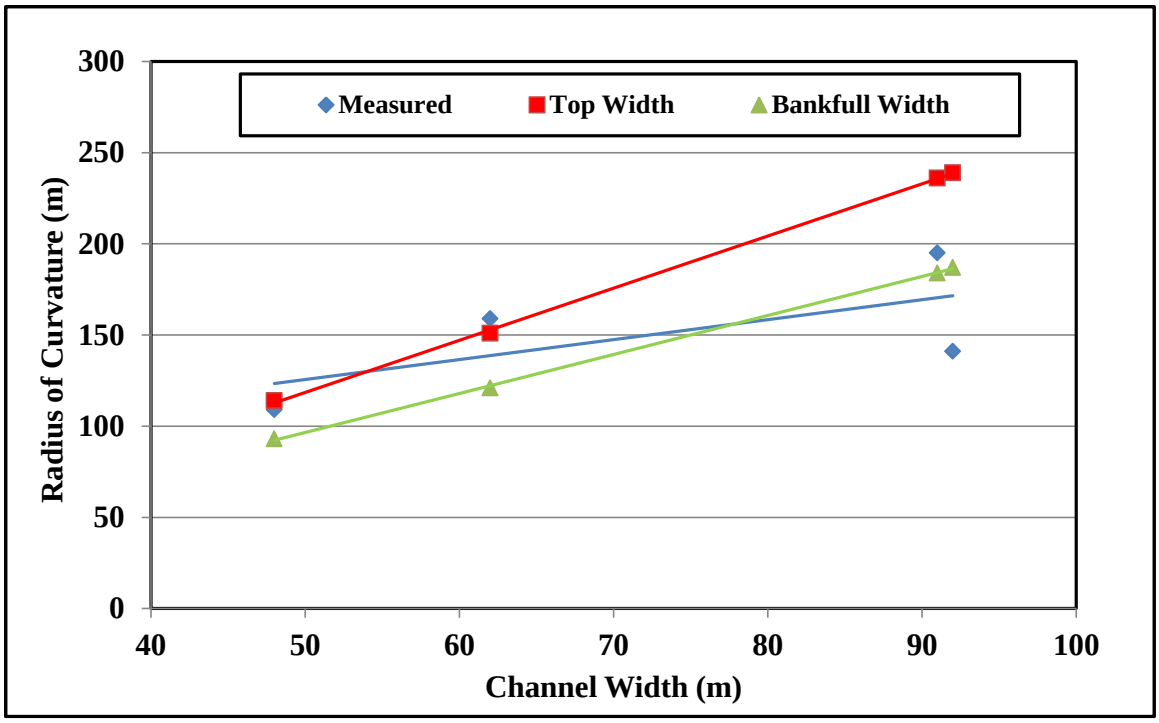

Figure 1.13. Measured and calculated radius of curvature for four reaches with a sinuosity greater than 1.2 on the Barren Fork Creek. The radius of curvature was calculated using Equation 4.9 ($R_c = 1.5*W^{1.12}$), where W is the measured bankfull width or top width.

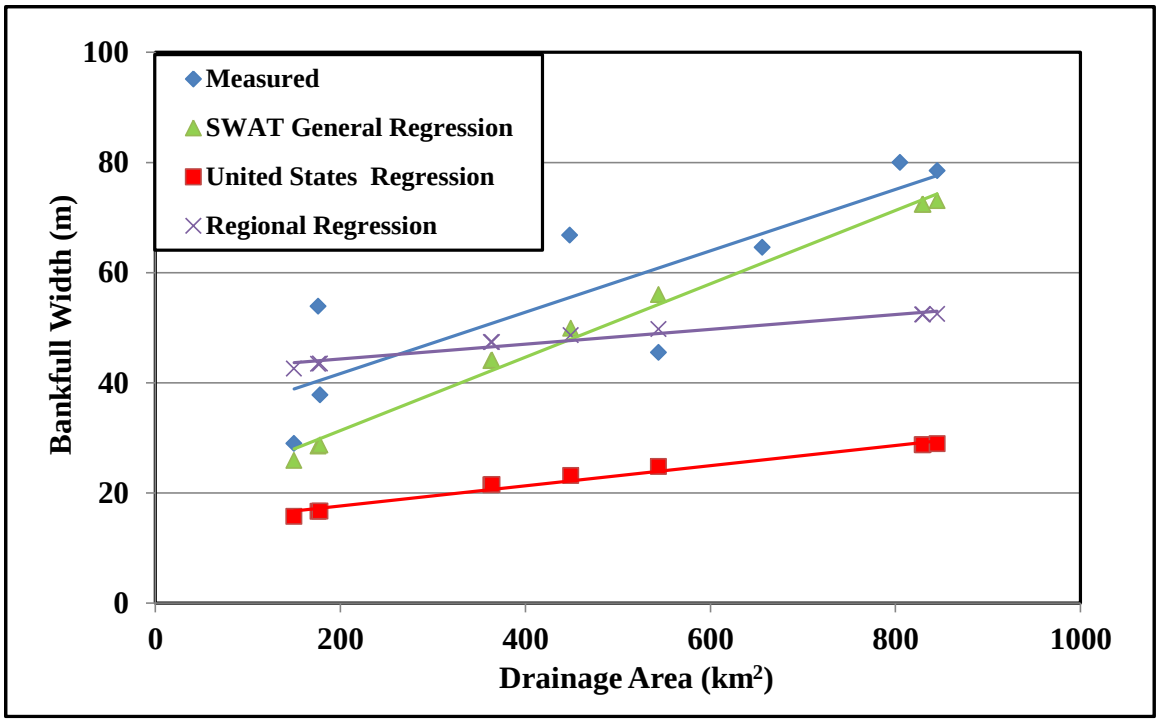

Figure 1.14. Measured bankfull width and calculated bankfull width using three empirical equations vs drainage area for the Barren Fork Creek.

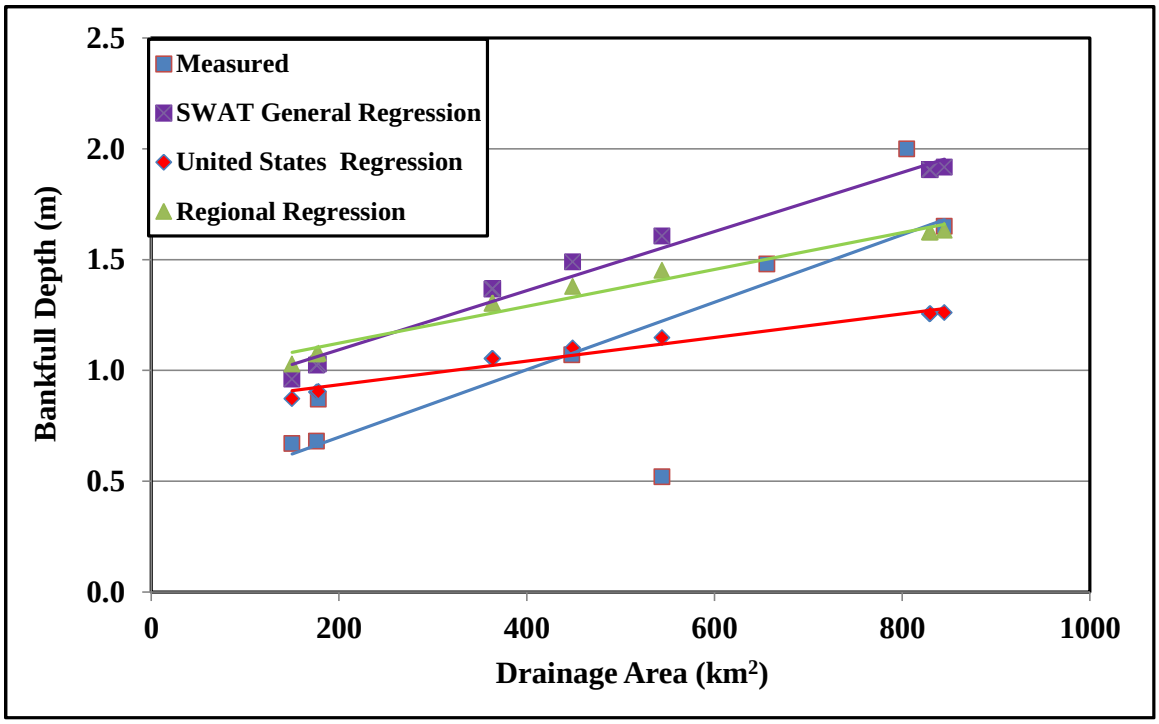

Figure 1.15. Measured bankfull depth and calculated bankfull depth using three empirical equations vs drainage area for the Barren Fork Creek.

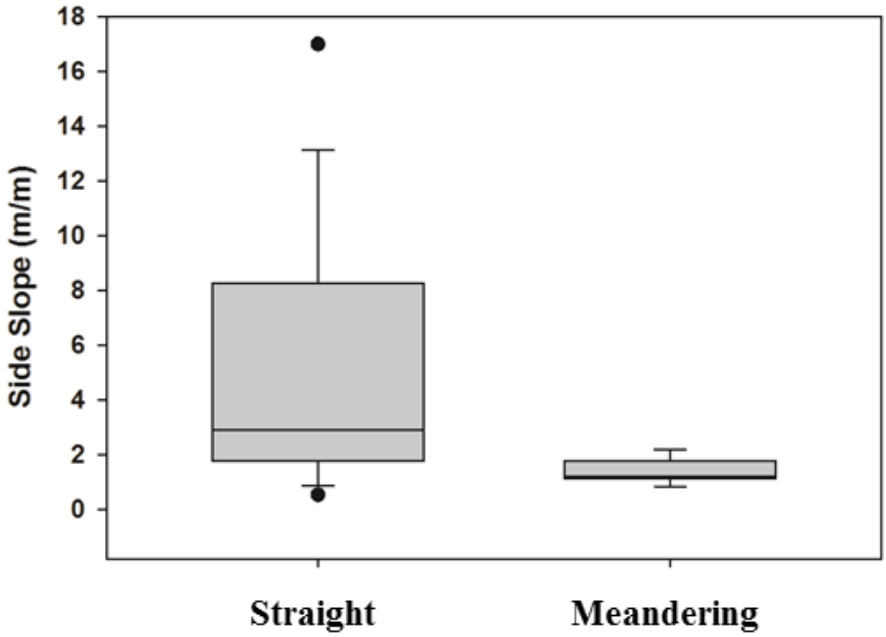

Figure 1.16. Measured side slopes for straight and meandering reaches on the Barren Fork Creek.

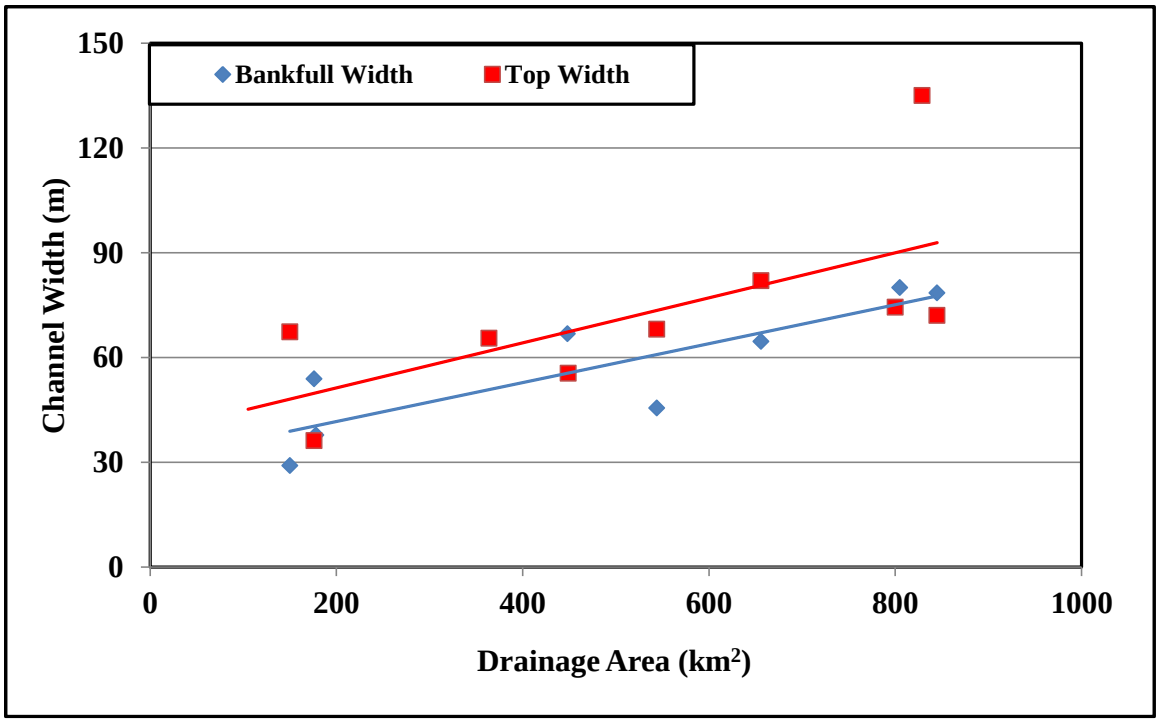

Figure 1.17. Measured straight reach top width and bankfull width for the Barren Fork Creek.

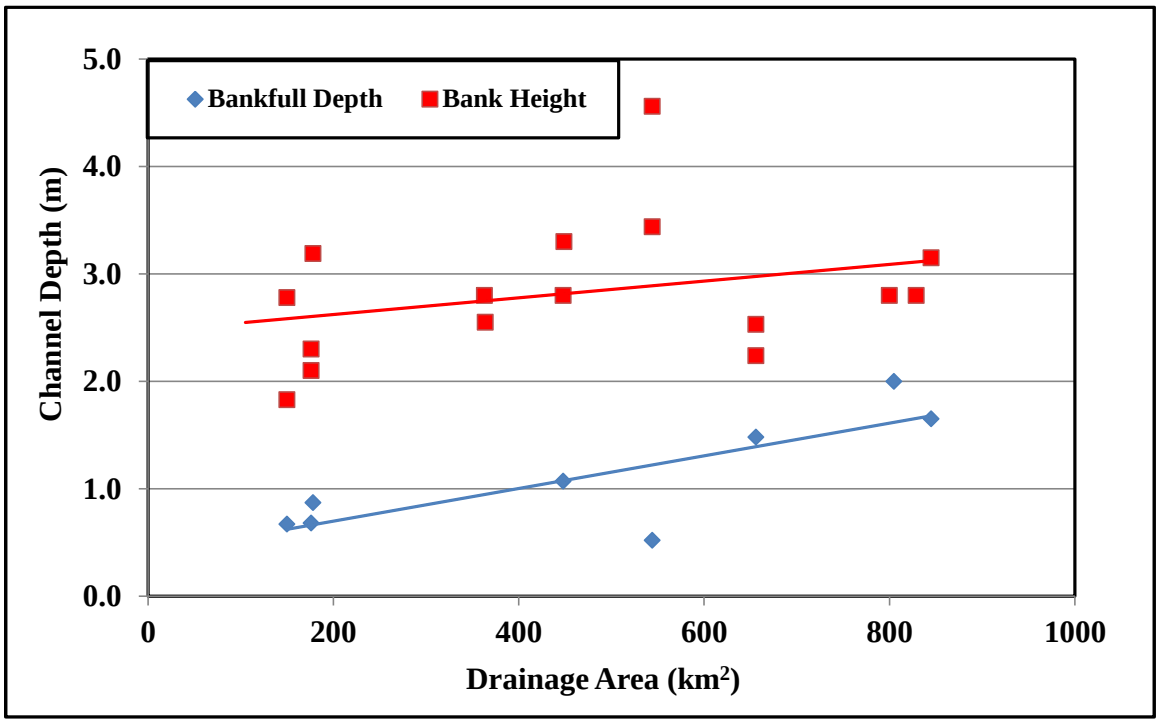

Figure 1.18. Measured straight reach bankfull depth and bank height for the Barren Fork Creek.

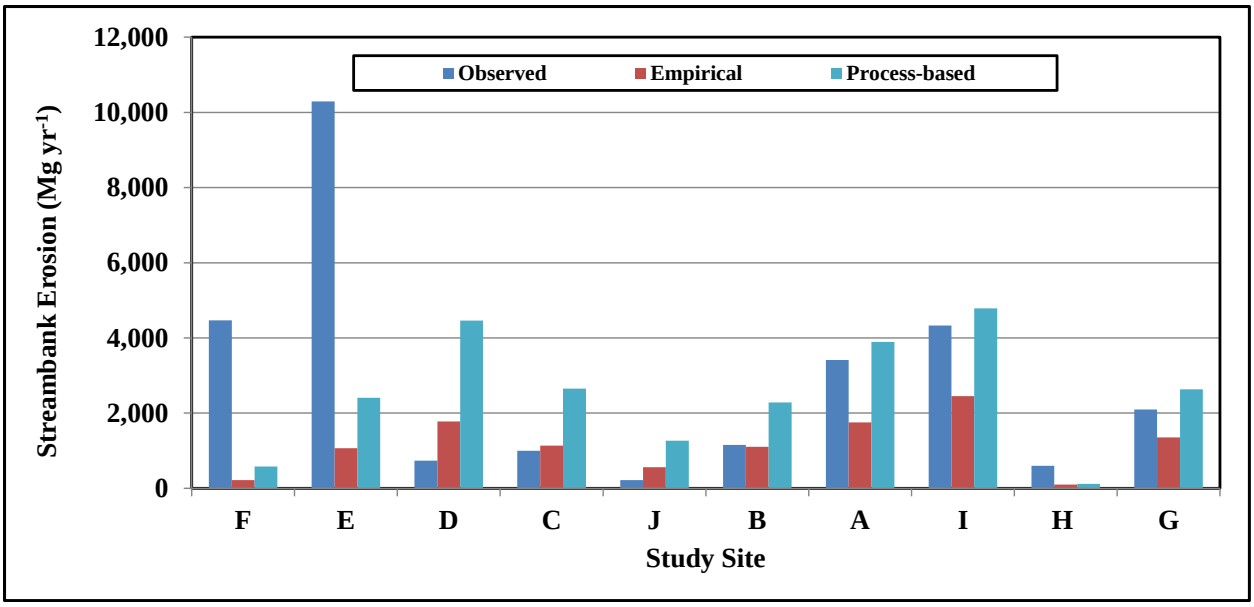

Figure 4.19. Measured and simulated streambank erosion using empirical and process-based applied shear stress equations using the SWAT model with default parameters at ten study sites on the Barren Fork Creek from 2004 to 2013. Empirical is the applied shear stress equation currently used by the SWAT model and process-based is the proposed process-based applied shear stress equation.

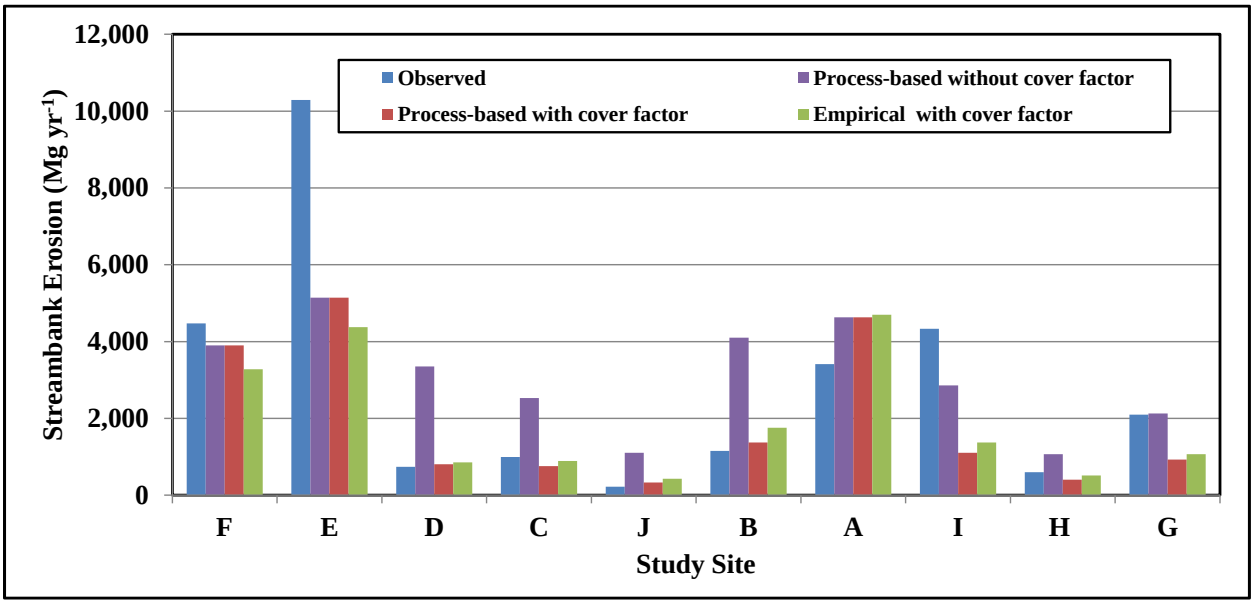

Figure 1.20. Observed streambank erosion compared to SWAT simulated erosion with and without the streambank cover factor for the Barren Fork Creek from 2004 to 2013. Empirical equation is the applied shear stress equation currently used by the SWAT model and process-based is the proposed process-based applied shear stress equation.

Figure 1.21. Streambank erosion at reach I on the Barren Fork Creek from National Agricultural Imagery Program aerial 2003 (left) to 2013 (right) images. The red line is the location of the reach in 2003.

CHAPTER 2

ESTIMATING STREAMBANK EROSION AND PHOSPHORUS LOADS FOR THE BARREN FORK CREEK WATERSHED USING A MODIFIED SWAT MODEL

Abstract

Phosphorus (P) and streambank erosion are problematic in the Barren Fork Creek watershed in northeast Oklahoma and northwest Arkansas. Previous SWAT modeling efforts of the watershed have not accounted for the contribution of stream banks as a P source due to lack of field data and model limitations. This is believed to be the cause for under predicting total and particulate P during large storm events. The objectives of this research were to model the streambank erosion and P for the Barren Fork Creek using a modified SWAT model. Measured streambank and channel parameters were incorporated into a flow-calibrated SWAT model and used to estimate streambank erosion and P for the Barren Fork Creek using the latest streambank-erosion routine and newly incorporated process-based applied shear stress equation. The predicted streambank erosion was 215,000 Mg yr^{-1} versus the measured 160,000 Mg yr^{-1}. Streambank erosion contributed 47% of the total P to the Barren Fork Creek and also improved P predictions compared to observed data, especially during the high flow events. Due to this influx of streambank P to the system and the current in-stream P routine's limitations, the in-stream P routine was modified by introducing a long-term storage coefficient, thus converting some of the particulate P to long-term storage. Of the total P entering the stream system, approximately 65% left via the watershed outlet and 35% was stored in the floodplain and stream system. This study not only provided local, state and federal agencies with accurate estimates of streambank erosion and P contributions for the Barren Fork Creek watershed, it demonstrated how watershed-scale model, such as SWAT, can be used to predict both upland and streambank P.

Introduction

Excess phosphorus (P) and sediment are two major stream and reservoir pollutants. Often non-point sources, such as livestock, urbanization and commercial fertilizer, and point sources are responsible for elevated P and turbidity. Currently, over $3.7 billion is spent in the United States annually on natural resource conservation (Monke and Johnson, 2010; White et al., 2014), with much of this spent on the implementation of conservation practices to reduce the quantity of P and sediment reaching waterways from agricultural activities. White et al. (2014) found that row crops and point sources were the most significant contributors of P reaching the Gulf of Mexico, although in some watersheds, streambanks can contribute up to 80% of the total sediment (Simon et al., 1996) and a significant quantity of total P (Kronvang et al., 2012; Laubel et al., 2003; Langendoen et al., 2012). Conservation practices aimed at reducing

P runoff from agricultural land and point sources will thus be less effective if streambank erosion is not addressed.

One area of concern is the highly-sinuous stream system of the Barren Fork Creek in northeast Oklahoma and northwest Arkansas. The Barren Fork Creek, along with its receiving waterbodies Illinois River and Tenkiller Ferry Lake, are on the Oklahoma 303(d) list of impaired waters due to excess P (DEQ, 2012). In the last sixty years, the once-clear waters have become eutrophic due to pollutant loads from urbanization and livestock production, especially poultry (Cooke et al., 2011). Although tens of millions of dollars have been spent on improving the water quality of one of Oklahoma's few state-designated scenic rivers, most of these monies have been used for the implementation of conservation practices in the upland areas. In previous SWAT modeling efforts of the Illinois River watershed (Storm et al., 2006; Storm et al., 2010; Storm and Mittelstet, 2015), streambank erosion was not addressed due to lack of data and model limitations. Due to the meandering stream system and highly erosive streambanks, P derived from streambank erosion is hypothesized to be the cause for underestimating P during the high flow events. Recent work by Miller et al. (2014) has strengthened this hypothesis. They found that 36% of the streambanks on the Barren Fork were unstable and contribute approximately 90 Mg of TP annually, almost half the total P reaching the watershed outlet.

In the last decade, the streambank-erosion routine in the Soil and Water Assessment Tool (SWAT) (Arnold et al, 1998) has undergone considerable improvements. The latest beta version, previously only tested on cohesive soils in the Cedar Creek watershed in Texas (Narasimhan et al., 2015), uses an excess shear stress equation to calculate the erosion rate, ε (m/s), given as:

$$\varepsilon = k_d(\tau_e - \tau_c) \tag{2.1}$$

where k_d is the erodibility coefficient ($cm^3\ N^{-1}\ s^{-1}$), τ_e is the effective shear stress ($N\ m^{-2}$), and τ_c is the soil's critical shear stress ($N\ m^{-2}$). The k_d and τ_c coefficients are functions of numerous soil properties. Improvements on predicting applied shear stress to streambanks were accomplished by incorporating sinuosity and radius of curvature to account for the effects of meander. Though the current routine uses an empirical equation to estimate the applied shear stress (Eaton and Millar, 2004), Mittelstet (Chapter 1) proposed an alternative process-based equation (USDA-ARS, 2000) for SWAT:

$$\tau = \gamma * R * S_f \tag{2.2}$$

where γ is the specific weight of water (N/m^3), R is the hydraulic radius (m) and S_f is the friction slope (m/m). The friction slope is computed using the following equation:

$$S_f = \frac{n^2 * Q^2}{A^2 * R^{\frac{4}{3}}} \tag{2.3}$$

where Q is the average flow rate (m^3), n is Manning's roughness coefficient and A is the area (m^2).

This study will test and validate this updated routine on a flow-calibrated SWAT model of the Barren Fork Creek watershed. Specifically, the objectives of this study are (1) to predict streambank erosion for the Barren Fork Creek using the proposed streambank-erosion routine (Chapter 1), (2) model P in the watershed with and without incorporating P derived from streambank erosion and (3) determine the significance of streambank erosion relative to upland P sources.

Methods

Study Site

The Barren Fork Creek watershed has a drainage area of 890 km^2 and is composed of approximately 55% forest, 24% well-managed pasture, 6% over-grazed pasture and 13% hay meadow (Storm and Mittelstet, 2015). The Barren Fork Creek, a fourth-order stream, is approximately 73 km in length and is located in the Ozark Highland Ecoregion in northeast Oklahoma and northwest Arkansas (Figure 2.1). The headwaters begin in Washington County, Arkansas, and flow through Adair County, Oklahoma before discharging into the Illinois River in Cherokee County, Oklahoma just north of Tenkiller Ferry Lake. Barren Fork Creek is a State-designated Scenic River and is on the Oklahoma 303(d) list for nutrient and sediment related impairments (USEPA, 2015b). Typical of the Ozark Highland Ecoregion, the watershed is characterized by cherty soils and gravel-bed streams (Heeren et al., 2012). The highly dynamic streambanks consist of alluvial gravel deposits underlying silty loam topsoil (Figure 2.2). The sinuous stream often has a critical bank on the outside of the meander and a gravel bed on the inside bank.

SWAT Model Description

SWAT is a basin-scale hydrological/water-quality model used to predict streamflow and pollutant losses from watersheds composed of mixed land covers, soils and slopes. The model was developed to assist water resource managers to assess water quantity and/or quality in large river watersheds and as a tool to evaluate the impact of agricultural conservation practices. The SWAT model, a product of over 30 years of model development by the US Department of Agriculture Agricultural Research Service, has been extensively used worldwide (Gassman et al., 2007, 2014). The model is process-based and can simulate the hydrological cycle, crop yield, soil erosion, and nutrient transport.

An ArcGIS interface can be used to develop model input of land cover, soils, elevation, weather, and point sources, and define the flow network. The interface divides the watershed into subbasins, which are further split into hydrological response units (HRUs). Each HRU has one soil type, one land use and one slope. The model uses the Modified Universal Soil Loss Equation (MUSLE) to calculate sediment yield for each HRU. This sediment, along with nutrients, are combined for each subbasin and routed through the stream reach. The water and sediment, along with any other pollutants, are routed from reach to reach until arriving at the watershed outlet. Many field-scale activities, such as planting dates, irrigation, fertilization, grazing, harvesting and tillage, are utilized by

SWAT as management options scheduled by date. Further details on the model inputs and the theoretical aspects of hydrology, nutrient cycling, crop growth and their linkages are provided in Neitsch et al. (2009).

This study used SWAT 2012 version 583 and the recently incorporated simplified in-stream P routine (White et al., 2012), which consists of two components. The first component represents the transformation of soluble P to particulate P (i.e. the uptake of soluble P by algae and P precipitation) and its interactions with sediment, which is based on an equilibrium P concentration (EPC). EPC is the concentration at which there is no net sorption or desorption from benthic sediments into the water column. If the EPC is greater than the concentration of soluble P in the water column, P moves from the benthos to the water column; the reverse occurs if the EPC is less than the soluble P. The second component represents the deposition and scour of particulate P (sediment-bound P and algal P) to/from the benthos, which is based on the ratio of flow to bankfull discharge.

SWAT Model Modifications

As Figure 2.3 illustrates, the Barren Fork Creek is very dynamic. Within ten years, sediment was deposited on the gravel bar and the riparian vegetation became fully established (see yellow arrows). Much of eroded particulate P, from both uplands and streambanks, is deposited on the floodplain or within the stream system, particularly on the non-critical bank. Since the water only overtopped its bank a few times from 2004 to 2013, most of the excess P is believed to be stored in the stream system.

A floodplain ratio, currently in the beta version of the streambank-erosion routine (Narasimhan et al., 2015), calculates the sediment and particulate P that settles on the floodplain using:

$$FP_{ratio} = \frac{area_1 - area_2 - area_3}{area_1} \tag{2.4}$$

where FP_{ratio} is a fraction of sediment and particulate P deposited in the floodplain, $area_1$ and $area_2$ are the total and top of the bank submerged cross sectional area (m^2), respectfully, and $area_3$ is the submerged cross sectional area from the top of bank to the total water depth multiplied by the top width (m^2). This equation assumes the velocity and particulate P are uniformly distributed.

The in-stream P routine scours all benthic P during large storm events, although much of the P deposited within the stream system is believed to remain stored in the stream system (Figure 2.3). Thus, in order to simulate the long-term storage of the particulate P, the in-stream P routine was modified.

Two new variables were added to the subroutine, F_{stor} and S_{max}. F_{stor} is the fraction of bankfull flow when P from the benthic pool is converted to long-term P storage, and ranges from 0 to 1. The flow corresponding to long-term P storage, Q_{stor} in $m^3\ s^{-1}$, is calculated using:

$$Q_{stor} = F_{stor} * Q_{bankfull} \tag{2.5}$$

where $Q_{bankfull}$ is the flow when the water reaches the top of the bank ($m^3 s^{-1}$). When the flow exceeds Q_{stor}, a storage ratio, S_{ratio}, is calculated using:

$$S_{ratio} = \frac{Q_{stor}}{Q} \quad (2.6)$$

where Q is the stream flow in $m^3 s^{-1}$. The quantity of P moved from the benthic P storage into the long term P storage is calculated using:

$$P_{lts} = (1 - S_{ratio}) * P_{benthic} \quad (2.7)$$

where P_{lts} is P moved to long term storage (kg), and $P_{benthic}$ in the P stored in the benthic pool (kg). Note that P in long term storage is stored indefinitely. To limit the quantity of P converted to long term storage, S_{max} is the maximum allowable S_{ratio}.

A sensitivity analysis was conducted on F_{stor} and S_{max}. Each parameter was varied from 0.25 to 1.0 and the results compared to the SWAT-predicted total P load without the new parameters, i.e. baseline conditions (Table 2.1). The greatest change occurred when both variables were at 0.25. As F_{stor} increases, more flow is required to convert P to long-term stored P. As S_{max} converges to 1.0, less P is converted to long term stored P.

SWAT Model Setup

The landcover dataset, developed from 2010 and 2011 Landsat images, was used as well as the 10-m USGS DEM and SSURGO soil data. The watershed had minor point sources at Westville, Oklahoma and Lincoln, Arkansas, two United States Geological Survey (USGS) stream gages located near Eldon, Oklahoma and Dutch Mills, Arkansas and three weather stations (Figure 2.4). The two point sources contributed an average of 2.5 kg of dissolved P and 0.63 kg of particulate P daily from 2004 to 2013. Management practices, litter application rates and Soil Test Phosphorus (STP) for each subbasin were obtained from the Illinois River SWAT model. The final SWAT model consisted of 73 subbasins, 2,991 HRUs and eight land uses: forest (55%), well-managed pasture (24%), over-grazed pasture (5.8%) hay meadow (13%) and other (2.2%).

Of the 73 subbasins, 36 were on the Barren Fork Creek. Streambank erosion for tributaries was ignored. Data to characterize each stream reach were obtained from aerial images, topography maps, 28 cross-sectional surveys (Chapter 1) and previous studies (Miller et al., 2014; Narasimhan et al., 2015). These data included bed slope, cover factor, sinuosity, radius of curvature, top width, streambank depth, area-adjustment factor, bank composition, side slope, τ_c , k_d and total and dissolved P. For each measured parameter, the values for each reach were derived either from (1) a longitudinal trend relating the variable to watershed area or distance to confluence with the Illinois River or (2) an average from measured data. The bed slope was measured using National Agricultural Imagery Program (NAIP) images and 1:24,000 topography maps, and used to derive the following equation:

$$BS = 4.3*10^{-9} * DA^2 - 6.7*10^{-6} * DA + 0.00369 \quad (2.8)$$

where *BS* is the bed slope (m m^{-1}) and *DA* is the drainage area (km^2).

Previous streambank modeling results showed that riparian protection significantly impacted the quantity of erosion in the watershed (Daly et al., 2015a; Chapter 1). In Chapter 1, a channel cover factor of 2.0 for the protected sites and a channel cover factor of 1.0 for the unprotected sites were used. Since only a portion of the streambank reaches were protected, a value between 1.0 and 2.0 was assigned to each reach proportional to the percentage of riparian protection (Narasimhan et al., 2015). The critical shear stress was then modified based on the equation proposed by Julian and Torres (2006):

$$\tau_c^* = \tau_c * CH_{\text{cov}} \tag{2.9}$$

where τ_c^* is the effective critical shear stress (N m^{-2}) adjusted for vegetation and CH_{COV} is channel cover factor (Julian and Torres, 2006).

The sinuosity for each reach was calculated by measuring both the stream length and straight-line distance for each reach using NAIP images. Based on the sinuosity, SWAT divided each reach into the fraction of straight (*1/sinuosity*) and meandering (*1*-(*1/sinuosity*)) reach sections. For example, for a 100 m reach with a sinuosity of 1.5, 67% (*1/1.5*) of the reach is defined as straight, or 67 m. The remaining reach section (*1*-(*1/1.5*)) or 33 m would be defined as a meander. Streambank erosion occurs on both banks for the straight reaches, but only one bank for the meandering sections. In this example, streambank erosion would occur on both banks for 67 m of the reach and on one bank for 33 m of the reach. Effective shear stress, calculated from Equations 2.2 and 2.3, is multiplied by a dimensionless bend factor, K_b, (Sin et al., 2012; Narasimhan et al., 2015) for the meandering section of each reach using:

$$K_b = 2.5 * \left(\frac{R_c}{W}\right)^{-0.32} \tag{2.10}$$

$$R_c = 1.5 * W^{1.12} \tag{2.11}$$

where R_c is the radius of curvature (m) and W is the top width (m).

Data from the cross-sectional surveys were used to estimate the *W*, streambank depth, side slope, area-adjustment factor and bank composition for each reach. These data were used with drainage area to derive:

$$W = 0.0765 * DA + 35.6 \tag{2.12}$$

where *W* is top width (m) and *DA* is the drainage area (km^2). Since here was no longitudinal trend, the average side slope (3.1:1) and streambank depth (2.84 m) were used for each reach. Since SWAT assumes a simple trapezoidal channel cross section, an area-adjustment factor was proposed (Chapter 1) to account for the heterogeneous cross-section given as:

$$A_{adj} = a * A \tag{2.13}$$

where A_{adj} is the adjusted channel cross-sectional area (m^2), *a* is a dimensionless adjustment factor less than or equal to 1.0 and *A* is the trapezoidal cross-sectional area. An average *α* of 0.78 was found for the surveyed cross sections (Chapter 1), which signifies that when flow is at the top of the bank, only 78% of the cross-sectional area is submerged**.** The percentage of gravel for each measured bank ranged from 0 to 100% with an average of 62% gravel and 38% cohesive (Figure 2.5).

Streambank data obtained from Miller et al. (2014) included τ_c and total and water soluble P for the soil. There was no longitudinal trend relating the τ_c with the *DA*. Therefore, an average τ_c of 5.6 Pa, a function of the measured d_{50}, was used. The k_d was calculated based on the k_d to τ_c relationship proposed by Hanson and Simon (2001):

$$k_d = 0.2 * \tau_c^{-0.5} \tag{2.14}$$

Although Equation 2.14 was derived using cohesive soils, the equation was successfully used for gravel layers at similar sites by Daly et al. (2015a) and Midgley et al. (2012) and thus will be used in this study. Total P concentrations for the streambanks from Miller et al. (2014) ranged from 250 to 427 mg P kg^{-1} soil, which were similar to Tufekcioglu (2010) (246 to 349 mg P kg^{-1} soil) and Zaimes et al. (2008) (360 to 555 mg P kg^{-1} soil). Water soluble P concentrations ranged from 1.2 to 8.1 mg P kg^{-1} soil. Total and water-soluble P for the streambank soil was obtained using:

$$TP = 1.7546 * d + 249.49 \tag{2.15}$$

$$WSP = 0.1121 * d + 0.3278 \tag{2.16}$$

where *TP* and *WSP* are the total and water soluble P in the streambank (mg P kg^{-1} soil) and *d* is the distance from the confluence of the Illinois River (km) (Figure 2.6). The P concentrations are higher upstream, believed to be a result of the higher density of poultry houses in Arkansas. The quantity of P eroded was adjusted based on the percentage of the bank containing cohesive soil, since gravel was assumed to not contain P.

Model Evaluation

Streamflow

SWAT was manually calibrated for monthly baseflow, peak flow and total flow at the USGS gage stations 07197000 and 07196900. A sensitivity analysis was conducted on eleven parameters based on previously used calibration parameters and SWAT documentation (Neitsch et al., 2009). Parameters were adjusted within the SWAT recommended range. Their sensitivity was calculated and used to determine the influence each parameter had on peak flow and baseflow. The streamflow was calibrated and validated from 2004 to 2013 and 1995 to 2003, respectively. The USGS Hydrograph separation program (HYSEP) was used to estimate baseflow (Sloto and Crouse, 1996).

Coefficient of Determination, R^2, and Nash-Sutcliffe Efficiency (NSE) were used to evaluate the model's performance (Moriasi et al., 2007). Model performance ratings for NSE for total monthly flow were the following: Very good >0.75, Good 0.65-0.75, Satisfactory 0.50-0.65, Unsatisfactory <0.50 (Moriasi et al., 2007).

Phosphorus

The SWAT in-stream P routine was calibrated and validated on a monthly time step from 2009 to 2013 and 2004 to 2008, respectfully, at the USGS gage station 07197000. The USGS gage station 07196900 was not used due to poor LOADEST results (Miller et al., 2014). R^2 and NSE were used to evaluate model performance. Note that the model was calibrated prior to and after the incorporation of the streambank erosion.

Streambank Erosion

Using a method by Heeren et al. (2012) and Miller et al. (2014), streambank erosion was measured using 2003 and 2013 NAIP images for each of the 36 SWAT defined reaches on the Barren Fork Creek (Figure 2.7). The NAIP images were used to estimate the average eroded width and length and then used to calculate the eroded area (*AE*, m^2). The total sediment loading (*TS, kg*) from each reach was calculated using:

$$TS = EA * D_{ts} * \rho_b \tag{2.17}$$

where D_{ts} is the streambank depth (m) from Miller et al. (2014) and Chapter 1, and ρ_b is the soil bulk density (g cm^{-3}). A weighted ρ_b based on the bank composition (Miller et al., 2014) was used to estimate the average ρ_b for the bank.

Results and Discussion

Streamflow

During calibration, six parameters were modified to obtain the best goodness-of-fit statistics for each gage station (Table 2.2). SWAT predictions at USGS gage station 07197000 were 'very good' (Moriasi et al., 2007) for the calibration and validation periods, with NSE of 0.82 and 0.78, respectfully. R^2 for the calibration and validation periods were 0.82 and 0.80, respectfully. At the upstream USGS gage station (0719690), calibration and validation predictions 'good' (Moriasi et al., 2007) based on the NSE of 0.72 and 0.70 for the calibration and validation periods, respectfully. R^2 for the calibration and validation periods were 0.72 and 0.71, respectfully**.**

Total Phosphorus without Streambank Erosion

Each of the in-stream P parameters was manually adjusted during P calibration (Table 2.3). Overall the model performed exceptionally well predicting total P, except for some of the peaks loads (Figure 2.8). During the calibration process, any attempt to increase the predicted total P for the peaks resulted in an over prediction for a number of

smaller events (Figure 2.8, see arrows). For the 2009 to 2013 calibration period, the R^2 was 0.82 and the NSE 0.60. The lower NSE was due to the under prediction of the total P during the large storm event in April 2011. The R^2 and NSE for the 2004 to 2008 validation period was 0.80 and 0.77, respectively. The predicted average annual P load from 2004 to 2013 originating from the uplands was 53.9 Mg yr^{-1}, with 42% from well-managed pasture, 32% from overgrazed pasture, 21% from hay meadows and 5.6% from forest.

Streambank Erosion

The measured streambank erosion for the Barren Fork Creek from 2003 to 2013 was 160,000 Mg yr^{-1}. The reach-weighted streambank erosion was 42 kg m^{-1} compared to 34 kg $m^{-1}$for Spavinaw Creek (Purvis, 2015), approximately 60 km north of the Barren Fork Creek. The Barren Fork Creek streambank erosion increased further downstream as reaches approached the confluence of the Illinois River. For example, the average erosion 0 to 25 km from the confluence with the Illinois River was 78 kg m^{-1}, compared to 28 kg m^{-1} 25 to 65 km from the confluence. Therefore, future streambank stabilization projects should focus their efforts on the lower 25 km of the creek.

The uncalibrated cover factors for the 36 reaches ranged from 1.0 to 2.0 with an average of 1.6 (Figure 2.9). Using these cover factors, the uncalibrated SWAT predictions compared to measured streambank erosion resulted in an R^2 and NSE of 0.36 and 0.33, respectively (Figure 2.10). SWAT simulated mass of eroded soil was 215,000 Mg yr^{-1} or a reach-weighted 40 kg m^{-1} from 2004 to 2013, which compares to the measured erosion of 160,000 Mg yr^{-1} or 42 kg m^{-1}. Some of this over prediction was due to assumptions in estimating the streambank-erosion parameters and failing to account for the armored banks. From personal observations, approximately 5% of the banks are armored, with the majority located in the head waters of the Barren Fork Creek. Armored banks, with a k_d of 0.0 cm^3 N^{-1} s^{-1}, would reduce the simulated erosion by approximately 10,800 Mg yr^{-1} and the relative error for the measured versus simulated erosion from 34 to 27%. SWAT-predicted streambank erosion was then calibrated by adjusting the cover factor, which modified τ_c and k_d. The average calibrated cover factor was 1.9 (Figure 2.9), which equates to τ_c of 11 Pa and k_d of 0.06 cm^3 N^{-1} s^{-1}.

Total Phosphorus with Streambank Erosion

The calibrated streambank erosion contributed a total of 48 Mg yr^{-1} of total P from 2004 to 2013, which is approximately half the total P estimated by Miller et al. (2014). The higher estimate by Miller et al. (2014) was likely due to the ten study sites not being representative of the entire creek. Two of their study sites had the second and third most erosion per length of stream (see ovals in Figure 2.10). The total P from the combined uplands and Barren Fork Creek streambanks from 2004 to 2013 was 103 Mg yr^{-1}, of which 47% originated from streambanks. Langendoen et al. (2012) found that 36% P entering Missisquoi Bay was from streambank erosion. Streambanks in Denmark contributed 21 to 62% of the annual P loads (Kronvang et al., 2012). This study supports other studies around the world that P derived from streambank erosion can be a significant source of P in a watershed. It should be noted that while the quantity of particulate P from

streambank erosion exceeded the particulate P from the upland area, the majority of the dissolved P originated from the upland areas. The dissolved P, which is easily accessible to aquatic plants, is more important to water quality than the tightly-bound particulate P. In addition, the two point sources contributed a small percent of the total P in the watershed (Figure 2.11).

After incorporating streambank-derived P into the SWAT model, the two proposed in-stream P routine variables were calibrated. F_{stor} was calibrated to 0.35 and S_{max} was calibrated to 0.25. If bankfull flow is 1000 m^3 s^{-1}, for example, P will be converted into long-term storage when flow exceeds 350 m^3 s^{-1}. At a flow of 7000 m^3 s^{-1}, 95% of the benthic P is converted to long-term storage. However, S_{max} limits the P converted to long-term storage to 75%.

P calibration improved with streambank erosion compared to without streambank erosion (Table 2.4). The R^2 and NSE improved for both the calibration and validation periods except for the R^2 for the calibration period, which was due to over predicting streamflow and P load in November 2011. The relative errors for total, dissolved and particulate P were all less than 6% for both the calibration and validation periods (Table 2.5). The inclusion of P from streambank erosion also improved the prediction of particulate and total P during large storm events (Figure 2.12), with most of the peaks comparing favorably with observed loads, except for the large storm in 2009.

From 2004 to 2013, approximately 103 Mg yr^{-1} of P entered the Barren Fork Creek from the upland areas, streambank erosion and point sources. Of this total, over 35 Mg yr^{-1} (39 kg yr^{-1} km^{-2}) was converted to long-term storage (Figure 2.13). Mittelstet (2015) estimated the total P stored in the Illinois River watershed at 7.7 to 290 kg yr^{-1} km^{-2} during the period of 1925 to 2015. Based on the results of this study, the total P stored in the Illinois River stream system is probably closer to 7.7 than 290 kg yr^{-1} km^{-2}. During this same time period, 75 kg yr^{-1} km^{-2} of total P left via the watershed outlet to the Illinois River and 1.7 kg yr^{-1} was deposited on the floodplain. A large quantity of P from the benthos was scoured and converted to long-term stored P in 2004. Therefore, the net P added to the benthos was -1.7 kg yr^{-1} km^{-2}. Of the total quantity of P added to the system, approximately 65% left via the outlet and 35% was stored in the stream system and floodplain.

Conclusions

The modified streambank-erosion routine, with the process-based applied shear stress equation and the area-adjustment factor, was applied to the Barren Fork Creek. Uncalibrated, the average reach-weighted predicted streambank erosion from 2004 to 2013 was 40 kg m^{-1} compared to the measured 42 kg m^{-1}. Over 100 Mg of P was added to the Barren Fork Creek annually from 2004 to 2013, of which 47% was from streambank erosion. Due to this influx of streambank P to the system and the current in-stream P routine's limitations, the in-stream P routine was modified by introducing a long-term storage coefficient. This long-term storage coefficient converted particulate P to long-term storage as a function of flow. P calibration with the proposed long-term storage coefficient improved P calibration results, especially for peak flow events. Of the total

quantity of P added to the system from 2004 to 2013, approximately 65% left via the watershed outlet and 35% was stored in the stream system and floodplain. This accumulation of P in the stream system, or legacy P, will likely be a source of P for several years or even decades.

The modified SWAT streambank-erosion routine produced reasonable estimates of streambank erosion. Incorporating particulate P from the streambank erosion can improve SWAT predicted P loads. Streambank erosion can be a significant contributor of P at a watershed scale and thus should be considered when addressing water quality in watershed management plans. For watersheds around the world with dynamic and eroding streambanks with elevated P, the modified streambank erosion and in-stream P routines can be used to improve modeling results and provide watershed managers a better understanding of the significance of both streambank erosion and streambank P in the watershed.

Table 2.1. Sensitivity of instream-phosphorus routine proposed parameters F_{stor} and S_{max} on SWAT predicted total phosphorus load. At baseline F_{stor} and S_{max} are equal to 0.35 and 0.25, respectively.

F_{stor}	S_{max}	Total P (kg yr^{-1})	Percent Change
Baseline	Baseline	101,200	N/A
0.25	0.25	74,200	-26.7
0.50	0.25	83,500	-17.5
0.75	0.25	89,900	-11.2
1.0	0.25	93,100	-8.0
0.35	0.25	78,600	-22.3
0.35	0.50	80,100	-20.8
0.35	0.75	84,200	-16.8
0.35	1.0	101,200	0

Table 2.2. SWAT default and calibrated parameter estimates used to calibrate flow on the Barren Fork Creek watershed SWAT model.

Original Value or Range	Calibrated Value or Range	Parameter	Description
0.95	0.85	ESCO	Soil evaporation compensation coefficient
0.05	0.25	RCHRG_DP	Aquifer percolation coefficient
0.048	0.75	ALPHA_BF	Baseflow Alpha Factor (Days)
39-94	-4	CN2	SCS curve number adjustment
0.0	10	CH_K2	Effective hydraulic conductivity in main channel alluvium (mm hr^{-1})
0.5	105	CH_K1	Effective hydraulic conductivity in tributary channel alluvium (mm hr^{-1})
0.014	0.05	Manning's n	Manning's 'n' in main channel

Table 2.3. SWAT default and calibrated in-stream phosphorus (P) model parameter estimates for the Barren Fork Creek watershed SWAT model.

Parameter	Default	Calibrated	Description
DI	250	90	Period of influence (d)
K_{in}	0.10	0.15	Soluble P transformation into the benthic sediment (hr^{-1})
K_{out}	0.10	0.001	Soluble P transformation out of the benthic sediment (hr^{-1})
F_{dep}	0.01	0.01	Fraction of bankfull discharge at 100% deposition
F_{eq}	0.15	0.26	Fraction of bankfull discharge at which scour and deposition of particulate P is at equilibrium
F_{scr}	0.80	0.75	Fraction of bankfull discharge at which all P is scoured from the streambed
SPT	0.01	0.001	Soluble to particulate transformation coefficient

Table 2.4. Calibration and validation statistics for SWAT predicted total phosphorus load with and without streambank erosion. NSE is Nash Sutcliff Efficiency.

Statistic	Without Streambank Erosion		With Streambank Erosion	
	Calibration	Validation	Calibration	Validation
R^2	0.82	0.80	0.80	0.95
NSE	0.60	0.77	0.78	0.95

Table 2.5. Observed and simulated total, dissolved and particulate phosphorus and their relative errors for the calibration (2009 to 2013) and validation periods (2004 to 2008) with and without streambank erosion.

	Total Phosphorus ($kg\ yr^{-1}$)	Error (%)	Dissolved Phosphorus (kg^{-1})	Error (%)	Particulate Phosphorus (kg^{-1})	Error (%)
Calibration						
Observed	59,500		16,800		42,700	
Simulated	60,000	0.84	16,700	-0.60	43,200	1.2
Validation						
Observed	55,800		18,100		37,700	
Simulated	57,800	3.6	19,100	5.5	38,700	2.7

Figure 2.1. Illinois River and Barren Fork Creek watersheds in northeast Oklahoma and northwest Arkansas.

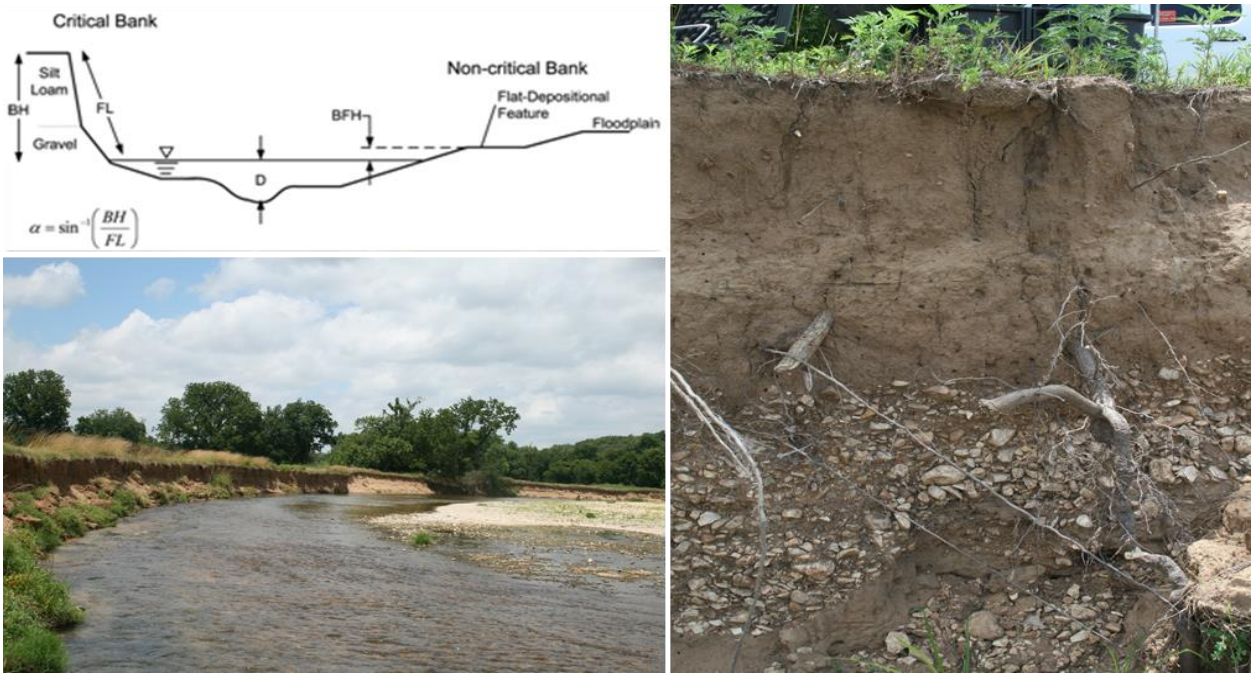

Figure 2.2. Typical stream channel profile in the Barren Fork Creek with one critical bank and one non-critical bank. Right image illustrates the underlying gravel layer and the silty loam topsoil for the critical bank (Heeren et al., 2012).

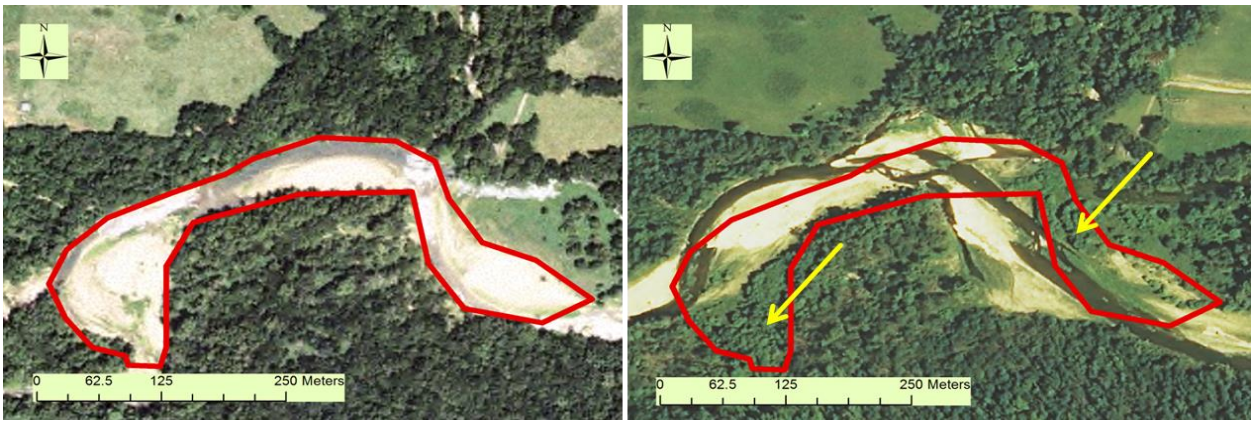

Figure 2.3. Barren Fork Creek reach illustrating the large quantity of streambank erosion and deposition that occurred from 2003 (left) to 2013 (right). Red lines illustrate the location of the gravel bar in 2003 and the yellow arrows show the newly established riparian vegetation.

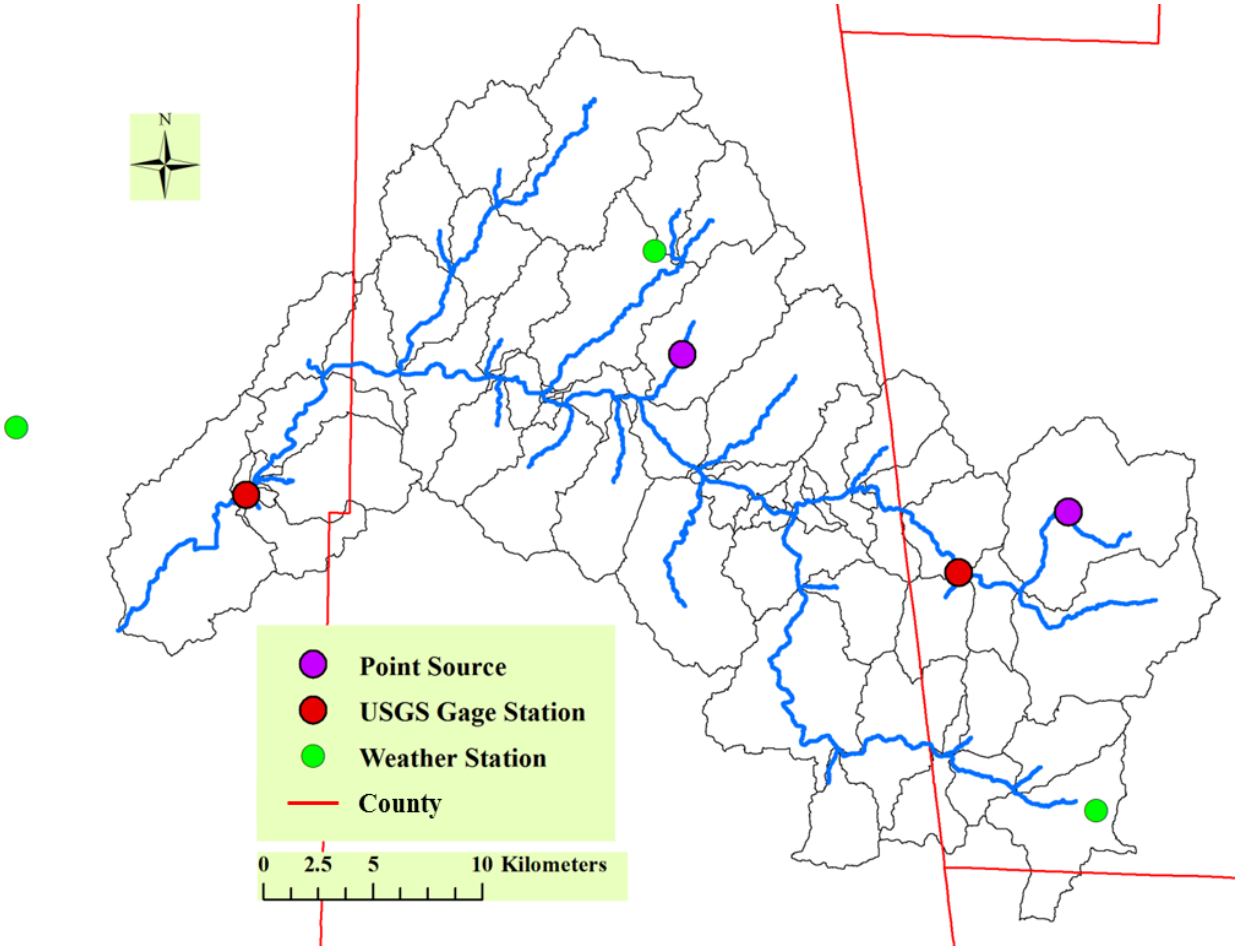

Figure 2.4. United States Geological Survey (USGS) gage stations, weather stations and point sources located in the Barren Fork Creek watershed in northeast Oklahoma and northwest Arkansas.

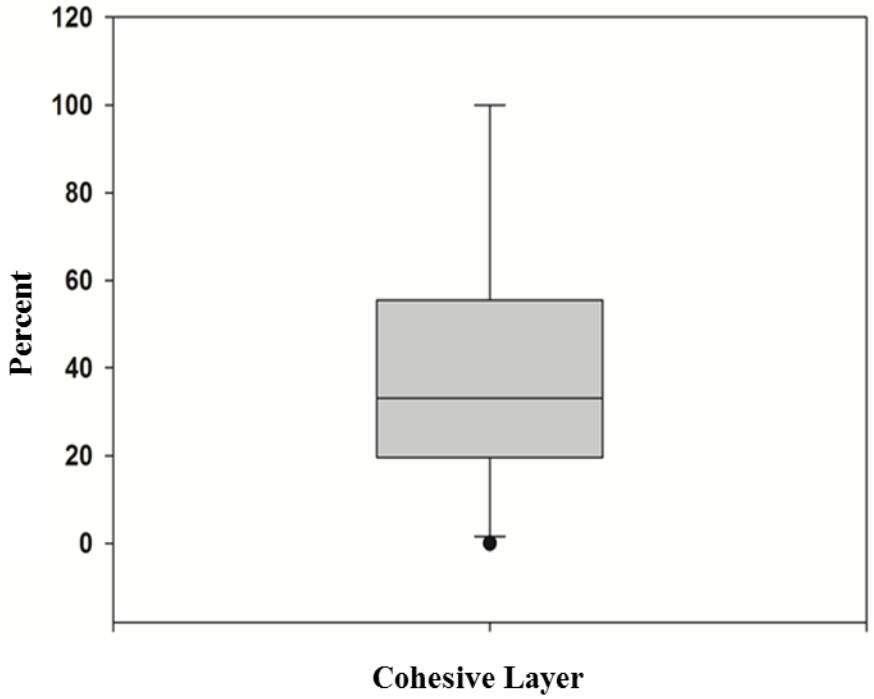

Figure 2.5. Percent cohesive layer for each of the surveyed banks.

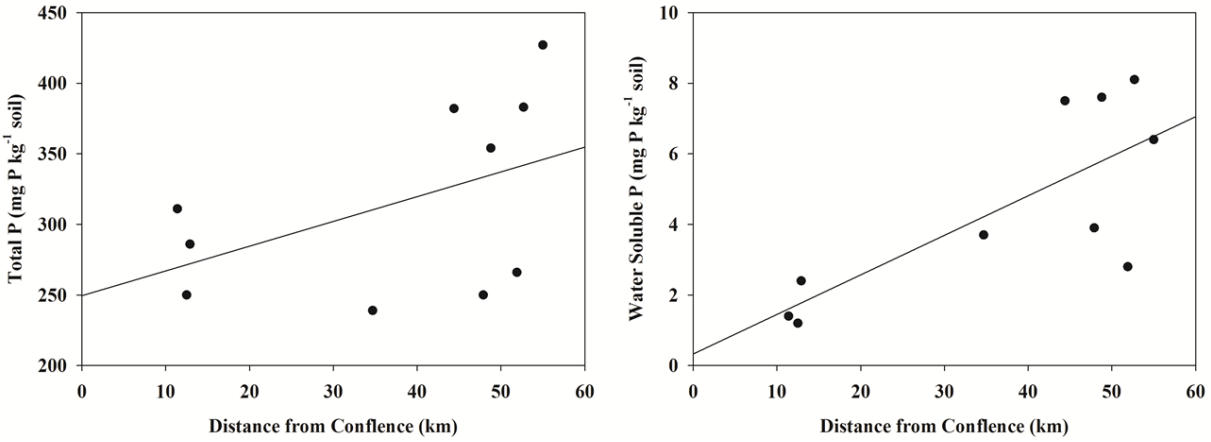

Figure 2.6. Total and water soluble phosphorus (P) concentrations for streambanks with distance from the Barren Fork Creek to the confluence with the Illinois River in Oklahoma.

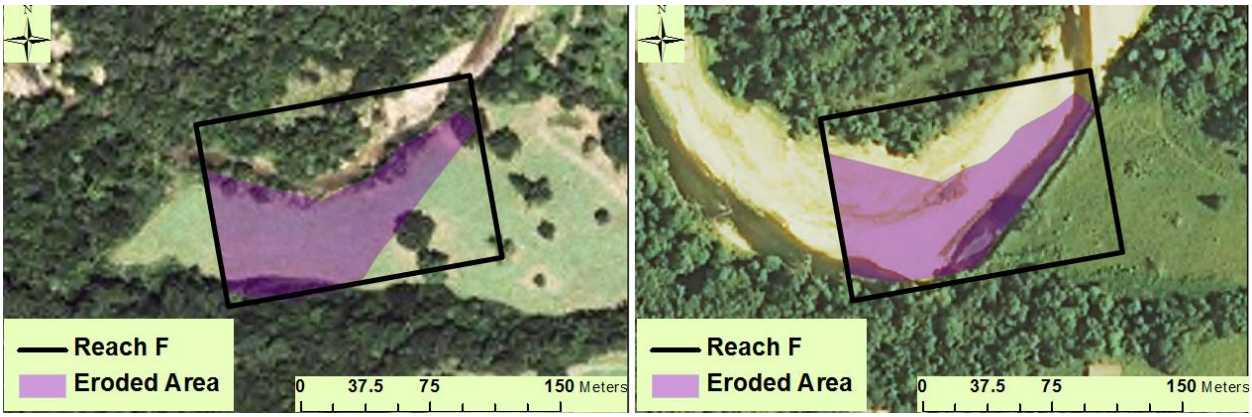

Figure 2.7. National Agricultural Imagery Program (NAIP) aerial images for 2013 (left) and 2013 (right) with polygons showing the bank retreat (purple) during the period.

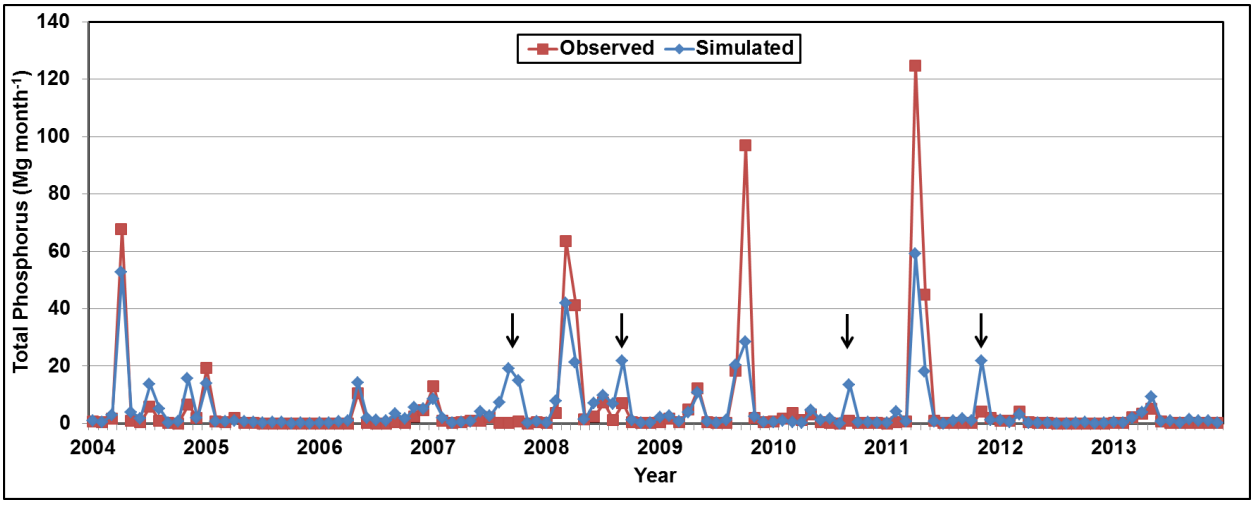

Figure 2.8. Time series illustrating monthly SWAT predicted and observed total phosphorus (P) load from 2004 to 2013 at the United States Geological Survey gage station 07197000 on the Barren Fork Creek. Black arrows indicate storm events where the SWAT model over predicted P.

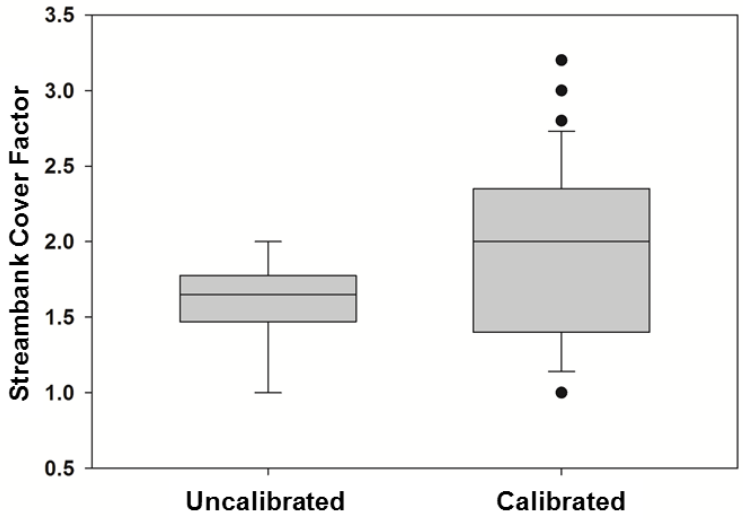

Figure 2.9. Uncalibrated and calibrated cover factors for the 36 reaches on the Barren Fork Creek.

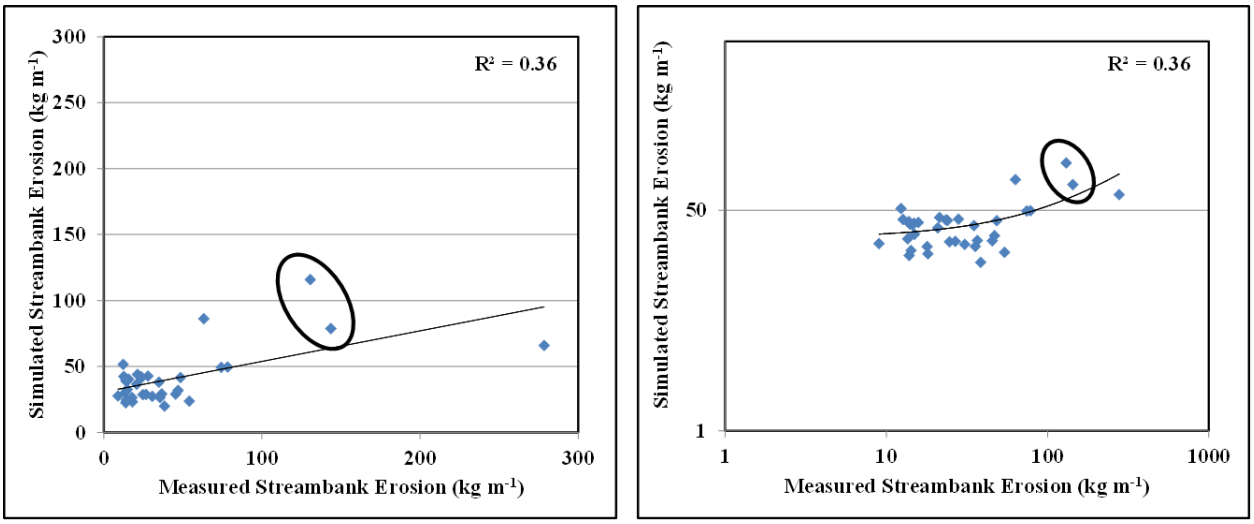

Figure 2.10. Measured vs uncalibrated SWAT streambank erosion predictions for the Barren Fork Creek from 2004 to 2013 on linear (left) and log (right) scales. The two circled points are two of the ten study sites from Miller et al. (2014), which were two of the most erosive reaches of the SWAT-defined 36 reaches on the Barren Fork Creek.

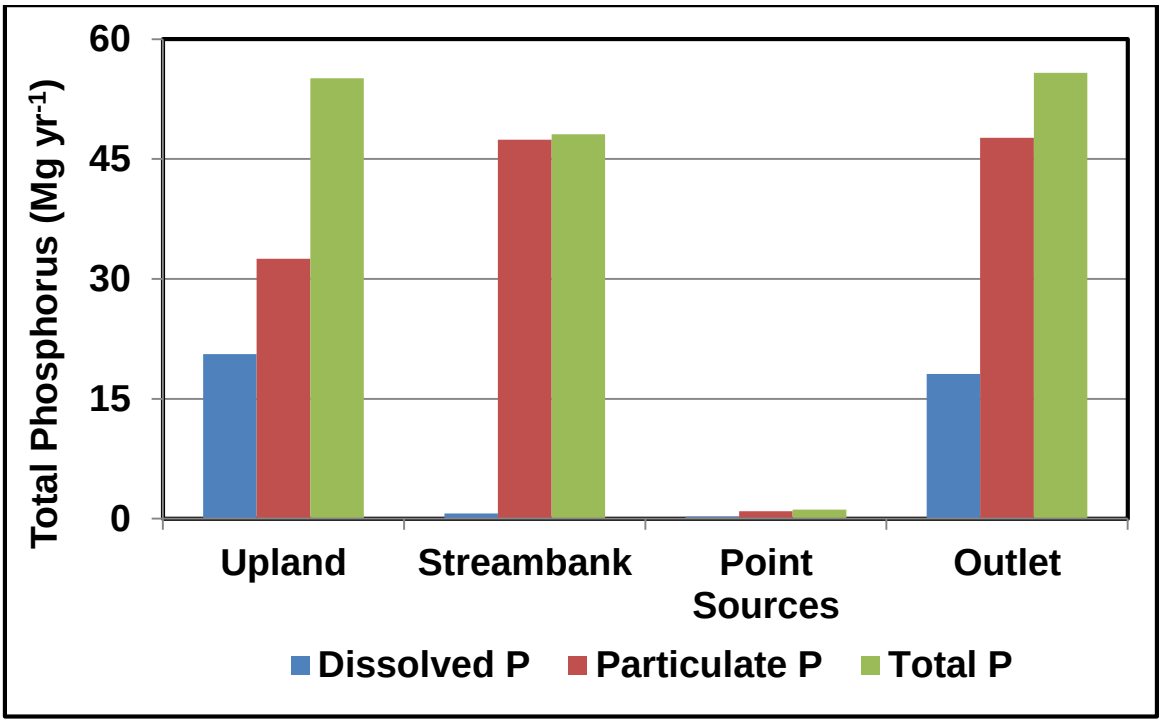

Figure 2.11. Average annual total phosphorus (P) contributions from the Barren Fork Creek watershed upland areas, streambank and point sources compared to the total P load reaching the outlet.

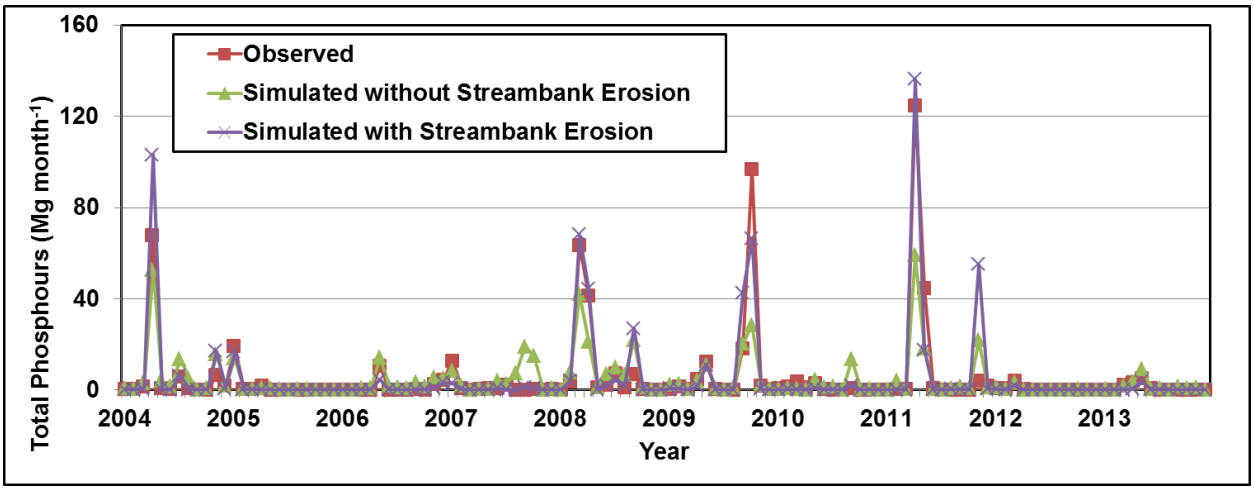

Figure 2.12. Monthly SWAT time series for observed and predicted total phosphorus load from 2004 to 2013 for the Barren Fork Creek watershed with and without streambank erosion.

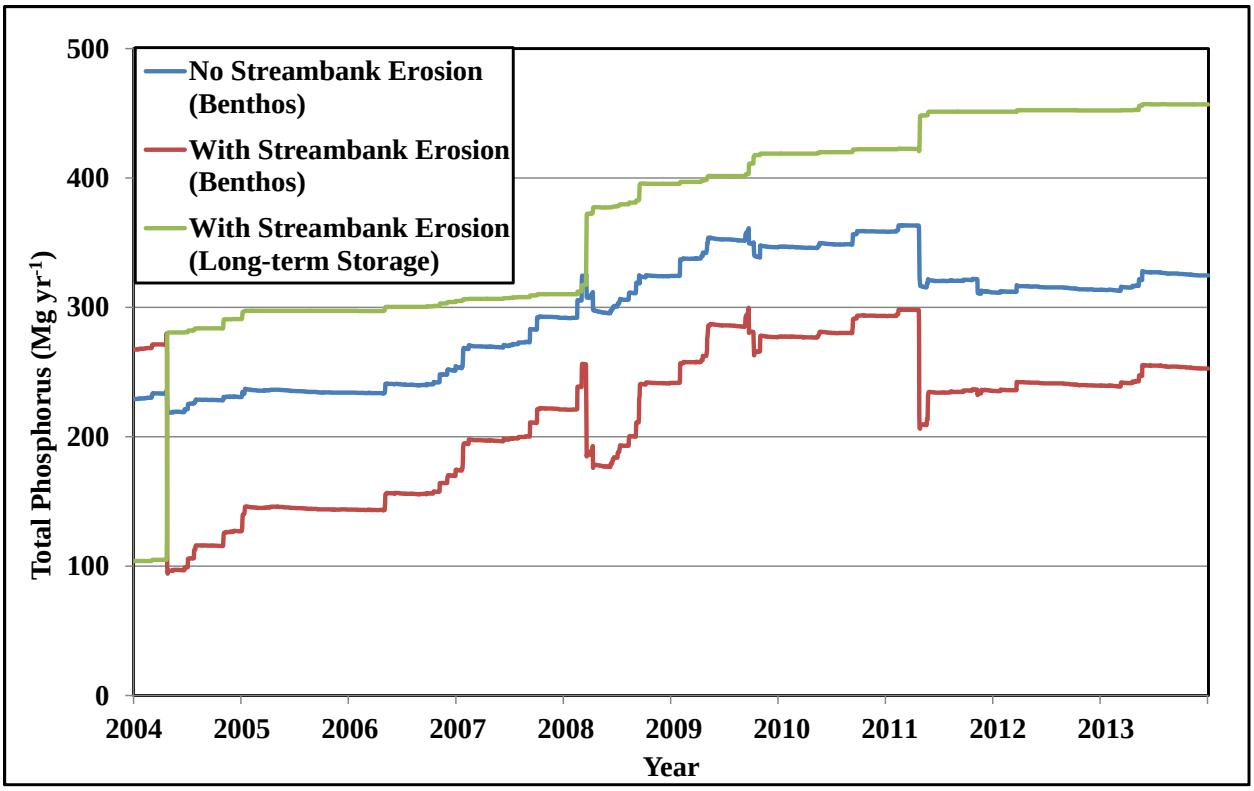

Figure 2.13. Total phosphorus stored in the benthos and long-term storage for SWAT predictions of the Barren Fork Creek from 2004 to 2013 with and without streambank erosion.

REFERENCES

Arnold J.G., R. Srinivasan, R.S. Muttiah and J.R. Williams. 1998. Large-area hydrologic modeling and assessment. Part 1: Model development. *J. Am. Water Resour. Assoc.* 34(1):73-89.

Bentley, 2015. FlowMaster Hydraulic Calculator Software. Available at: https://www.bentley.com/en/products/product-line/hydraulics-and-hydrology-software/flowmaster.

Bieger, K, H. Rathjens, P.M. Allen and J.G. Arnold. 2015. Development and evaluation of bankfull hydraulic geometry relationships for the physiographic regions of the United States. *J. Am. Water Resour. Assoc.* Paper No. JAWRA-13-0228-P.

Chaubey, I., A.S. Cotter, T.A. Costello and T.S. Soerens., 2005. Effect of DEM data resolution on SWAT output uncertainty. *Hydrol. Proc.* 19(3):621-628.

Cooke, D.G., E.B. Welch and J.R. Jones. 2011. Eutrophication of Tenkiller Reservoir, Oklahoma, from nonpoint agricultural runoff. *Lake Reserv. Manage*. 27(3):256-270.

Daly, E.R., G.A. Fox, A.T. Al-Madhhachi and D.E. Storm. 2015b. Variability of fluvial erodibility parameters for streambanks on a watershed scale. *Geomorphology* 231:281-291.

Daniel, T.C., A.N. Sharpley and J.L. Lemunyon. 1998. Agricultural phosphorus and eutrophication; a symposium overview. *J. Environ. Qual*. 27:251-257.

DEQ. Oklahoma Department of Environmental Quality, 2012. Integrated Water Quality Assessment. http://www.deq.state.ok.us/wqdnew/305b_303d/.

Dey, S. Fluvial Hydrodynamics, GeoPlanet: Earth and Planetary Sciences, DOI: 10.1007/978-3-642-19062-9_9, Springer-Verlag Berlin Heidelberg 2014. pp. 529.

Dutnell, R.C., 2004. Development of bankfull discharge and channel geometry relationships for natural channel design in Oklahoma using a fluvial geometric approach. Master's Thesis, University of Oklahoma, Norman, Oklahoma.

Eaton, B.C. and Millar, R.G. 2004. Optimal alluvial channel width under a bank stability constraint. *Geomorphology* 62:35-45.

Fisk, H.N. 1947. Fine-grained alluvial deposits and their effects on Mississippi River activity, Vol. 2. U.S. Army Corps Eng., Waterways Exp. Stn., Vicksburg, 74 plates.

Fox, G. A. and G.V. Wilson. 2010. The role of subsurface flow in hillslope and streambank erosion: A review. *Soil Sci. Soc. Am. J*., 74(3), 717–733.

Friedkin, J.F. 1945. A Laboratory Study of the Meandering of Alluvial Rivers. U.S. Army Corps Eng., Waterways Exp. Stn., Vicksburg, 40 pp.

Gassman, P.W., M.R. Reyes, C.H. Green, and J.G. Arnold. 2007. The Soil and Water Assessment Tool: Historical development, applications, and future research directions. *Trans. ASABE* 50(4):1211-1250.

Gassman, P.W., Balmer C., Siemers M., Srinivasan, R. The SWAT literature database: overview of database structure and key SWAT literature trends. 2014. Available at: https://www.card.iastate.edu/swat_articles/.

Gibson, S. 2013. The USDA-ARS bank stability and toe erosion model (BSTEM) in HEC-RAS. Advances in Hydrologic Engineering. Davis, CA: USACE, Institute for Water Resources, Hydrologic Engineering Center.

Hanson, G.J. and A. Simon. 2001. Erodibility of cohesive sediment in the loess area of the Midwestern USA. *Hydrol. Proc.* 15:23–28.

Harmel, R.D., C.T. Haan, and R.C. Dutnell. 1999. Evaluation of Rosgen's streambank erosion potential assessment in northeast Oklahoma. *J. Am. Water Resourc. Assoc.* 35(1):113-121.

Heeren, D.M., Mittelstet, A.R., Fox, G.A., Storm, D.E., Al-Madhhachi, A.T., Midgley, T.L., Stringer, A.F., Stunkel, K.B. and Tejral R.B. 2012. Using rapid geomorphic assessments to assess streambank stability in Oklahoma Ozark streams. *Trans. ASABE*. 55(3): 957–968.

Johnson, P.A. and T.M. Heil. 1996. Uncertainty in estimating bankfull conditions. *J. Am. Water Resour. Assoc.* 32(6):1283-1291.

Julian, J.P. and R. Torres. 2006. Hydraulic erosion of cohesive river banks. *Geomorphology.* 76:193-206.

Kocian, M.J. Assessing the accuracy of GIS-derived stream length and slope estimates. Master's thesis, University of Minnesota, 2012.

Kronvang, B., J. Audet, A. Baattrup-Pedersen, H.S. Jensen and S.E. Larson. 2012. Phosphorus loads to surface waters from bank erosion in a Danish lowland river basin. *J. Envion. Qual.* 41:304-313.

Langendoen, J., A. Simon, L. Klimetz, N. Bankhead and M.E. Ursic. 2012. Quantifying sediment loadings from streambank erosion in selected agricultural watersheds draining to Lake Champlain. US Department of Agriculture, Agricultural Research Service, National Sedimentation Laboratory, Watershed Physical Processes Research Unit, Oxford, Mississippi.

Laubel, A., B. Kronvang, A.B. Hald and C. Jensen. 2003. Hydromorphological and biological factors influencing sediment and phosphorus loss via bank erosion in small lowland rural streams in Denmark. *Hydrol. Proc.* 17(17):3443-3463.

Merritt, W.S., Letcher, R.A. and Jakeman, A.J. 2003. A review of erosion and sediment transport models. *Environ. Modell. Softw.* 18:761-799.

Micheli, E.R. and J.W. Kirchner. 2002. Effects of wet meadow riparian vegetation on streambank erosion. Measurements of vegetated bank strength and consequences for failure mechanics. *Earth Surf. Process. Landforms* 27:687-697.

Midgley, T.L., G.A. Fox and D.M. Heeren. 2012. Evaluation of the bank stability and toe erosion model (BSTEM) for predicting lateral streambank retreat on composite streambanks. *Geomorphology* 145-146:107-114.

Millar, R.G. 2005. Theoretical regime equations for mobile gravel-bed rivers with stable banks. *Geomorphology* 64(3-4): 207-220.

Miller, R.B., G.A. Fox, C.J. Penn, S. Wilson, A. Parnell, R.A. Purvis and K. Criswell. 2014. Estimating sediment and phosphorus loads from streambanks with and without riparian protection. *Agric. Ecosyst. Environ.* 189:70-81.

Mittelstet, A.R., D.M. Heeren, G.A. Fox, D.E. Storm, M.J. White and R.B. Miller. 2011. Comparison of subsurface and surface runoff phosphorus transport rates in alluvial floodplains. *Agric. Ecosyst. Environ.* 141:417-425.

Monke, J., and R. Johnson. 2010. Actual Farm Bill spending and cost estimates. Rep. Congr. 7-5700/R41195. Congr. Res. Serv. Washington, DC. http:// www.nationalaglawcenter.org/assets/crs/R41195.pdf

Moriasi, D.N., J.G. Arnold, M.W. Van Liew, R. L. Bingner, R.D. Harmel and T.L. Veith. 2007. Model evaluation guidelines for systematic quantification of accuracy in watershed simulations. *Trans. ASABE* 50(3):885-900.

Narasimhan, B., P. Allan, L. Arnold and R. Srinivasan. 2015. Development and testing of a physically based model of stream bank erosion for coupling with a basin-scale hydrologic model SWAT. *Hydro. Proc.* In Reviw.

Nash, J. E., and J. V. Sutcliffe. 1970. River flow forecasting throughconceptual models: Part 1. A discussion of principles. *J. Hydrology* 10(3):282-290.

Neitsch, S.L., J.G. Arnold, J.R. Williams. 2011. Soil and Water Assessment Tool User's Manual Version 2009. Blackland Research Center.

Partheniades, E. 1965. Erosion and deposition of cohesive soils. *J. Hydraul. Div.* ASCE. 91:105-139.

Purvis, R. *Sediment and phosphorus loads from streambank erosion and failure: a source of legacy phosphorus in watersheds*. Master's Thesis, Oklahoma State University. Stillwater, Oklahoma, 2015.

Simon, A., M. Rinaldi, and G. Hadish, 1996 Channel evolution in the loess area of the midwestern United States. Sixth Federal Interagency Sedimentation Conference, Las Vegas, pp III-86 to iIII-93.

Simon, A., and S.E. Darby. 1999. The nature and significance of incised river channels, In *Incised River Channels*, 3-18. S.E. Darby and A. Simon, eds. Chichester, UK: John Wiley and Sons.

Simon, A., R. L. Bingner, E. J. Langendoen, and C. V. Alonso. 2002. Actual and reference sediment yields for the James Creek Watershed, Mississippi. USDA Agricultural Research Service National Sedimentation Laboratory Research Report No. 31.

Sin, K. C.I. Thornton, A.L. Cox and S.R. Abt. 2012. Methodology for calculating shear stress in a meandering channel. Colorado State University, Fort Collins, Colorado.

Sloto, R.A. and M.Y. Crouse. 1996. HYSEP: A computer program for streamflow hydrograph separation and analysis: U.S. Geological Survey Water-Resources Investigations Report 96-4040, 46 p.

Staley, N.A., T. Wynn, B. Benham and G.Yagow. 2006. Modelling channel erosion at the watershed scale: Model review and case study. Center for TMDL and Watershed Studies, Biological Systems Engineering, Virginia Tech.

Soil Survey Staff, Natural Resources Conservation Service, United States Department of Agriculture. Soil Survey Geographic (SSURGO) Database. Available online at http://sdmdataaccess.nrcs.usda.gov/. Accessed May 10, 2012).

Storm, D.E., M.J. White and M.D. Smolen. 2006. Illinois River upland and in-stream phosphorus modeling: Final Report submitted to the Oklahoma Department of Environmental Quality. Submitted June 28, 2006. Oklahoma State University, Department of Biosystems and Agricultural Engineering, Stillwater, Oklahoma 74078.

Storm, D.E., P.R. Busteed, A.R. Mittelstet and M.J. White. 2010. Oklahoma/Arkansas Illinois river basin using SWAT 2005: Final Report submitted to the Oklahoma Department of Environmental Quality. Submitted October 8, 2009. Oklahoma State University, Department of Biosystems and Agricultural Engineering, Stillwater, Oklahoma 74078.

Storm, D.E. and A.R. Mittelstet. 2015. Watershed Based Plan Support for the Illinois River and Spavinaw Creek Watersheds. DRAFT FINAL REPORT. Oklahoma Conservation Commission for the US EPA Region VI. Oklahoma State University, Department of Biosystems and Agricultural Engineering, Stillwater, Oklahoma 74078.

Tufekcioglu, M. 2010. Stream bank soil and phosphorus losses within grazed pasture stream reaches in the Rathbun Watershed in southern Iowa. Ph.D. Dissertation, Iowa State University, Ames, Iowa.

USDA ARS, 2013. Bank Stability and Toe Erosion Model Homepage. USDA Agricultural Research Service National Sedimentation Laboratory. Oxford, MS. http://www.ars.usd.gov/research/docs.htm?docid=5044. Accessed September 12, 2014.

USDA ARS, 2000. CONCEPTS – Conservational Channel Evolution and Pollutant Transport System. USDA Agricultural Research Service National Sedimentation Laboratory. Oxford, MS. http://www.ars.usd.gov/research/docs.htm?docid=5044. Accessed July 21, 2015.

USEPA, 2015a. National Summary of Impaired Waters and TMDL Information. U.S. Environmental Protection Agency. Available at: http://iaspub.epa.gov/waters10/attains_nation_cy.control%3Fp_report_type=T.

USEPA, 2015b. Progress towards Adopting Total Nitrogen and Total Phosphorus Numeric Water Quality Standards. Environmental Protection Agency. Available at: http://www2.epa.gov/nutrient-policy-data/progress-towards-adopting-total-nitrogen-and-total-phosphorus-numeric-water.

USGS, 2004. Determination of channel-morphology characteristics, bankfull discharge, and various design-peak discharges in western Montana. U.S. Department of the Interior. U.S. Geological Survey: Available at http://pubs.usgs.gov/sir/2004/5263/pdf/sir_2004_5263.pdf. Accessed on September March 10, 2015.

Walling, D.E., P.N. Owens and G.J.L. Leeks. 1999. Fingerprinting suspended sediment sources in the catchment of the River Ouse, Yorkshire, UK. *Hydro. Proc.* 13(7):955-975.

Wechsler, S. P. 2007. Uncertainties associated with digital elevation models for hydrologic applications: a review. *Hydrol. Earth Syst. Sci*. 11:1481-1500.

Williams, G.P. 1986. River meanders and channel size. *J. Hyrol.* 88:147-164.

White, M.J., C. Santhi, N. Kannan, J.G. Arnold, D. Harmel, L. Norfleet, P. Allen, M. DiLuzio, X. Wang, J. Atwood, E. Haney and M. Vaughn Johnson. 2014. Nutrient delivery from the Mississippi River to the Gulf of Mexico and effects of cropland conservation. *J. Soil Water Conserv.* 69(1):26-40.

Wilson, C. G., R. A. Kuhnle, D. D. Bosch, J. L. Steiner, P. J. Starks, M. D. Tomer, and G. V. Wilson. 2008. Quantifying relative contributions from sediment sources in Conservation Effects Assessment Project watersheds. *J. Soil Water Conserv.* 63(6):523-531.

Zaimes, G.N., R.C. Schultz, and T.M. Isenhart. 2008. Total phosphorus concentrations and compaction in riparian areas under different riparian land-uses of Iowa. *Agric. Ecosyst. Environ*. 127:22-30.

APPENDIX A

BARREN FORK CREEK CROSS SECTIONS

A total of 28 cross-sections were surveyed on the Barren Fork Creek using a laser level, measuring tape and survey rod: eight at cross-over points, nine at meanders and eleven at straight cross sections (Figure A.1). These data were then used to derive regression equations or averages for each of the streambank parameters used in the SWAT model.

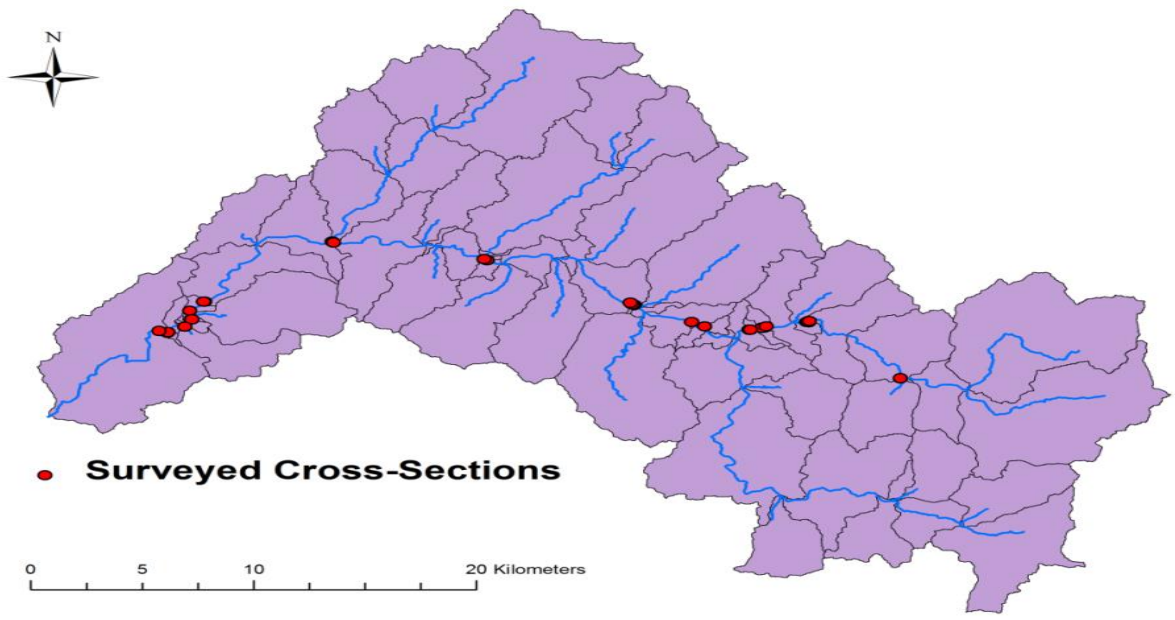

Figure A.1. Locations of the 28 cross sections surveyed on the Barren Fork Creek.

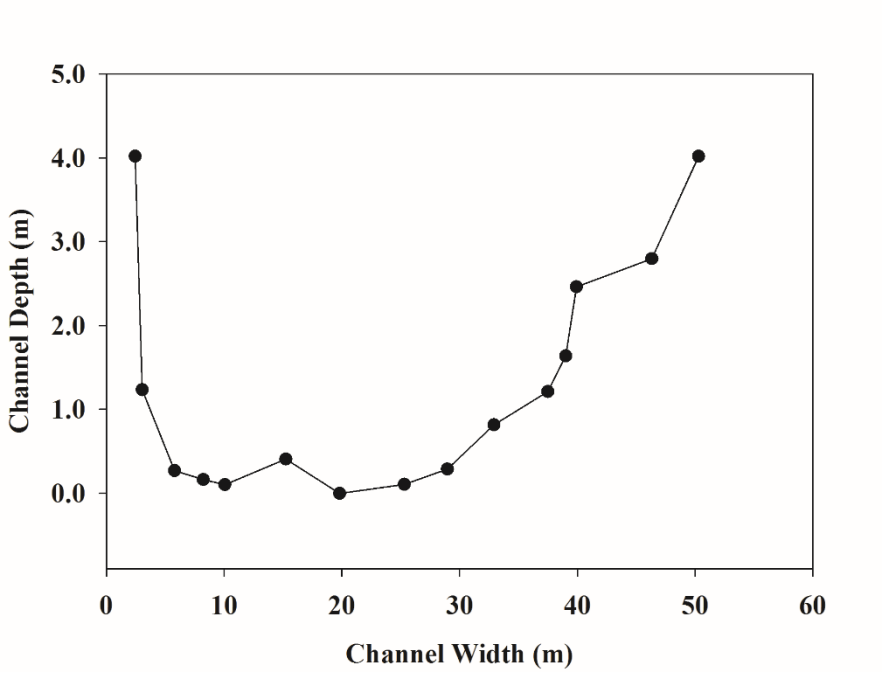

Figure A.2. Cross-sectional survey located on a straight reach at the U.S. Geological Survey gage station near Dutch Mills, Arkansas (365480 N, 3971663 E) on the Barren Fork Creek.

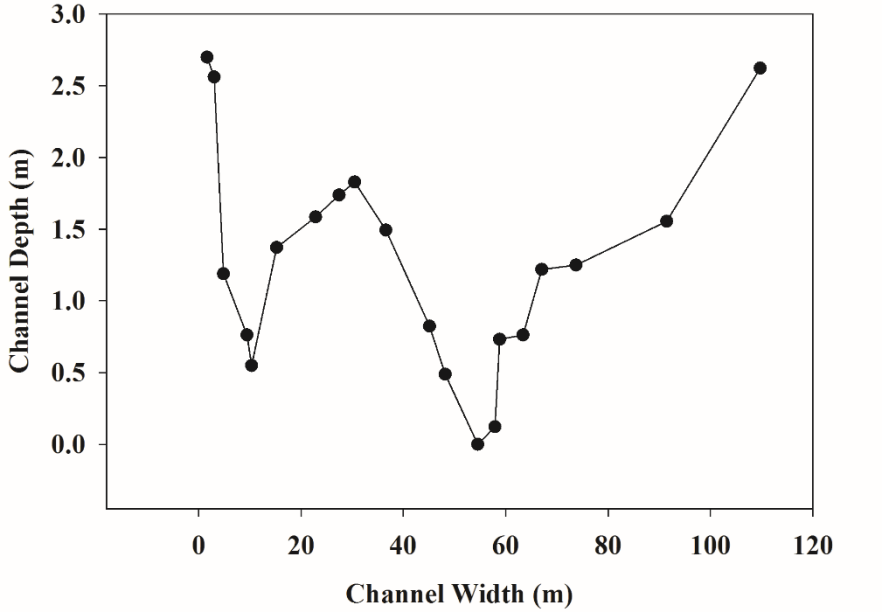

Figure A.3. Cross-sectional survey located on a straight reach at 361417 N, 3975506 E on the Barren Fork Creek.

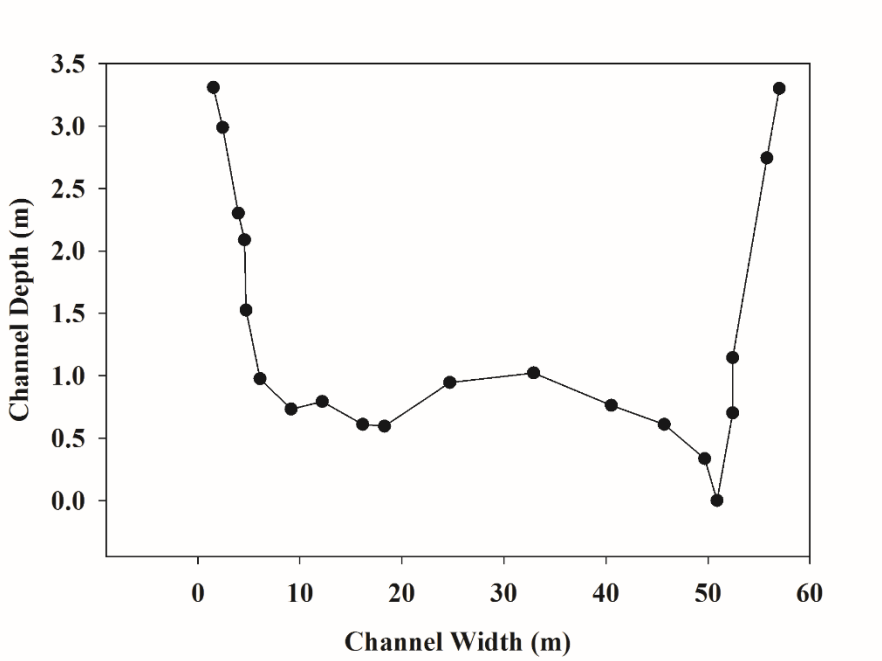

Figure A.4. Cross-sectional survey located at a cross-over at 361364 N, 3975435 E on the Barren Fork Creek.

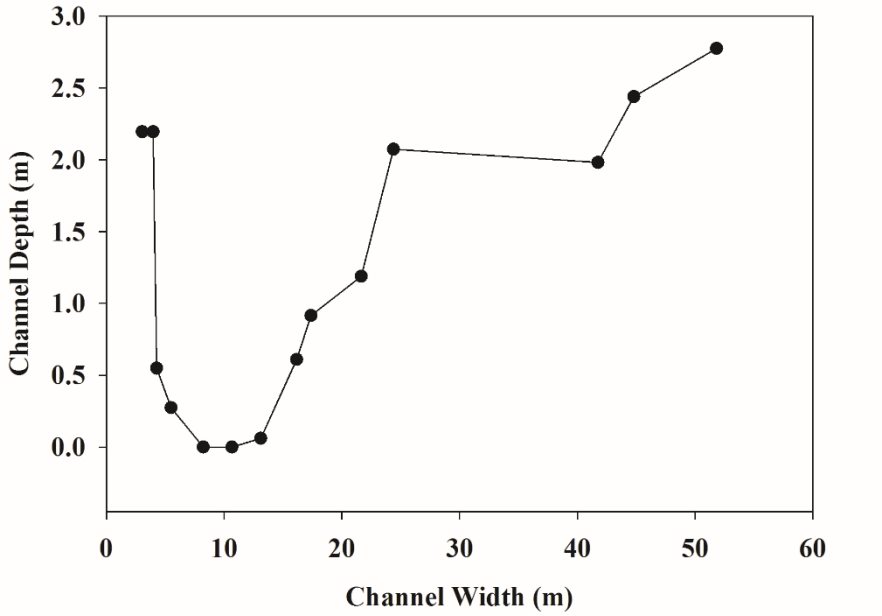

Figure A.5. Cross-sectional survey located on a meander at 361272 N, 3975458 E on the Barren Fork Creek.

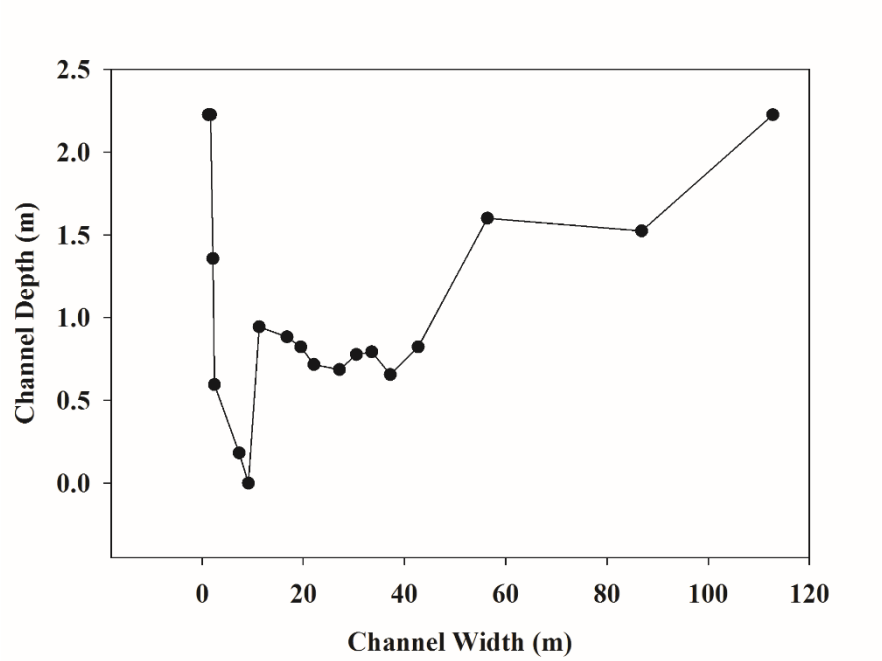

Figure A.6. Cross-sectional survey located at a cross-over at 359447 N, 3975165 E on the Barren Fork Creek.

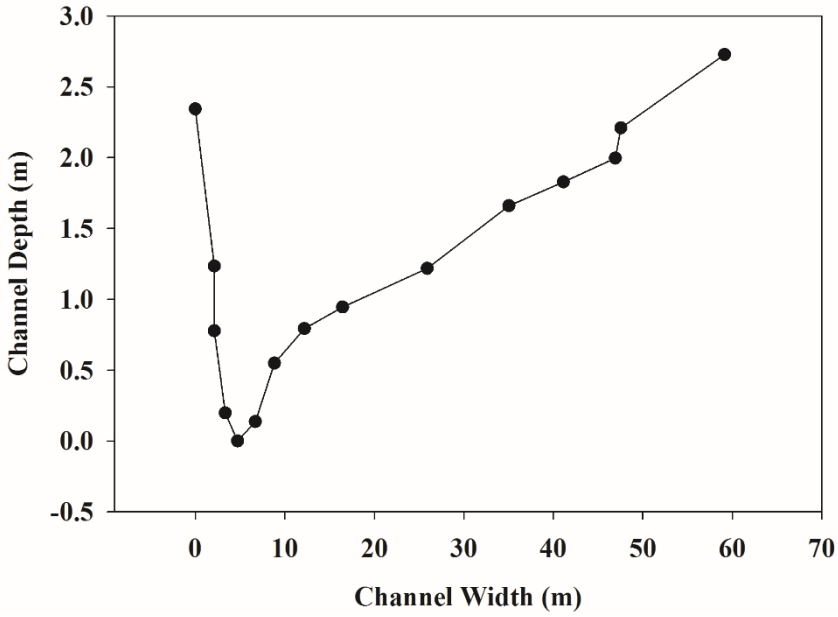

Figure A.7. Cross-sectional survey located on a meander at 3594405 N, 3975097 E on the Barren Fork Creek.

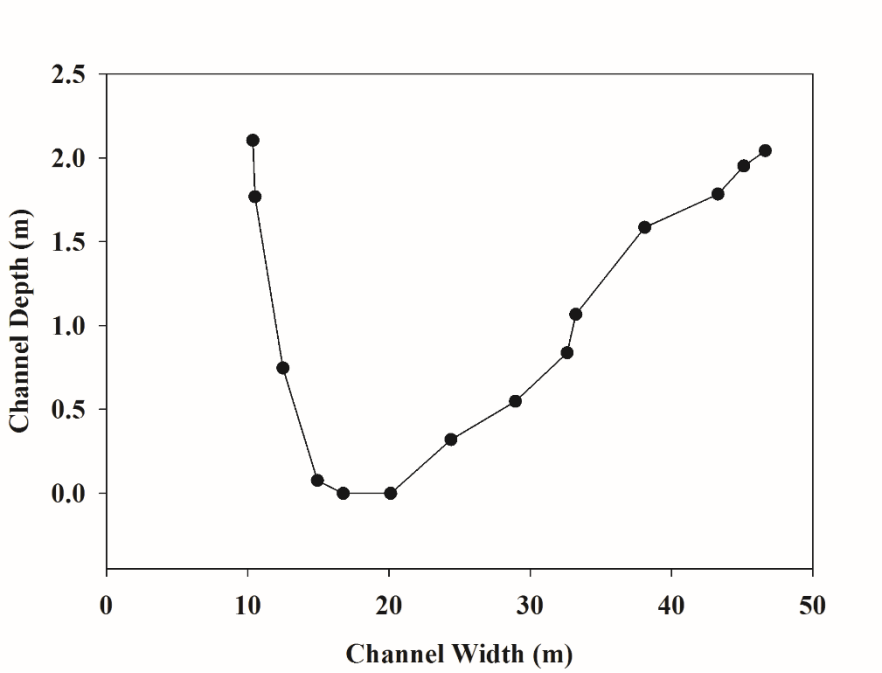

Figure A.8. Cross-sectional survey located on a straight reach at 359273 N, 3975070 E on the Barren Fork Creek.

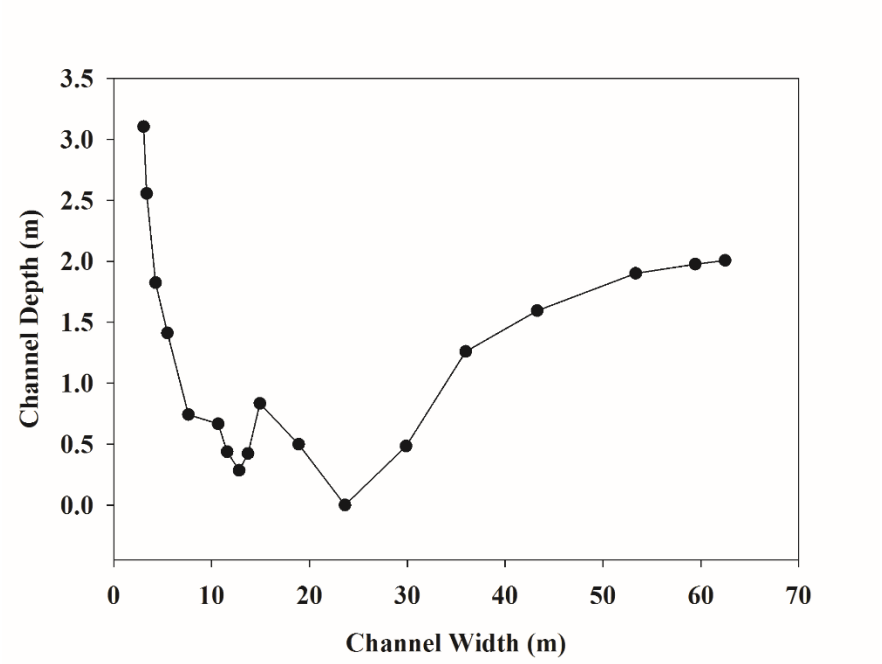

Figure A.9. Cross-sectional survey located at a cross-over at 358773 N, 3974947 E on the Barren Fork Creek.

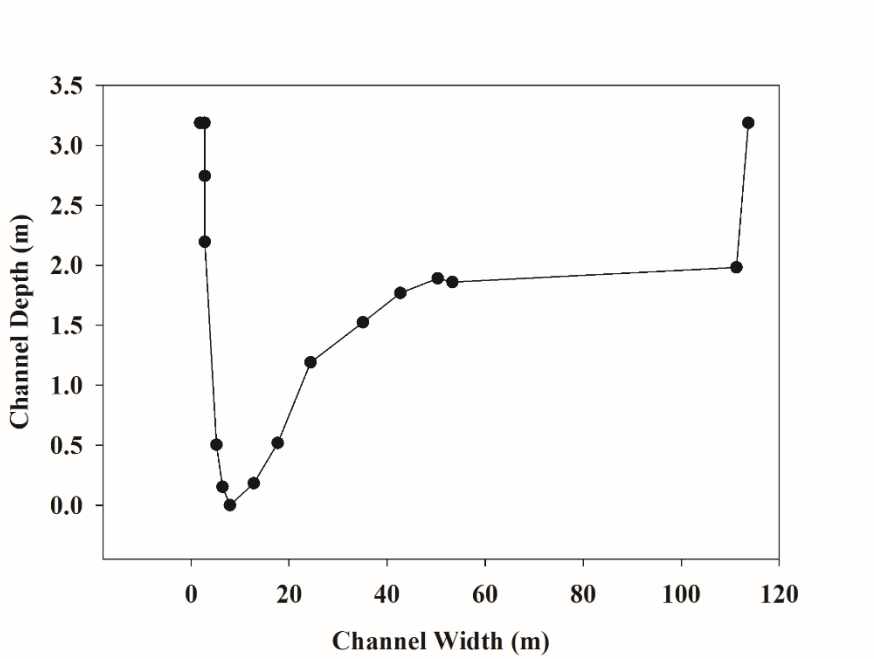

Figure A.10. Cross-sectional survey located on a meander at 358705 N, 3974940 E on the Barren Fork Creek.

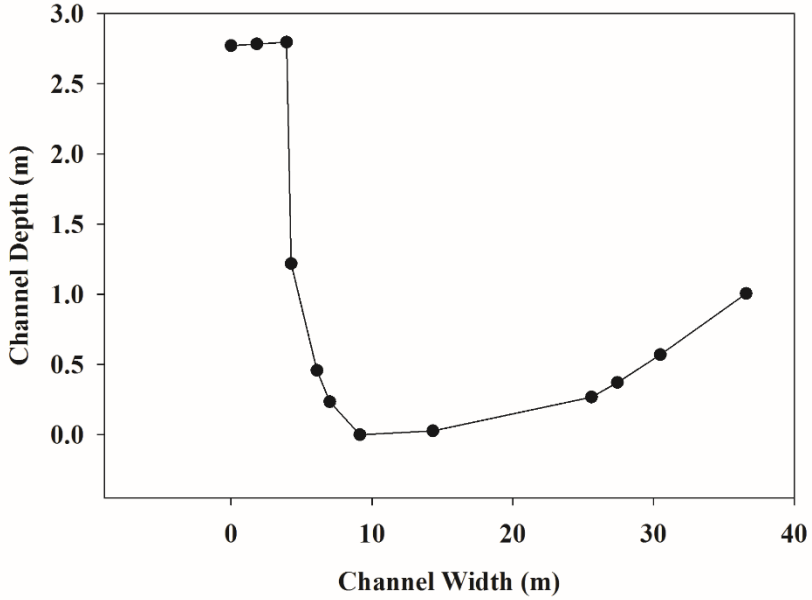

Figure A.11. Cross-sectional survey located on a meander at 356712 N, 3975175 E on the Barren Fork Creek.

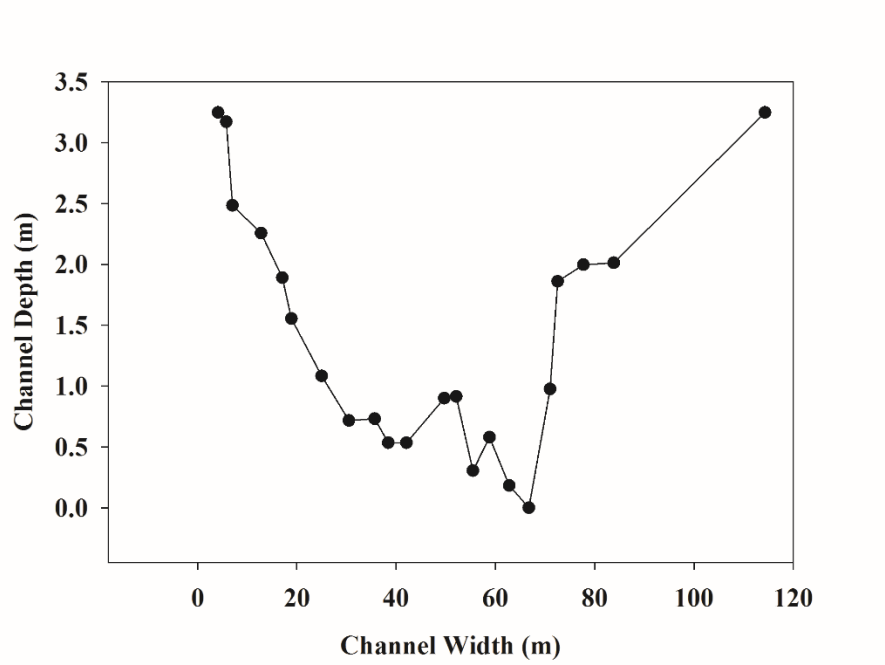

Figure A.12. Cross-sectional survey located at a cross-over at 353555 N, 3976619 E on the Barren Fork Creek.

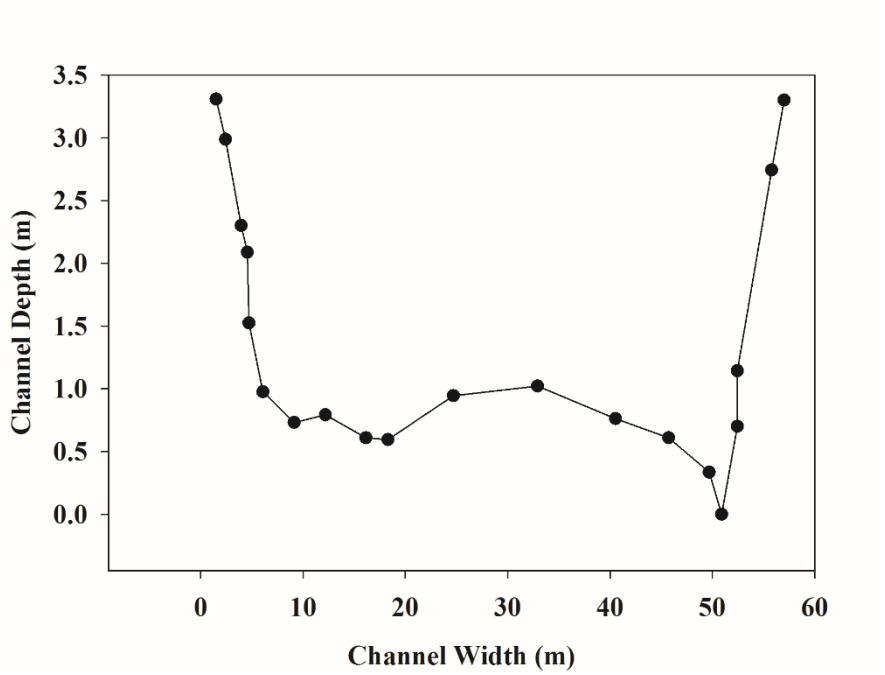

Figure A.13. Cross-sectional survey located on a straight reach at 353469 N, 3976687 E on the Barren Fork Creek.

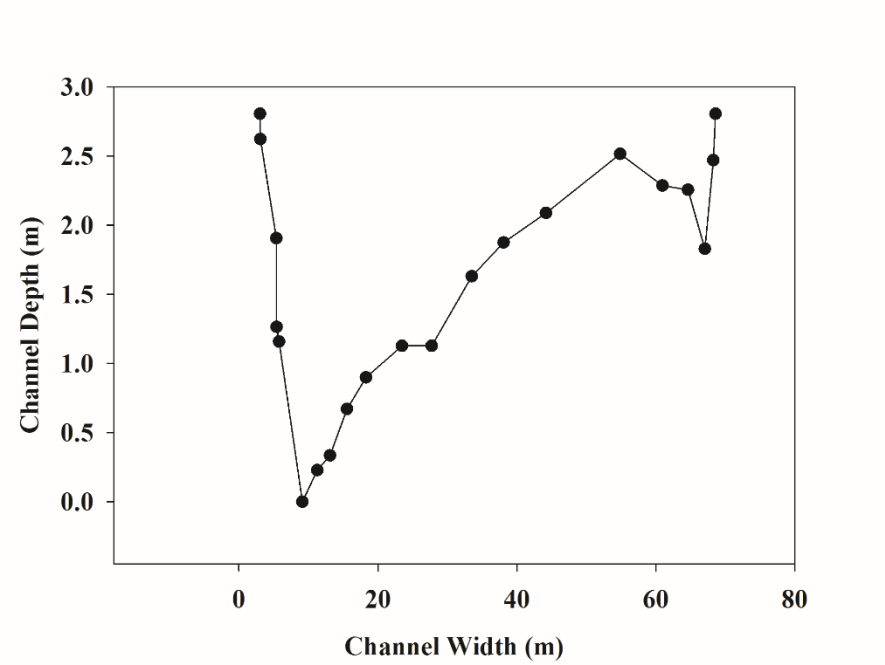

Figure A.14. Cross-sectional survey located on a meander at 353356 N, 3976777 E on the Barren Fork Creek.

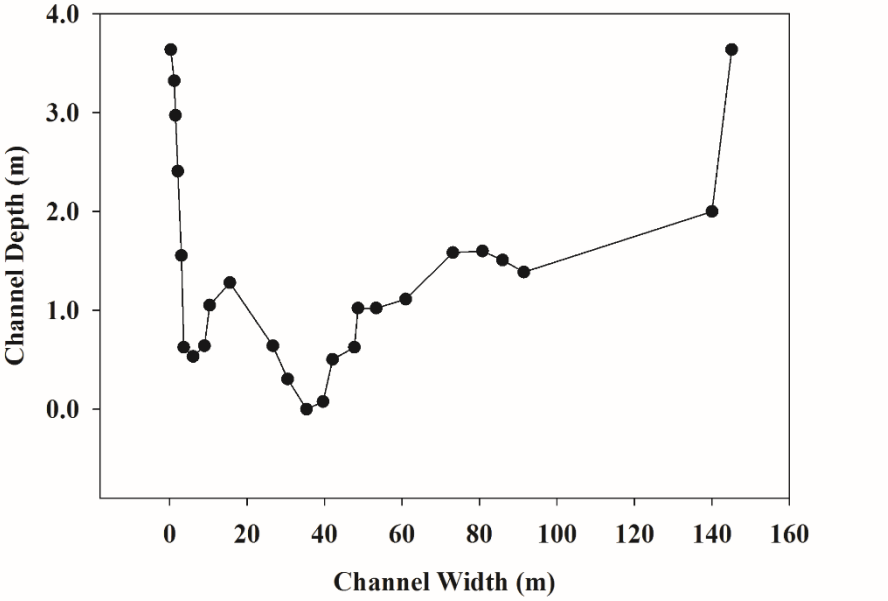

Figure A.15. Cross-sectional survey located on a cross-over at 346927 N, 3979630 E on the Barren Fork Creek.

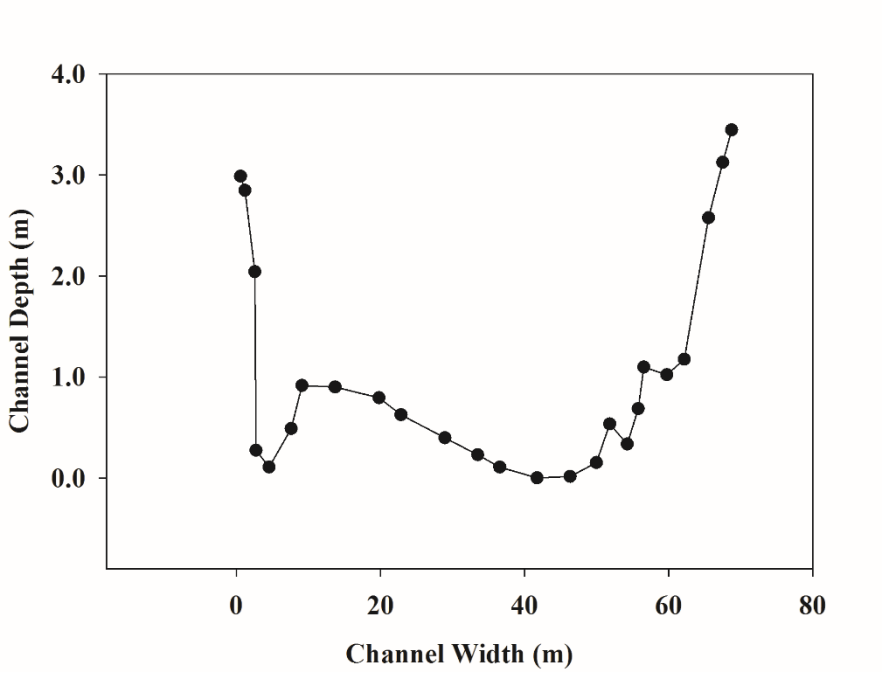

Figure A.16. Cross-sectional survey located on a straight reach at 346884 N, 3979651 E on the Barren Fork Creek.

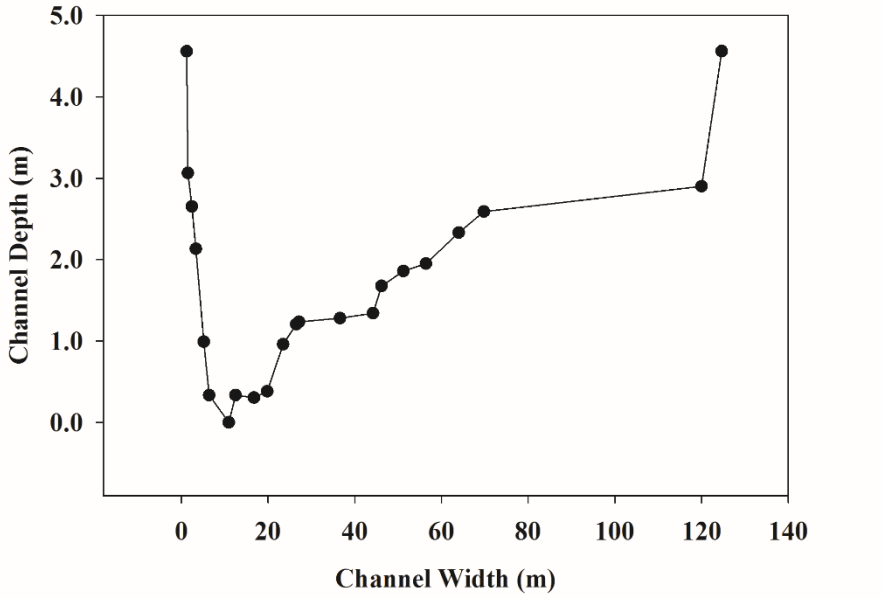

Figure A.17. Cross-sectional survey located on a meander at 346815 N, 3979706 E on the Barren Fork Creek.

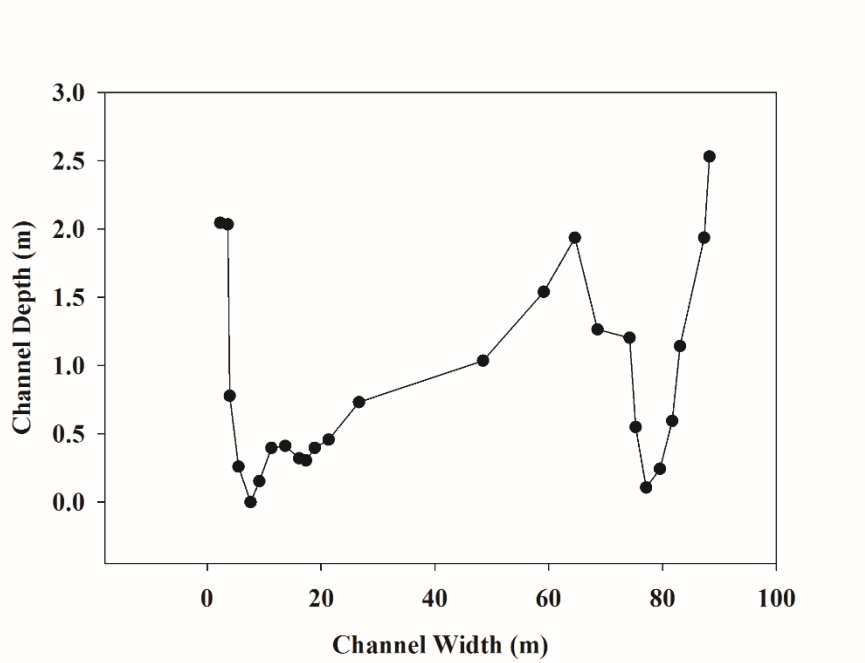

Figure A.18. Cross-sectional survey located on a meander at 340047 N, 3980843 E on the Barren Fork Creek.

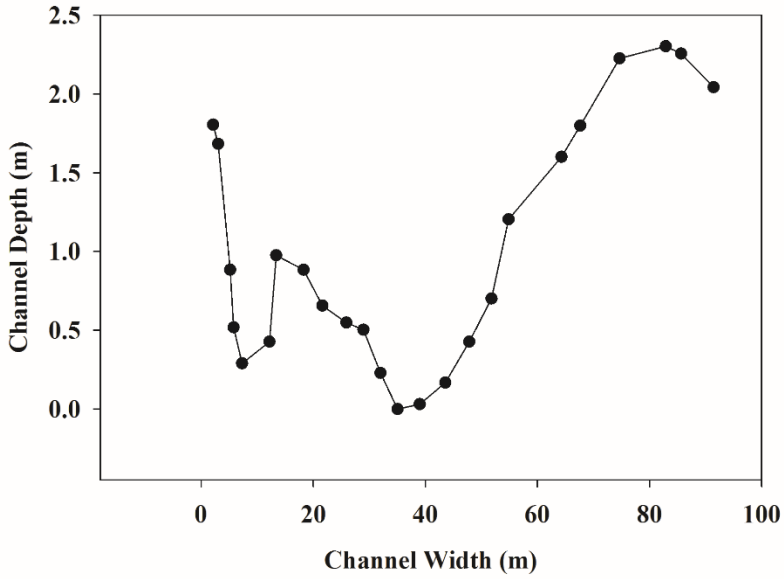

Figure A.19. Cross-sectional survey located on a cross-over at 340029 N, 3980855 E on the Barren Fork Creek.

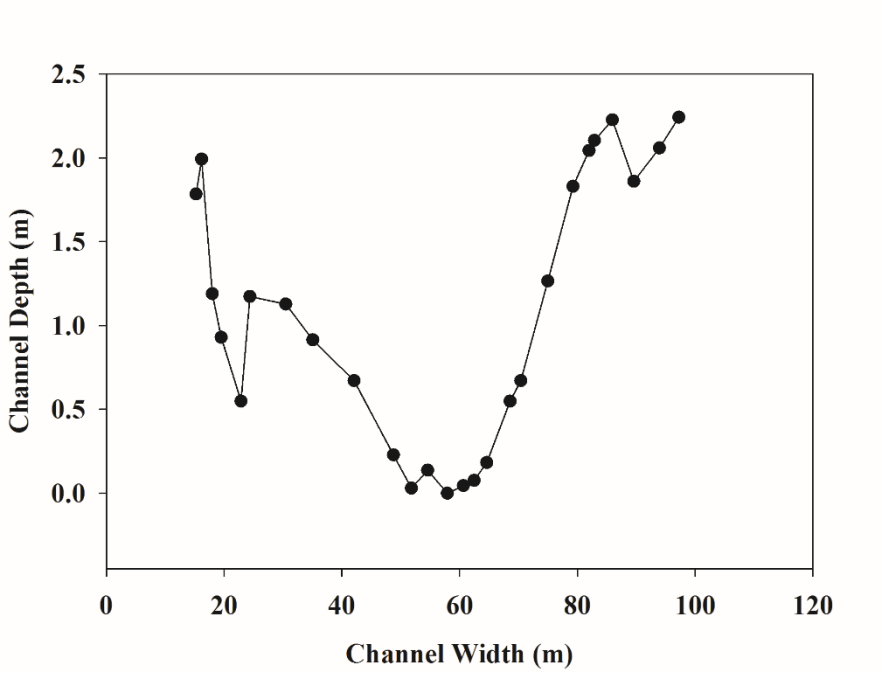

Figure A.20. Cross-sectional survey located on a straight reach at 339979 N, 3980899 E on the Barren Fork Creek.

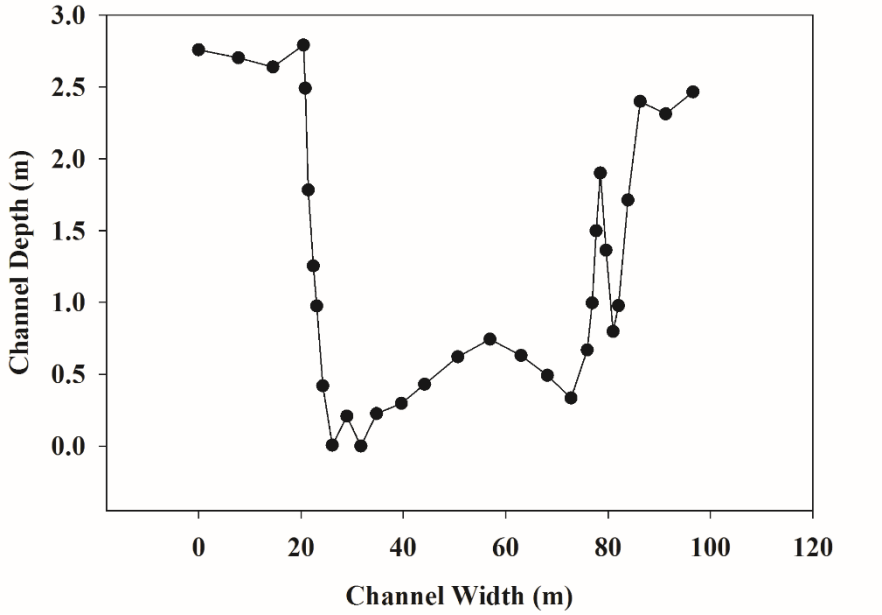

Figure A.21. Cross-sectional survey located on a straight reach at 333579 N, 3976229 E on the Barren Fork Creek.

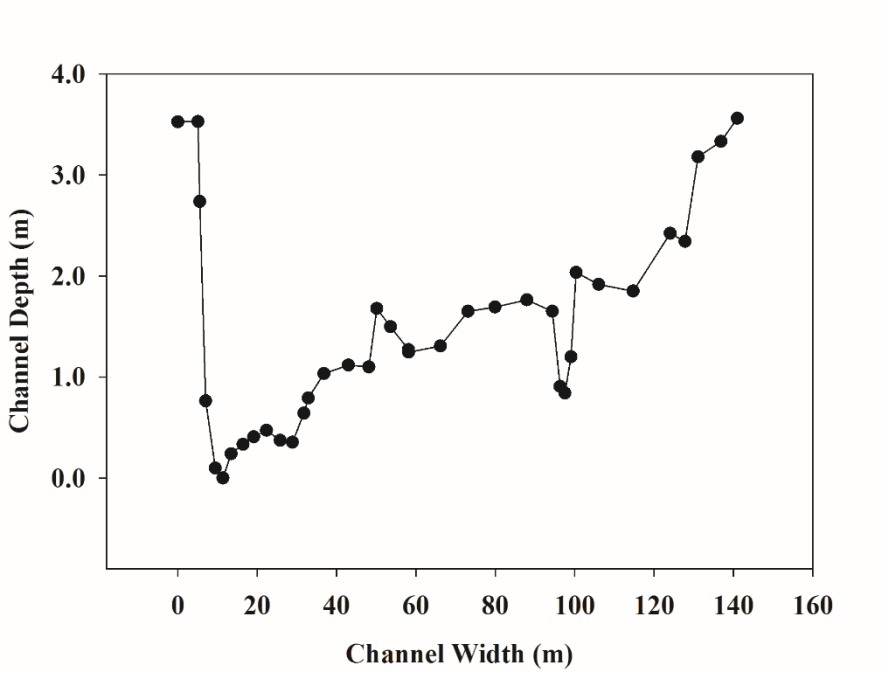

Figure A.22. Cross-sectional survey located on a straight reach at 333451 N, 3975536 E on the Barren Fork Creek.

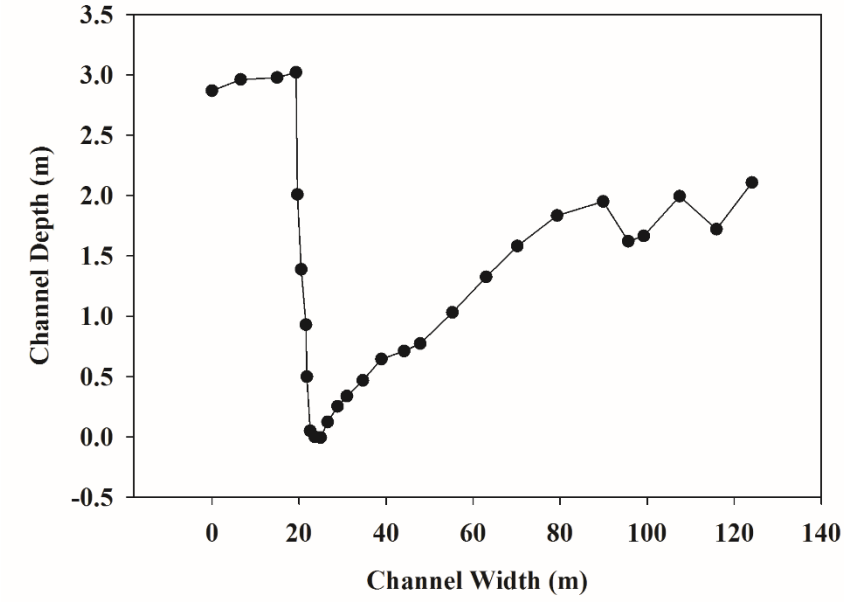

Figure A.23 Cross-sectional survey located on a meander at 333413 N, 3975106 E on the Barren Fork Creek.

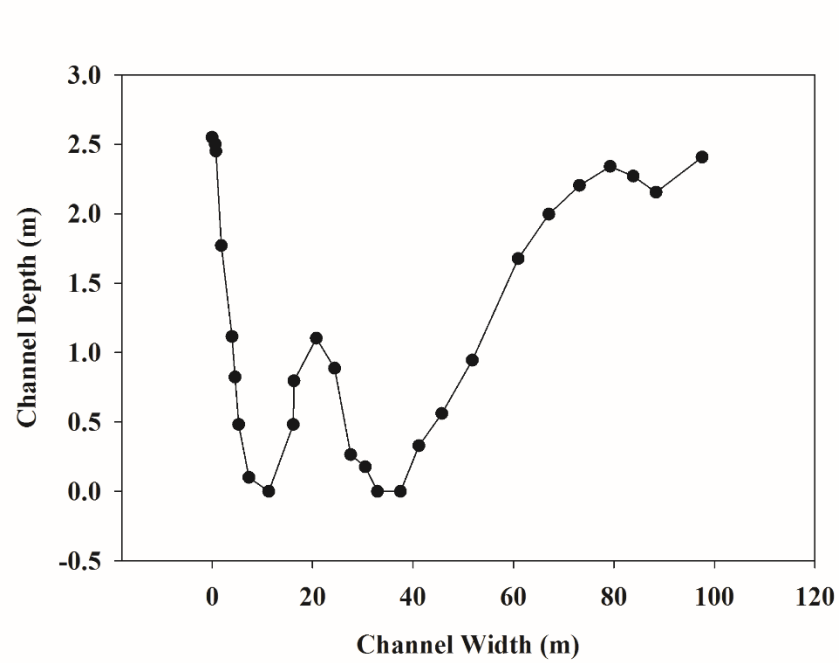

Figure A.24. Cross-sectional survey located on a straight reach at 332633 N, 3974785 E on the Barren Fork Creek.

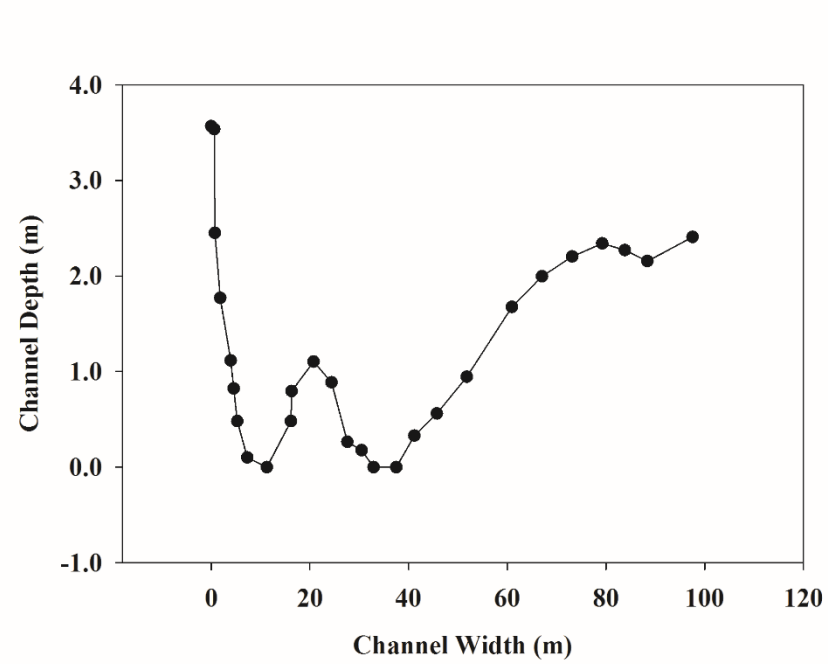

Figure A.25. Cross-sectional survey located on a cross-over at 332596 N, 3974712 E on the Barren Fork Creek.

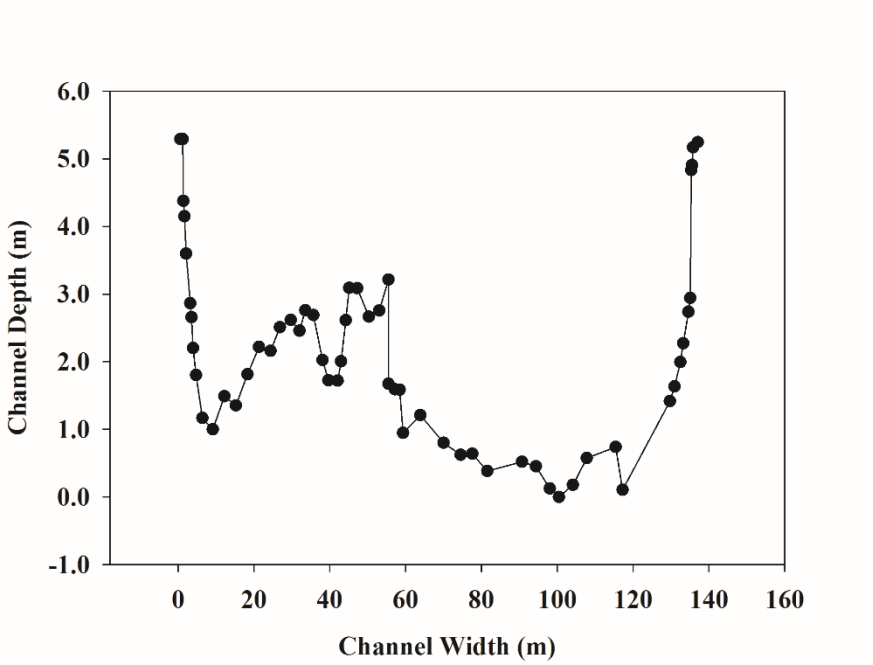

Figure A.26. Cross-sectional survey located on a straight reach at the U.S. Geological Survey gage station near Eldon, Oklahoma (334227 N, 3976830 E) on the Barren Fork Creek.

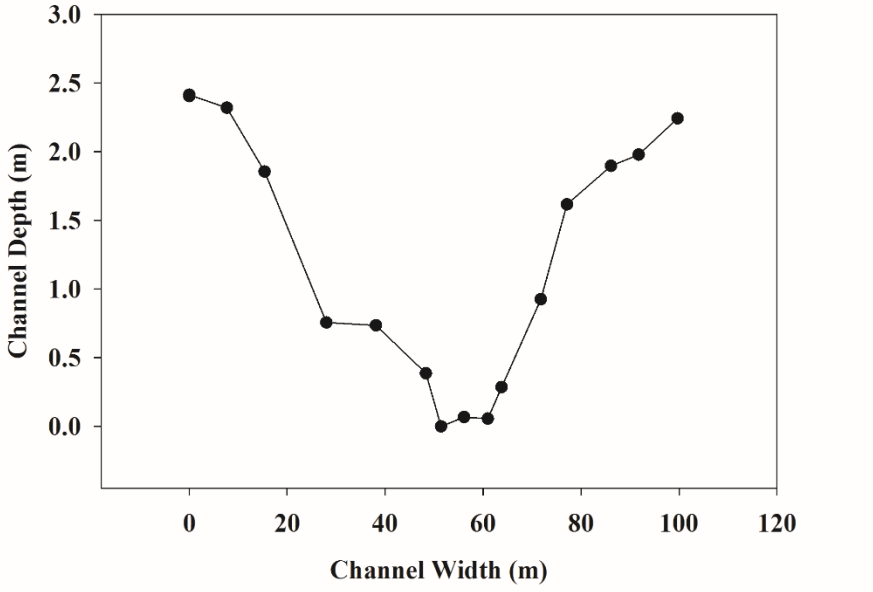

Figure A.27. Cross-sectional survey located on a cross-over at 332644 N, 3974899 E on the Barren Fork Creek.

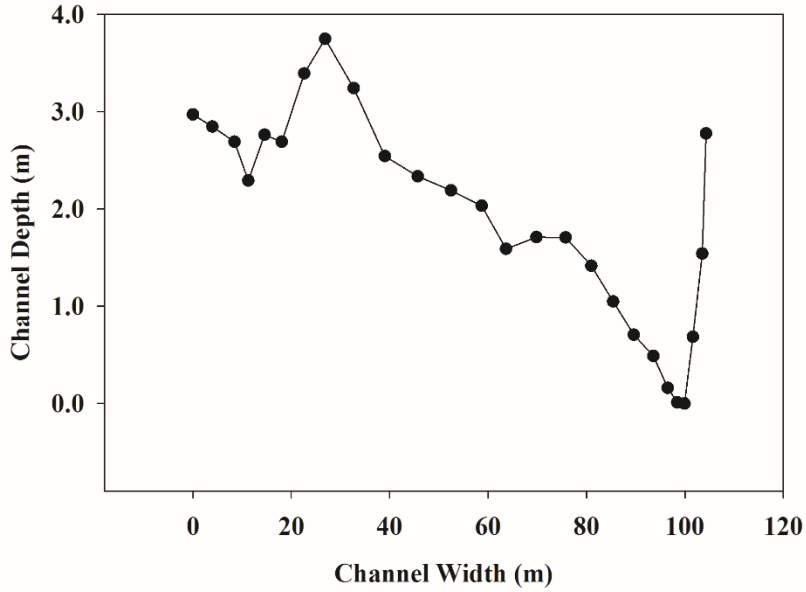

Figure A.28. Cross-sectional survey located on a meander at 332274 N, 3974867 E on the Barren Fork Creek.

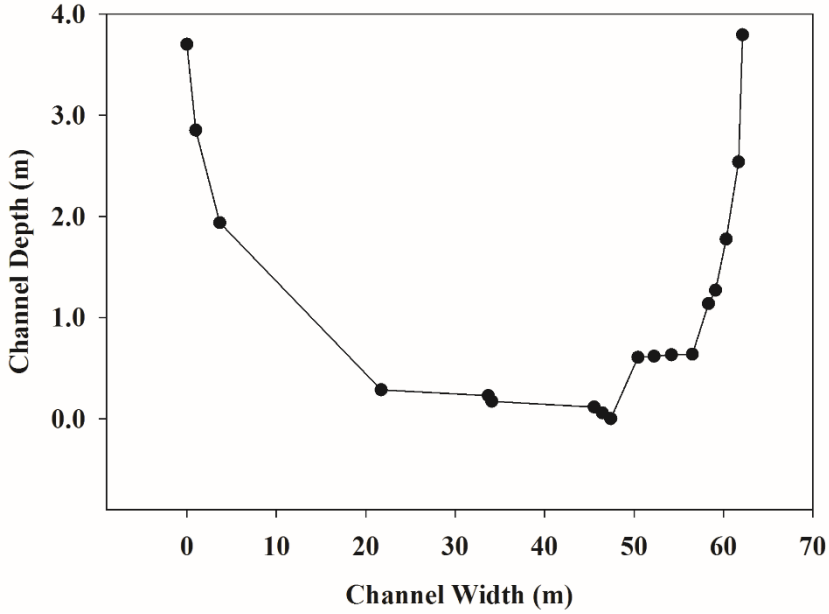

Figure A.29. Cross-sectional survey located on a straight reach at 331669 N, 3973131 E on the Barren Fork Creek.